creative commons
COMMONS DEED

저작자표시-비영리-변경금지 2.0 대한민국

이용자는 아래의 조건을 따르는 경우에 한하여 자유롭게

- 이 저작물을 복제, 배포, 전송, 전시, 공연 및 방송할 수 있습니다.

다음과 같은 조건을 따라야 합니다:

저작자표시. 귀하는 원저작자를 표시하여야 합니다.

비영리. 귀하는 이 저작물을 영리 목적으로 이용할 수 없습니다.

변경금지. 귀하는 이 저작물을 개작, 변형 또는 가공할 수 없습니다.

- 귀하는, 이 저작물의 재이용이나 배포의 경우, 이 저작물에 적용된 이용허락조건을 명확하게 나타내어야 합니다.
- 저작권자로부터 별도의 허가를 받으면 이러한 조건들은 적용되지 않습니다.

저작권법에 따른 이용자의 권리는 위의 내용에 의하여 영향을 받지 않습니다.

이것은 이용허락규약(Legal Code)을 이해하기 쉽게 요약한 것입니다.

Disclaimer

dCollection

약학박사학위논문

Synthesis and Anti-inflammatory evaluations of Novel Catecholopyrimidine derivatives for the treatment of Atopic Dermatitis

아토피성피부염치료를위한

새로운카테콜로피리미딘유도체의합성및항염증평가

2019 년 02 월

서울대학교대학원

약학과약품분석학전공

Baskaran Purushothaman

약학박사학위논문

Synthesis and Anti-inflammatory evaluations of Novel Catecholopyrimidine derivatives for the treatment of Atopic Dermatitis

아토피성 피부염 치료를 위한

새로운 카테콜로피리미딘 유도체의 합성 및 항염증 평가

지도교수 송 준 명

이 논문을 약학박사학위논문으로 제출함

2019 년 02 월

서울대학교 대학원

약학과 약품분석학전공

Baskaran Purushothaman

Baskaran Purushothaman 의 박사학위논문을 인준함 **2019 년 02 월**

위 원 장	박 정 일 (인)
부 위 원 장	송 준 명 (인)
위 원	이 상 국 (인)
위 원	이 지 연 (인)
위 원	박 성 수 (인)

Abstract

Synthesis and Anti-inflammatory evaluations of Novel Catecholopyrimidine derivatives for the treatment of Atopic Dermatitis

Baskaran Purushothaman

College of Pharmacy

The Graduate School

Seoul National University

Atopic dermatitis (AD) is a chronic inflammatory skin disease affecting millions of people worldwide. Dysregulated cytokine release from activated immune cells is the major underlying cause of AD. For the past decades, the discovery of phosphodiesterase 4 (PDE4) inhibitors as anti-inflammatory drugs for the treatment of atopic dermatitis (AD) have been investigated. However, a fewer number of drugs only approved by the United States federal drug administration (US-FDA). PDE4 is a major cyclic adenosine monophosphate (cAMP) hydrolyzing enzyme and play an important role in the inflammatory response. PDE4 enzyme is primarily found in inflammatory

and immune cells. Selective inhibition of PDE4 enzyme favorably suppresses the production of inflammatory cytokines and subsequently arrest the development of atopic dermatitis via modulating the intracellular cAMP levels. Considering the side effects of corticosteroids, selective inhibition of PDE4 could constitute an effective alternative therapy for the treatment of atopic dermatitis (AD).

In this work, a series of novel catechol based compounds bearing a pyrimidine as the core have been designed and synthesized. In chapter I, introduction to atopic dermatitis and PDE4 enzyme is presented. In chapter II, design, synthesis, molecular docking, *in-vitro* and *in vivo* properties of the synthesized compounds is presented. In vitro PDE4 enzyme assay confirmed that compounds **1** and **23** specifically inhibits PDE4B enzyme. The *in-vivo* animal study of the active compounds **1** and **23** were analyzed using DNCB-induced Balb/c and NC/Nga mice. The animal study confirmed that compound **23** suppressed the levels of pro-inflammatory cytokines such as TNF-α, IL-4, IL-5, and IL-17. Moreover, compound **23** significantly reduced the infiltrative CD4+ T-helper cells, mast cells and IgE levels in atopic tissue. Thus, the *in-vitro* and *in-vivo* data suggested that compound **23** specifically inhibited the PDE4B enzyme and the symptoms of the AD in atopic mice.

Taken together, this work suggested that compound **23** could be an effective PDE4B inhibitor for the potential treatment of AD.

Keywords: atopic dermatitis; phosphodiesterase-4; molecular docking; catecholopyrimidine; dinitrochlorobenzene.

Student Number: 2013-31348

Table of contents

Chapter-I

Introduction

1.1. Atopic dermatitis……...1

1.2. Causes of Atopic dermatitis…….1

1.3. Symptoms of AD……2

1.4. Therapy for AD…….3

1.5 Targets and Current developments for the treatments of atopic dermatitis…….4

1.6. PDE4 inhibitors currently in development for AD……7

1.7.Phosphodiesterase-4 (PDE4) and cyclic adenosine monophosphate (cAMP)…….9

Chapter-II

Design, synthesis, and anti-inflammatory evaluations of catecholopyrimidine derivatives

2.2. Medicinal chemistry design strategy…….13

2.3. Results

2.3.1. Synthesis of small molecules……15

2.3.2. In vitro PDE4 enzyme assay of synthesized compounds……..22

2.3.3. Molecular docking study of active compound 23……..30

2.3.4. X-ray crystal structure of active compound 23…….36

2.4. THE IN VIVO ANIMAL STUDY OF ACTIVE COMPOUNDS 1 and 23

2.4.1. Compound 23 treatment alleviates AD-like symptoms in BALB/c mice……..37

2.4.2. Histological observation of compound 23 treated BALB/c mice……40

2.4.3. Compound 23 treatment suppress the inflammatory mediators……41

2.4.4. Compounds 1 and 23 alleviates AD-like Symptoms in NC/Nga Mice…….43

2.4.5. Histological observation of the NC/Nga mice skin……48

2.4.6. PDE4B Inhibitors Improves Intracellular cAMP Levels in Macrophage……...51

2.4.7. Effect of Novel PDE4 Inhibitors on DNCB-Induced Inflammatory Mediators……..53

3. Discussion……..56

4. Conclusions……61

5. Materials and methods……..62

5.1. Synthesis of intermediates…….64

5.2. General procedure for the synthesis of compounds 1-6, 8-10, 13, 14, 16, 22, and 24-26…….....70

5.3. General procedure for the synthesis of compounds 7, 11, and 18……..70

5.4. General procedure for the synthesis of compounds 12, 15, 17, 19-21 and 23…….....72

5.5. Reaction conditions and spectroscopic characterization of compounds 1-26…….73

5.6. In vitro assay of compounds…...……96

5.7. Molecular docking…….....97

5.8. X-ray crystallography…….98

5.9. In vivo animal study: Animals…….....100

5.10. In vivo animal study using BALB/c mice: Sensitization and challenge…….....100

5.10.1. Evaluation of skin lesion……..101

5.10.2. Histopathological analysis……..101

5.10.3. Measurement of serum IgE, and tissue TNF-α in BALB/c mice…….....102

5.11. In vivo animal study using NC/Nga mice: Sensitization and Challenge……..103

5.11.1. Evaluation of Skin Lesion……104

5.11.2. Histopathology and Immunohistochemistry…….....104

5.11.3. Analysis of Intracellular cAMP and TNF-α…….105

5.11.4. Measurement of Serum IgE, and Tissue IL-4, 5, 17, and IFN-γ…….....106

5.11.5. Statistical Analysis……..106

6. References……143

List of Figures

Figure 1. Causes of atopic dermatitis……2

Figure 2. Steroids currently in clinical use……4

Figure 3. PDE4 inhibitors currently available and in development for AD……..**.....**7

Figure 4. Chemical structure of cAMP and GMP……..11

Figure 5. The degradation of cAMP by PDE4 enzyme……..11

Figure 6. Design strategy of compounds and chemical structures of different PDE4 inhibitors……13

Figure 7. Designing the PDE4 Inhibitors……14

Figure 8. The structure activity relationship (SAR) of the pyrimidine nucleus against PDE4……..24

Figure 9. Dose dependent inhibition of PDE4 isoenzymes by compound **23**…….**.....**28

Figure 10. Binding mode of compound **23** and rolipram in the catalytic domain of PDE4B……34

Figure 11. Binding mode between the compound **23** and PDE4B catalytic binding site……..35

Figure 12. Molecular docking of compound **23** with PDE4 A, B, C, and D enzymes……...35

Figure 13. The ORTEP diagram of compound **23**……..36

Figure 14. Epidermal skin score, scratching frequency, epidermal thickness of compound **23** treated AD induced BALB/c mice……39

Figure 15. H&E staining, the serum IgE and tissue TNF-α levels in control, DNCB, compound **23** and DNCB+compound **23** co-treated experimental mice……...42

Figure 16. Atopic dermatitis-induced NC/Nga mice were co-treated with either compound-**1** or compound-**23**……45

Figure 17. Epidermal skin score, scratching frequency thickness of the dorsal skin of experimental mice of compound **1** and **23** treated AD induced NC/Nga mice were compared with control and DNCB-treated mice…….46

Figure 18. Subiliac lymph node size and weight. Spleen weight in experimental animals……..47

Figure 19. H&E staining of dorsal skin of experimental animals (NC/Nga mice)……49

Figure 20. Toluidine blue staining of mast cells and Serum IgE level of compound **1** and **23** treated mice…….....50

Figure 21. cAMP and TNF-α levels in the cell lysate of compound **1** and **23** treated LPS stimulated Raw 264.7 cells…….....52

Figure 22. Serum cytokines level in experimental mice were quantified by ELISA……53

Figure 23. Immunohistochemical staining of cytokines deposited in the dorsal skin tissue of experimental animals……...55

Figure 24. ^{1}H and ^{13}C NMR spectrum of compounds **1-26**…..…….....115-140

Figure 25. ^{1}H-^{1}H COSY and HMBC spectrum of active compound **23**…….141

Figure 26. NOEOSY and HSQC spectrum of active compound **23**….142

Scheme Legends
Scheme 1. General synthetic scheme: Synthesis of compounds **1-8**…….17
Scheme 2. General synthetic scheme: synthesis of compounds **11-26**….19
Scheme 3. Synthetic scheme for compounds **9** and **10**…….20
Scheme 4. Synthesis of compounds **11** and **18**……..21
Scheme 5. Synthesis of compounds **16** and **21**……..21
List of tables
Table 1. New targets and compounds for AD…….6
Table 2. Synthesized compounds and its PDE4B IC_{50} values……...25
Table 3. The IC_{50} values of selected compounds on various PDEs……..29
Table 4. X-ray crystal data for compound-**23**……..108

List of abbreviations

AD: Atopic dermatitis

PDE4: Phosphodiesterase-4

cAMP: cyclic adenosine monophosphate

cGMP: cyclic guanosine monophosphate

IL: Interleukin

IFN: Interferon

IgE: Immunoglobulin E

TNF-α: tumor necrosis factor-α

COPD: chronic obstructive pulmonary disease

CNS: central nervous system

LPS: Lipopolysaccharides

CD4: cluster of differentiation 4

$POCl_3$: phosphoryl chloride

DIPEA: N,N-diisopropylethylamine

m-CPBA: m-chloroperoxybenzoic acid

EDCI: N-Ethyl-N′-(3-dimethylaminopropyl)carbodiimide hydrochloride

HOBt: Hydroxybenzotriazole

DMF: N, N-Dimethylformamide

ORTEP: Oak Ridge Thermal Ellipsoid Plot Program

DNCB: 2,4-Dinitrochlorobenzene

TR-FRET: time resolved-fluorescence resonance energy transfer

COSY: Correlation spectroscopy

HMBC: Heteronuclear Multiple Bond Correlation

NOESY: Nuclear Overhauser effect spectroscopy

HSQC: Heteronuclear single quantum coherence

Chapter-I

1. Introduction

1.1. Atopic dermatitis

Atopic dermatitis (AD) is the most common inflammatory skin disease affecting young children, at a prevalence rate of 15 – 25% globally [1, 2]. The clinical evidence suggested that the AD is one of the most common chronic inflammatory skin disorder associated with hyper-reactivity to environmental triggers and it is characterized by eczematous skin plaques and intense itch (pruritus). Pruritus has a major impact on the quality of sleep and is associated with profound negative effects on the quality of life for AD patients [3]. Earlier data showed the disease is affecting only >7 years old children with prevalence rate of 25%, however the recent data shows that AD is also very popular among adults with 7-10% prevalence rate. Data from the WHO Global Burden of Diseases initiative indicate that at least 230 million people worldwide have AD.

1.2. Causes of Atopic dermatitis

The family history of AD is one the strongest known evidence for the AD. The presence of AD in parents is estimated to increase the risk of developing

AD in their children's up to 3-5 fold [4, 5]. AD also involves complex interplay between multiple environmental (Regions with low ultraviolet light exposure or dry climatic conditions) and immunological factors [6]. The other factors/causes of AD include airborne allergens (animal dander, house dust mites, molds and pollens), cigarettes, microorganism (Staphylococcus aureus), and food allergy (Children's allergic to cow's milk, eggs, fish, peanuts). The causes of atopic dermatitis are shown in figure 1.

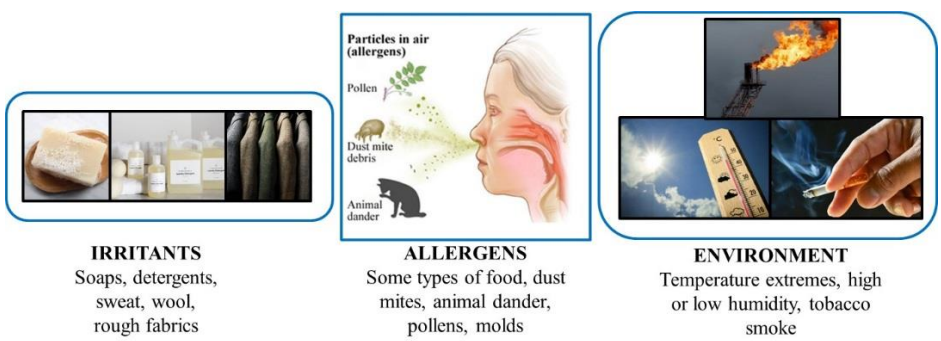

Figure 1. Causes of atopic dermatitis.

1.3. Symptoms of AD

Eczematous skin lesions, scaling, and unbearable itching (pruritus) are the clinical features of AD [7]. It leads to the psychological difficulties such as anxiety, anger, and depression. Sensitization of lymphocytes to infiltrating allergens due to epidermal barrier dysfunction is considered to be the primary cause of the disease. Activated lymphocytes at the dermis region

constitutively secrete abnormal levels of inflammatory cytokines (e.g. IL-4, 5, and 17) and contribute to the inflammation of the skin [8]. Several epidermal changes have been observed in both affected and non-affected skin of patients with AD, such as increased pH, easy irritability, reduced water retention, increased permeability to low molecular mass chemicals and increased susceptibility to infection. Sensitized T-helper lymphocyte cells, antigen-presenting cells (APC), neutrophils, and mast cells release a set of immunological mediators, which collectively determine the severity and longevity of AD [8].

1.4. Therapy for AD

The topical corticosteroids therapy used for AD for past five decades, and provide excellent therapeutic effect. However, long-term use of corticosteroids is associated with side effects such as skin atrophy, acne rosacea, and stretch marks. Topical calcineurin inhibitors such as, tacrolimus and pimecrolimus is also used as first line therapy for mild AD. Antihistamines such as cetirizine and levocetirizine has been also used for mild AD. However, less or/and insufficient evidence to use of these drugs in the treatment of AD. Systemic treatment such as systemic corticosteroids and phototherapy can be also applied for alternative therapy for the AD. Oral

corticosteroids such as cyclosporine, azathioprine, prednisone, methotrexate, and mycophenolate mofetil used for AD. Few steroids currently in clinical use is shown in figure 2. These drugs also showed side effects such as hepatotoxicity, dizziness, headache, abdominal pain, vascular disorders (vasculitis), gastrointestinal disorders (nausea, vomiting). To overcome these side effects, PDE4 inhibition has become an attractive alternative therapy for atopic dermatitis diseases.

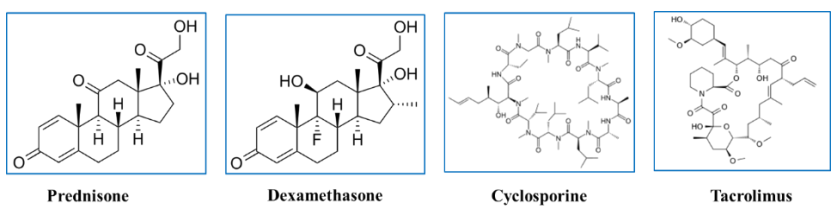

Figure 2. Steroids currently in clinical use.

1.5. Targets and Current developments for the treatments of atopic dermatitis

In many years topical or oral corticosteroids only used for AD. The development of new therapies are needed to overcome the side effects of steroid based drugs. Drug development for AD is currently ongoing with many biologics and small molecule inhibitors in clinical trials targeting different pathways, including suppressing activated immune pathways, improving the epidermal barrier, reducing the itch. Most agents in phase 2

trials. The blocking of IL-4, IL-5, IL-13, IL-22, and IL-31 cytokines is attractive target for the AD. The IL-4 inhibitor, dupilumab in adolescents with moderate-to-severe AD has been completed phase II study in Europe and the United States. The IL-5 inhibitor mepolizumab, which has been approved in the United States for severe asthma. However, the phase II clinical trials for AD is not fulfilled. IL-17 inhibitor secukinumab is also completed phase II trials for moderate to severe AD. The anti–IL-31 receptor α (IL31Rα) antibody nemolizumab is also significantly inhibited pruritus in patients with moderate to severe AD in a phase II clinical trial. The IL-31 antibody BMS-981164 is completed a phase I clinical trial for AD. The neurokinin 1 receptor (NK1R), tradipitant is completed a phase II study for moderate to severe AD. JAK inhibitors is one of the novel target for the AD and it can block a range of cytokine, growth factor, and hormone receptor signalling pathways. Many JAK inhibitors in the development for AD. For example, JAK1/2 inhibitor baricitinib is completed for phase II study and JAK 1 inhibitor upadacitinib is in phase II trials. Many other oral/topical JAK inhibitors are currently being tested for AD. The histamine receptor type 4 (H4R) antagonist, ZPL389 is completed for moderate to severe AD in phase II trials.

Table 1. New targets and compounds for AD.

Target	Compound	Atopic dermatitis indication	Current status	Ref
IL-4/IL-13R	Dupilumab	Moderate to severe	Phase –II trial	9
IL-5	Mepolizumab	Moderate to severe	Terminated	10
IL-13	Tralokinumab Lebrikizumab	Moderate to severe	Phase-II trial completed	11
IL-17	Secukinumab	Moderate to severe	Phase-II trial completed	12
IL-33	Etokimab	Moderate to severe	In phase-IIa trial	13
IL-22	Fezakinumab	Moderate to severe	In phase-IIa trial	14
IL-31Rα	Nemolizumab	Moderate to severe	Phase –II trial	15
IL-31	BMS-981164	Moderate to severe	phase I study completed	16
NK1R	Tradipitant	Moderate to severe	Phase II study completed	17
IgE	Ligelizumab	Moderate to severe	Phase III study	18
JAK1 and JAK2	Baricitinib	Moderate to severe	Phase II study completed	19
JAK1	Upadacitinib	Moderate to severe	Phase II study completed	20
JAK and SYK	ASN002	Moderate to severe	Phase IIa study completed	21
JAK1 and JAK3	Tofacitinib	Mild to moderate	Phase IIa study	22
JAK 1, 2 and 3	Delgocitinib	Mild to moderate	Phase III trial	23
JAK 1 and 2	Ruxolitinib	Moderate to severe	Phase IIb trial	24
H4R	ZPL389	Moderate to severe	Phase IIa study completed	25
PDE4	Crisaborole	Mild to moderate	Approved	26
PDE4	Roflumilast	Moderate	Phase IIa trial	27
PDE4	RVT-501	Mild to moderate	Phase II trail	28
PDE4	Apremilast	Mild to moderate	Phase II trail	29
PDE4	LEO-29102	Mild to moderate	Phase I study completed	30

1.6. PDE4 inhibitors currently in development for AD

The intracellular levels of cAMP have been implicated in the reduction of lymphocyte-derived cytokine and chemokines. However, PDE4 present in the inflammatory cells diminish the intracellular levels of cAMP through the hydrolysis of cyclic nucleotides. Increased level of PDE4 in cell from AD patients have been reported and targeting the PDE4 using specific

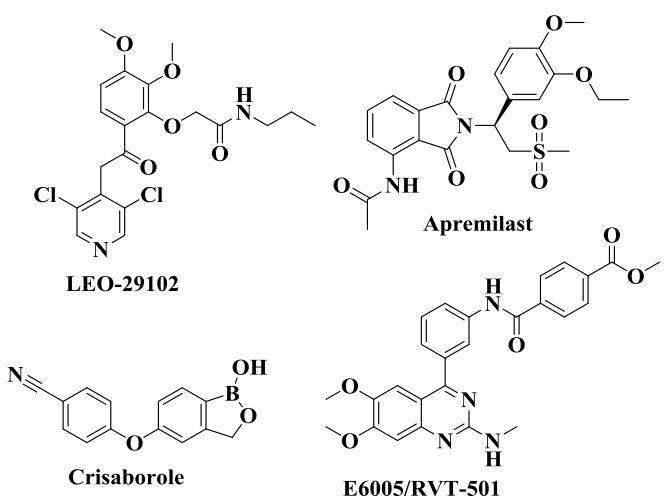

Figure 3. PDE4 inhibitors currently available and in development for AD.

inhibitors is believed to decrease the secretion of proinflammatory mediators in AD patients. Recently, crisaborole a topical boron-based compound that selectively inhibits the PDE4 and has been approved by the US FDA for mild to moderate AD. This drug is available as 2% ointment. The other topical

PDE4 inhibitor that are currently in development for treatment of AD includes E6005/RVT-501, DRM02, OPA-15406/MM36, and LEO-29102 is also completed phase II study for mild to moderate AD. The topical PDE4 inhibitor, E6005/RVT- 501 evaluated for phase 1 and 2 clinical studies. The results are promising in in children and adults in Japan. However, these drugs not yet studied for phase 3 clinical trials. The oral PDE4 inhibitor apremilast is approved for psoriatic arthritis and patients with moderate to severe plaque psoriasis and now in phase II study for AD. The clinical study of apremilast was conducted in patients with AD. The results are promising, however, diarrhea and nausea were more common side effects. These gastrointestinal side effects are not seen in the topical formulations of PDE4 inhibitors than oral PDE4 inhibitors. The limited topical treatments for patients with AD have led to development of novel nonsteroidal targeted therapies. PDE4 plays a role in the regulation of the inflammatory cells with AD. Thus it making the PDE4 is the novel and desired target for AD. The topical corticosteroids and calcineurin inhibitors affects broad range of cytokines involved in AD. However, the mechanism of PDE4 inhibitors is different from the corticosteroids. Overall, the clinical evidences suggested that targeting the PDE4 enzyme may be a safe and effective approach to the management of AD.

1.7. Phosphodiesterase-4 enzyme (PDE4) and Cyclic adenosine monophosphate (cAMP)

Cyclic adenosine monophosphate (cAMP) regulates numerous metabolic reactions. The regulatory function of the cAMP is generally cell dependent. cAMP-mediated protein kinase-A (PKA) signaling negatively regulates the expression of pro-inflammatory cytokines in lymphocytes and macrophages [31, 32]. Elevated intracellular levels of cyclic adenosine monophosphate (cAMP) have been implicated in the reduction of lymphocyte -derived cytokine and chemokines. However, Phosphodiesterases (PDEs) present in the inflammatory cells diminish the intracellular levels of cAMP through the hydrolysis of cyclic nucleotides [33, 34]. The chemical structure of cAMP and cGMP and degradation of cAMP by PDE4 enzyme are shown in figure 4 and 5. Phosphodiesterases are enzymes that hydrolyze cAMP and cyclic guanosine mono phosphate (cGMP) into their inactive form of 5'-adenosine mono phosphate (5'AMP) and 5'- guanosine mono phosphate (5'GMP), respectively (Figure 5) [35]. PDEs are subdivided into 11 different groups based on sequence similarity, biochemical properties, and inhibitor selectivity. PDEs are further classified into: (i) cAMP-specific (PDE4, 7, and 8); (ii) cGMP- specific (PDE5, 6, and 9); and (iii) specific to both cAMP and cGMP (PDE1, 2, 3, 10, and 11) [36, 37] based on their affinity to cAMP or cGMP.

Among the cAMP-specific PDEs, PDE4 enzymes are significantly expressed in inflammatory cells including mast cells, eosinophils, neutrophils, T cells, and macrophages. Four isoforms of PDE4 have been discovered so far, i.e., PDE4A, B, C, and D. Earlier, it has been reported that PDE4B is the predominant isoform of PDE4 expressing in lymphocytes and macrophages [38]. It has been reported that the inhibition of PDE4D is responsible for the emetic side effects [39]. Selective inhibition of the PDE4B may provide a means to achieve efficacy while potentially mitigating the adverse effects such as nausea and emesis. Thus, research efforts mainly focusing on the selective PDE4B inhibitors to minimize the side effects [40-43]. The degradation of cAMP by PDE4 enzyme can cause immune cell activation and release of proinflammatory cytokines such as TNF-α, IL-4, IL-5, IL-17 and IFN-γ. Inhibition of PDE4B in lymphocytes and macrophages could effectively elevate intracellular cAMP levels, which can effectively suppress the expression of inflammatory cytokines [44].

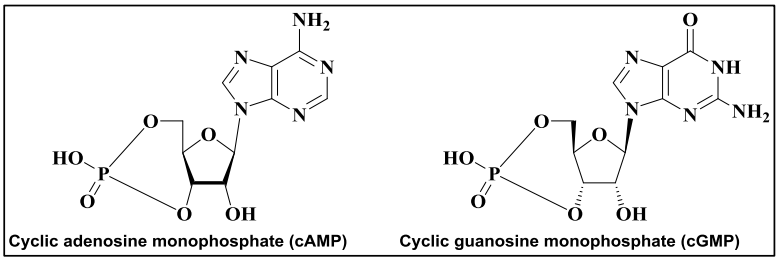

Figure 4. Chemical structure of cyclic adenosine monophosphate (cAMP) and cyclic guanosine monophosphate (cGMP).

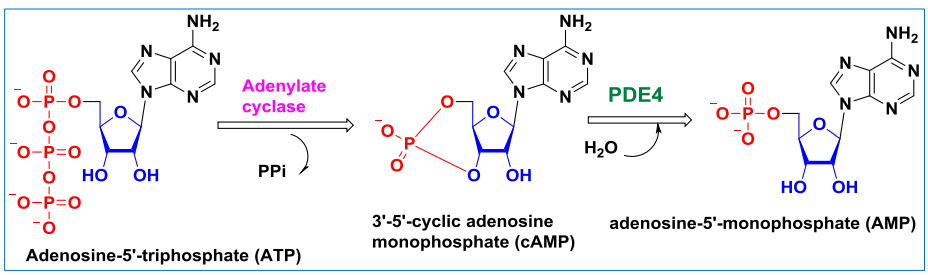

Figure 5. The degradation of cAMP by PDE4 enzyme.

Antihistamines and corticosteroids are widely used to treat inflammatory skin diseases (AD), but side effects, such as skin-atrophy, present a serious issue [45, 46]. PDE4B inhibition has become an attractive alternative therapy for inflammatory diseases such as psoriasis, psoriatic arthritis, chronic obstructive pulmonary disease (COPD) and rheumatoid arthritis [47, 48]. It has to be noted that overexpression of PDE4 enzyme has been reported in the activation of lymphocytes and degranulation of mast cells [49-51]. Several

oral PDE4 inhibitors are in clinical trials. For example, roflumilast as a potential second generation PDE4B inhibitor, recently approved by FDA. However, several reports suggested that roflumilast causes nausea and emesis as its major side effects due to abnormalities that resulted in the gastrointestinal tract (GIT) and the central nervous system (CNS), respectively [52-55]. Apart from the antagonist role in the regulation of pro-inflammatory mediators, the second messenger cAMP has been implicated in the regulation of virtually every physiological process, including the opening of ion channels, muscle relaxation, cellular differentiation, neuro muscular interaction, carbohydrate and lipid metabolism, and cell death mechanism [56-61]. Due to these active roles, it seems that side effects are inevitable for the long-term administration of oral PDE4 inhibitors. Thus, a great deal of clinical attention is required while administering oral PDE4 inhibitors. Conversely, topical application of PDE4 inhibitors can be an optimal choice to treat AD, since it is expected to exhibit less interference to cAMP-relevant metabolism. Recently, phase-2 clinical trials of roflumilast, apremilast and LEO-29102, a PDE4 inhibitors, has been completed for AD [62, 63]. Nonetheless, a safe and side-effect free non-steroidal anti-inflammatory PDE4 inhibitors is still needed for the treatment of allergic inflammatory disorders.

Chapter II

2. Design, synthesis, and anti-inflammatory evaluations of catecholopyrimidine derivatives

2.2. Medicinal chemistry design strategy

In order to develop a next generation novel PDE4 inhibitor, we rationally designed the compounds by covalently combining the available ligands such as catechol (3,4-dialkoxyphenyl) moiety with pyrimidine core into a single active molecule. Design strategy and chemical structures of different PDE4 inhibitors are shown in Figure 6 and 7.

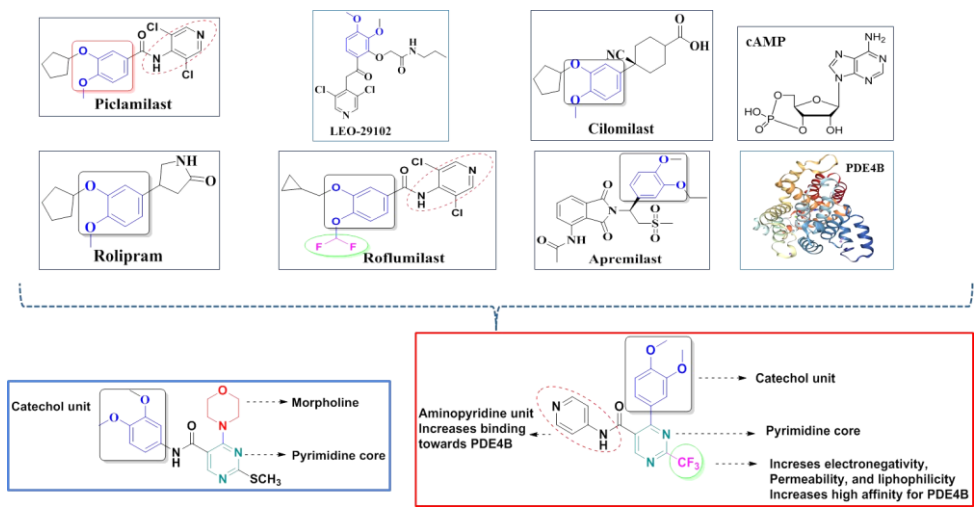

Figure 6. Design strategy of compounds and chemical structures of different PDE4 inhibitors.

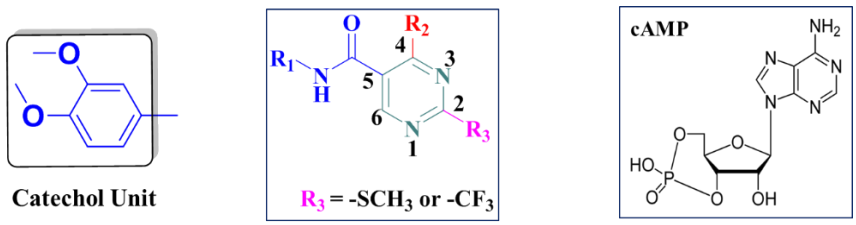

Figure 7. Designing the PDE4 Inhibitors.

The functionalization of catechol moiety to the pyrimidine core is one of the novel approaches for ligand based PDE4 drug discovery (Figure 7). In addition to that, the catechol pyrimidine core is a potential bioisostere of adenosine and also mimics the nucleotide part of the cAMP. The co-crystal structure of the 3,4-dialkoxyphenyl (catechol ether) functionalized compounds (e.g. rolipram, cilomilast, roflumilast, and apremilast) bound to PDE4B active site has revealed that the hydrophobic interactions with residues in the bivalent metal binding pocket(M pocket) and glutamine pocket (Q pocket) are very important for their PDE4 inhibition activity [66].Pyrimidine derivatives, such as pyrido[3',2':4,5]furo[3,2-d]pyrimidine and other pyrimidine heterocyclic compounds have been extensively described for their PDE4 inhibitory activity [64, 65]. The phenyl pyrimidine, 5,5-dioxo-7,8-dihydro-6H-thiopyrano[3,2-d]pyrimidine, and pyridazino[4,5-b]indolizines derivatives also reported as selective PDE4B inhibitors [41,

42,67]. In drug design strategy, trifluoromethyl (-CF_3) group introduced to the pyrimidine core to enhances the drug likeliness of newly synthesized compounds. Many reports also suggested that the -CF_3 functionalized compounds offers the characteristics of high electronegativity, enhanced permeability to cell membrane, increased lipophilicity for a particular affinity to a target protein, and minimized drug metabolism [68, 69]. These characteristics enhances the drug likeliness of newly synthesized compounds.

2.3. Results

2.3.1. Synthesis of small molecules

The synthesis of morpholine and catechol functionalized pyrimidine core compounds is depicted in **Scheme 1 and 2**. The condensation reaction of diethyl ethoxymethylenemalonate with different substituted amidines, such as trifluoromethylacetamidine or S-methylisothiourea hemisulfate salt, in the presence of sodium ethoxide as alkaline catalyst, provides 2-(trifluoromethyl) or 2-(methylthio)pyrimidinone **(i)**. The chlorination of (trifluoromethyl) or 2-(methylthio)pyrimidinone with $POCl_3$ at 100° C yielded Ethyl 4-chloro-2-(methylthio)4-chloro-2-(trifluoromethyl)pyrimidine-5-carboxylate (**Scheme 1 and 2, (ii)**). The nucleophilic substitution (S_N2) reaction of chloropyrimidine **(ii)** with morpholine provided the corresponding

morpholinopyrimidine esters (**Scheme 1**, **(iii)**) in the presence of DIPEA in 2-propanol. These morpholinopyrimidine ester were hydrolyzed to the corresponding acids **(iv)** by using aqueous NaOH in ethanol. To this pyrimidine acid intermediates **(iv)** different aromatic amines were coupled by acid-amine reaction to get morpholinopyrimidine carboxamides (**v, 1-8**). The library of catecholopyrimidine carboxamides **11-26** were synthesized from Ethyl 4-chloro-2-(methylthio) or Ethyl 4-chloro-2-(trifluoromethyl)pyrimidine-5-carboxylate **(ii)**.The classical Suzuki cross-coupling reaction of chloropyrimidine intermediates **(ii)** with 3,4-dimethoxyphenylboronic acid in the presence of tris(dibenzylideneacetone)dipalladium[0] and potassium fluoride under thermal heating provides the Ethyl 4-(3,4-dimethoxyphenyl)-2-(trifluoromethyl)pyrimidine-5-carboxylate or Ethyl 4-(3,4-dimethoxyphenyl)-2-(methylthio)pyrimidine-5-carboxylate (**Scheme 2**, **(vi)**) in good yields. The Suzuki cross-coupling reaction was optimized to get catecholopyrimidine compounds by following previously published procedure [70]. When we use 1.5 equivalent of 3,4-dimethylphenylboronic acid, intermediate **(vi)** was produced in 74% yield. This is followed by the ester hydrolysis of intermediates-**(vi)** with 1N NaOH in ethanol, providing the corresponding 4-(3,4-dimethoxyphenyl)pyrimidine-5-carboxylic acids

(**Scheme 2, (vii)**). Compounds **16** and **21** were synthesized from the oxidation of **13** and **20** by m-CPBA used as oxidant (**Scheme 5**).

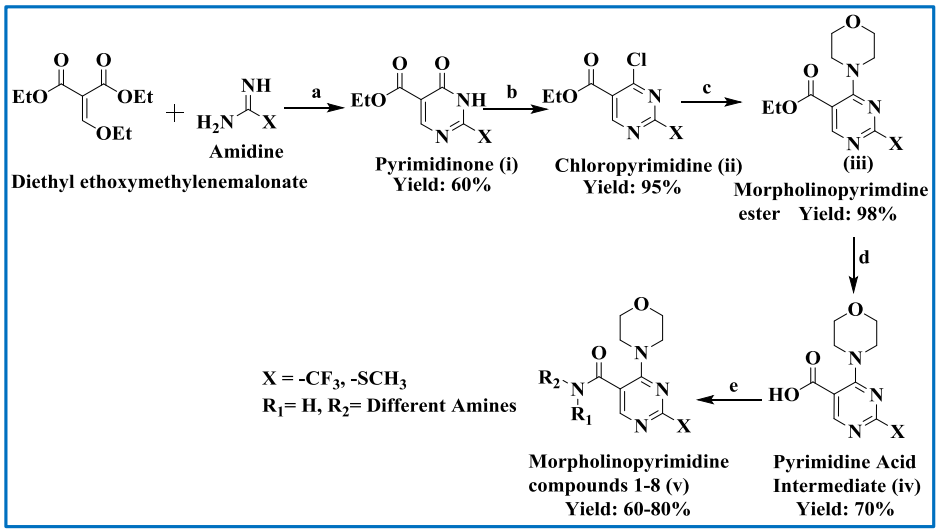

Scheme 1. General synthetic scheme: Synthesis of compounds 1-8. Reagents and conditions: (a) sodium ethoxide, EtOH, 78 ^{0}C, 8h; (b) $POCl_3$, 100^{0}C, 3h; (c) morpholine, DIPEA, 2-propanol, RT, 3 h; (d) 1N NaOH, EtOH, RT, 4h; (e) selected amines, EDCI, HOBt, DIPEA, DMF, RT or $(COCl)_2$, $DMF_{(cat)}$, DCM, 0^{0}C→RT.

The catecholopyrimidine compounds **11** and **18** were synthesized according to a previously reported procedure [46]. Briefly, the acid derivatives4-(3, 4-dimethoxyphenyl)-2-(methylthio or trifluoromethyl)pyrimidine-5-carboxylic

acid, **(iv)** or **(vii)** were activated using oxalylchloride to afford pyrimidine acid chlorides such as 4-(3,4-dimethoxyphenyl)-2-(trifluoromethyl or methylthio)pyrimidine-5-carbonyl chloride. This was followed by the reaction of *p*-nitrophenol, obtaining pyrimidinenitrophenol ester compounds, (4-nitrophenyl 4-(3,4-dimethoxyphenyl)-2-(trifluoromethyl or methylthio)pyrimidine-5-carboxylate) which were reacted with amino-3,5-dichloropyridine in the presence of sodium hydride as base at 0°C to obtain final products **11** and **18**. The synthetic scheme of compounds **11** and **18** were described in scheme 4. A library consisting of morpholino (**Scheme 1, (v)**) and catecholopyrimidine (**Scheme 2, (viii)**) carboxamides were prepared by treating corresponding acid intermediates (**(iv), (vii)**) respectively, with a variety of aromatic and aliphatic amines using solution-phase synthesis. The acid-amine coupling reaction was performed by either acid-activating agent EDCI with Hunig's base or the activation of acid intermediates by vilsmeier reaction. In the vilsmeier reaction, addition of oxalyl chloride and catalytic amount of DMF to the acid intermediate at 0^0C formed acid chloride by. Different substituted aromatic and aliphatic amines were then reacted to this to form the final product. The compounds' novelty was checked, and they were not present in any accessible academic database (e.g., PubChem, Scifinder). The structure and molecular weight of the compounds were

verified by NMR, IR, and ESI-mass spectroscopy. We further characterized the active compound **23** by 2D NMR (COSY, NOESY, HMBC, and HSQC) spectroscopy to assign all of the protons and carbons of compound **23**.

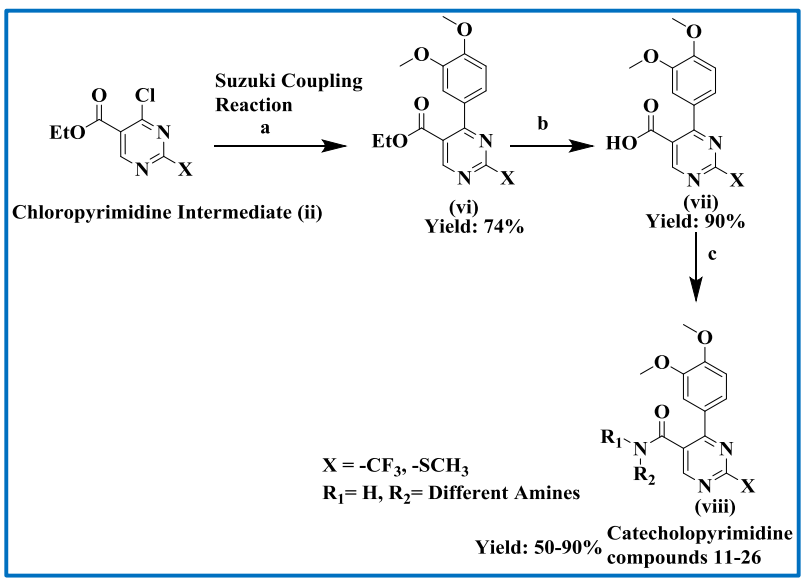

Scheme 2. General synthetic scheme: synthesis of compounds 11-26. Reagents and conditions: (a) 3,4-dimethoxyphenylboronic acid, $Pd_2(dba)_3$, $P(t\text{-}Bu)_3$, KF, THF (dry), 65^0C, 14h; (b) NaOH, EtOH, 6 h, reflux; (c) Amines, EDCI, HOBt, DIPEA, DMF or $(COCl)_2$, $DMF_{(cat)}$, DCM, $0^0C \rightarrow RT$.

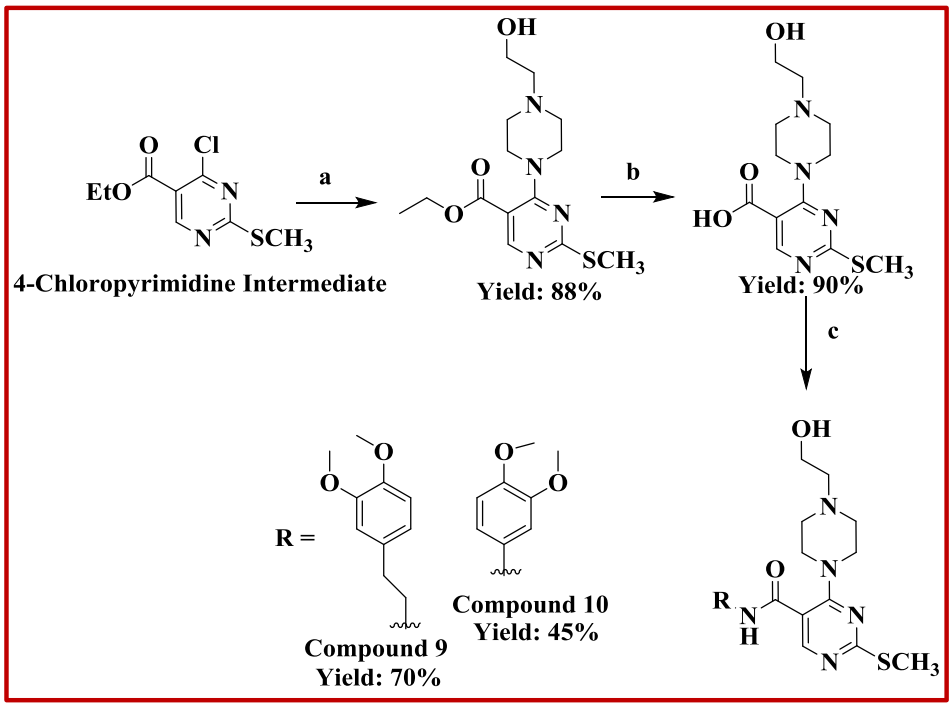

Scheme 3. Synthesis of compounds **9** and **10**. Reagents and conditions: (a) DIPEA, 2-propanol, RT; (b) NaOH, EtOH, 6 h, reflux; (c) Amines, EDCI, HOBt, DIPEA, DMF or $(COCl)_2$, $DMF_{(cat)}$, DCM, $0^0C \rightarrow RT$.

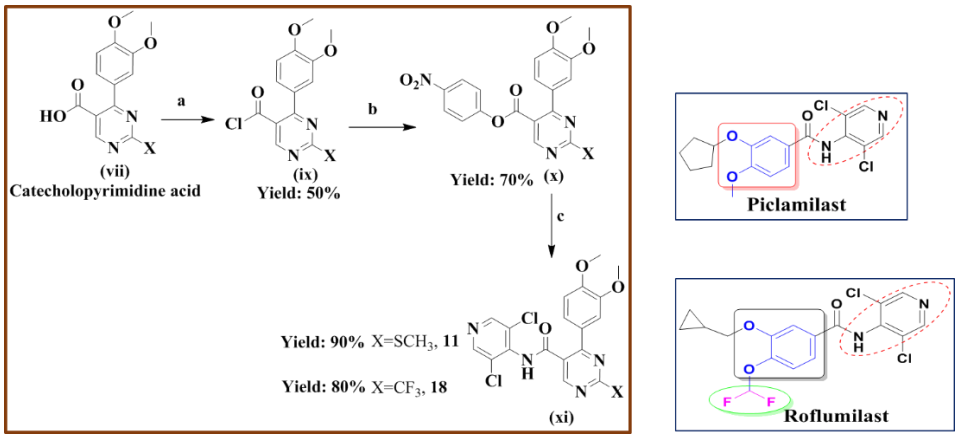

Scheme 4. Synthesis of compound **11** and **18**. Reagents and conditions: a) oxalyl chloride, dichloromethane, 0°C to RT; b) *p*-nitrophenol, dichloromethane, RT; c) amino-3,5-dicloropyridine, NaH, DMF, 0°C to RT.

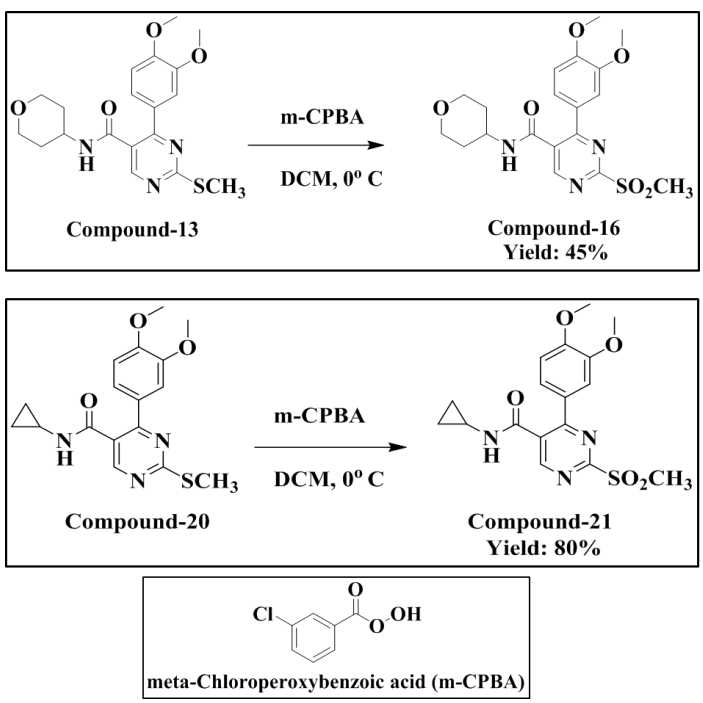

Scheme 5. Synthesis of compounds **16** and **21.**

2.3.2. In vitro PDE4 enzyme assay of synthesized compounds

The library of synthesized compounds was tested for dose-related PDE4B enzyme inhibition at different concentrations ranging from 1 nM–5000 nM using rolipram as a control drug. IC_{50} values for the compounds were calculated based on the molar concentration of PDE4B inhibitor required for 50% inhibition of the cAMP substrate into 5'AMP. We have studied the structure activity relationship (SAR) of the pyrimidine nucleus against PDE4B enzyme to get active compound (Figure 8). The different functional groups were substituted at 2, 4, and 5^{th}-positions of pyrimidine nucleus and their PDE4B inhibitory potential was evaluated. The main catechol (3, 4-dimethoxyphenyl) scaffold was functionalized with different substituents at the 4^{th}- and 5^{th}-positions of the $-CF_3$ or $-SCH_3$ functionalized pyrimidine nucleus to determine the precise molecular feature required for PDE4 inhibition. Firstly, we have introduced and fixed the morpholine ring to the 4^{th} position of the pyrimidine nucleus (i.e. morpholinopyrimidine). Then different aromatic amines were coupled at the 5^{th} position of the morpholinopyrimidine acid by EDCI coupling reaction to get morpholinopyrimidine carboxamides and interpreted their PDE4 inhibitory activity. In particular, the acid-amine coupling reaction of aromatic amine such as 3,4-dimethoxyphenyl (catechol) amine to the 2-(trifluoromethyl) or

2-(methylthio)-4-morpholinopyrimidine-5-carboxylic acid, significantly enhanced PDE4B inhibition activity (e.g., Compound **1, 5,** and **8**). We have introduced catechol moiety to the 4^{th} position of pyrimidine nucleus to improve the inhibitory activity of the compounds against PDE4B. Interestingly, the Suzuki coupling reaction of 3,4-dimethoxyphenylboronic acid at the 4^{th} position of the pyrimidine nucleus obtained catecholopyrimidine intermediate (**Scheme 2, (vii)**). Substitution of aromatic amine, such as 4-aminopyridines, to the catecholopyrimidine intermediate **(vii)** drastically increased PDE4B-inhibitory activity.

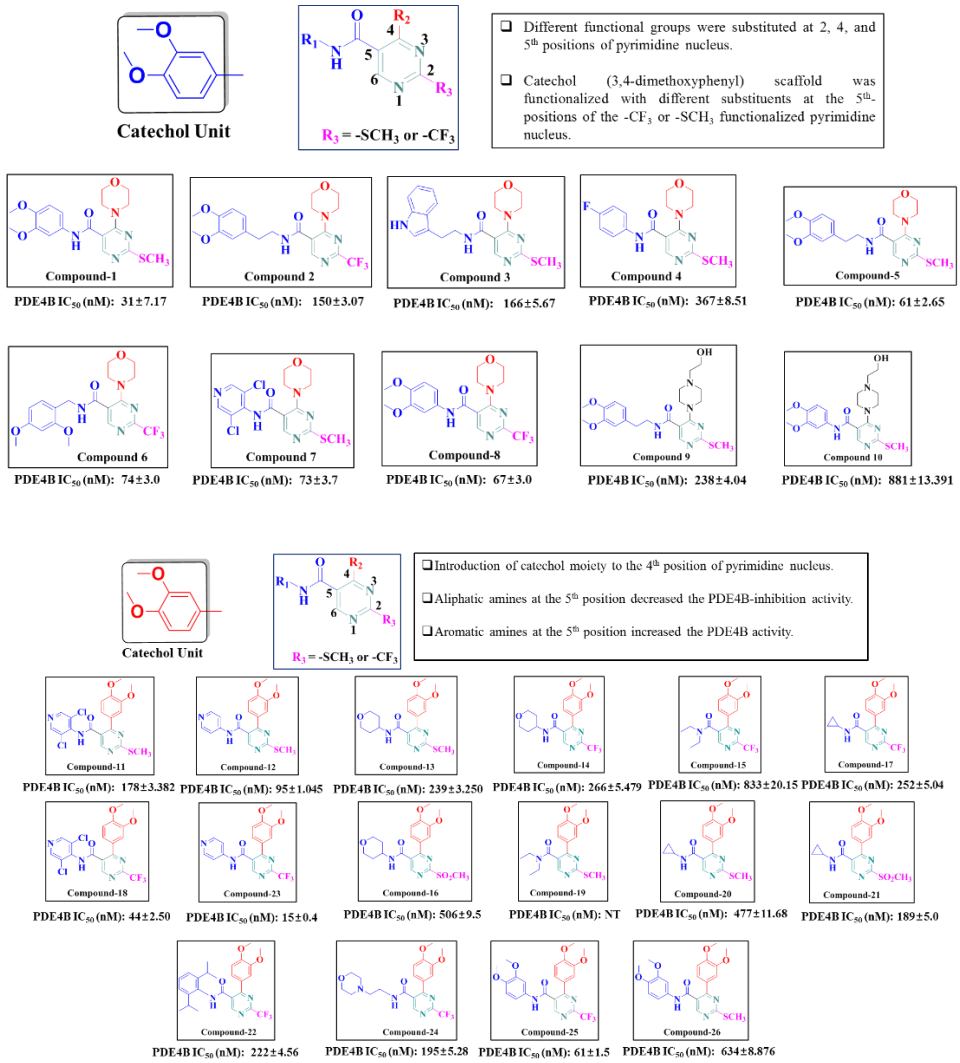

Figure 8. The structure activity relationship (SAR) of the pyrimidine nucleus against PDE4.

Table 2. Synthesized compounds and its PDE4B IC_{50} values

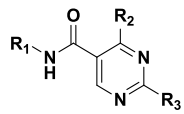

Compounds Number	R_1	R_2	R_3	*PDE4B* IC_{50}*(nM)*[a]
1	3,4-dimethoxyphenyl	Morpholine	$-SCH_3$	**31±7.17**
2	2-(3,4-dimethoxyphenyl)ethyl	Morpholine	$-CF_3$	150±3.07
3	2-(1H-indol-3-yl)ethyl	Morpholine	$-SCH_3$	166±5.67
4	4-fluorophenyl	Morpholine	$-SCH_3$	367±8.51
5	3,4-dimethoxyphenylethyl	Morpholine	$-SCH_3$	61±2.65
6	2,4-dimethoxyphenylmethyl	Morpholine	$-CF_3$	74±3.0
7	3,5-dichloro-4-pyridyl	Morpholine	$-SCH_3$	73±3.7
8	3,4-dimethoxyphenyl	Morpholine	$-CF_3$	67±3.0
9	2-(3,4-dimethoxyphenyl)ethyl	2-(piperazin-1-yl)ethan-1-ol	$-SCH_3$	238±4.046
10	3,4-dimethoxyphenyl	2-(piperazin-1-yl)ethan-1-ol	$-SCH_3$	881±13.391
11	3,5-dichloro-4-pyridinyl	3,4-dimethoxyphenyl	$-SCH_3$	178±3.382
12	4-pyridinyl	3,4-dimethoxyphenyl	$-SCH_3$	95±1.045
13	4-tetrahydropyranyl	3,4-dimethoxyphenyl	$-SCH_3$	239±3.250
14	4-tetrahydropyranyl	3,4-dimethoxyphenyl	$-CF_3$	266±5.479
15	N,N-diethyl	3,4-dimethoxyphenyl	$-CF_3$	833±20.15
16	4-tetrahydropyranyl	3,4-dimethoxyphenyl	$-SO_2CH_3$	506±9.5
17	cyclopropyl	3,4-dimethoxyphenyl	$-CF_3$	252±5.04
18	3,5-dichloro-4-pyridinyl	3,4-dimethoxyphenyl	$-CF_3$	44±2.50
19	N,N-diethyl	3,4-dimethoxyphenyl	$-SCH_3$	NT[b]
20	cyclopropyl	3,4-dimethoxyphenyl	$-SCH_3$	477±11.68
21	cyclopropyl	3,4-dimethoxyphenyl	$-SO_2CH_3$	189±5.0
22	2,6-diisopropylaniline	3,4-dimethoxyphenyl	$-CF_3$	222±4.56
23	4-pyridinyl	3,4-dimethoxyphenyl	$-CF_3$	**15±0.4**
24	2-morpholinoethanyl	3,4-dimethoxyphenyl	$-CF_3$	195±5.28
25	3,4-dimethoxyphenyl	3,4-dimethoxyphenyl	$-CF_3$	61±1.5
26	3,4-dimethoxyphenyl	3,4-dimethoxyphenyl	$-SCH_3$	634±8.876
Rolipram (μM)	-	-	-	1.27±0.05

[a] Data reported are the mean of three independent experiments. [b]NT = not tested.

Remarkably, the compounds (e.g., Compound **18**, **23**, and **25**) bearing a catechol moiety to the 4th position of the pyrimidine nucleus exhibited excellent PDE4 inhibitory ability, compared to that of catechol moiety substituted at the 5th position. This was also observed in the results of4-aminopyridine-substituted at 5th position of pyrimidine acid intermediates (e.g., **7**, **12**, **18**, and **23)** (See Table 2). However, coupling of aliphatic amines at the 5th position of 4-(3, 4-dimethoxyphenyl)-2-(methylthio) pyrimidine-5-carboxylic acid decreased the PDE4B-inhibition activity (e.g. **15** and **17**). The compound **23** showed fifty-five time's higher activity than compound **15**, this modification reveals that the catechol moiety is ideal and required for PDE4B inhibition activity. Generally, the -CF_3 functionalization to the 2nd position of the pyrimidine nucleus exhibited better PDE4B activity (compounds **6, 8, 18, 23,** and **25**) compared with thiomethyl (-SCH_3) substituted compounds. In conclusion, catechol-pyrimidine based small molecules **1**, **5**, **8**, **18**, **23**, and **25** exhibited excellent PDE4B inhibitory activity, with IC_{50} values in the nanomolar range. In particular, the IC_{50} values of compound **1** and **23** are 31±7.17nM and 15±0.4 nM, respectively. Table 2 shows the IC_{50} values of synthesized small molecule inhibitors. Further to find whether the most active compounds **1, 5, 8, 18** and **23** possess the selectivity against PDE4B, enzyme inhibition assay against PDE1A, PDE3B, PDE11A, and all the

isoforms of PDE4 enzyme (PDE4A, B, C, and D) was performed. Result depicted in Table-2 showed that catechol at the 4th position of pyrimidine nucleus has more preference for PDE4 enzyme over other PDEs (PDE1A, PDE3B and PDE11A). For example, the compound **23** selectively inhibited the PDE4B compared to the other PDEs and PDE4 iso-enzymes, and up to several fold higher PDE4B inhibitory activity than rolipram. The dose dependent inhibition of PDE4 isoenzymes and other PDEs by compound **23** are shown in Figure.9. Compound **23** showed seven-fold higher selectivity towards PDE4B compared to the PDE4D. However, the compounds **1** and **8** bearing a 3,4-dimethoxyphenyl (catechol) group at the 5th position of pyrimidine core showed low selectivity for PDE4B over PDE1A, PDE3B and PDE11A (Table 3).

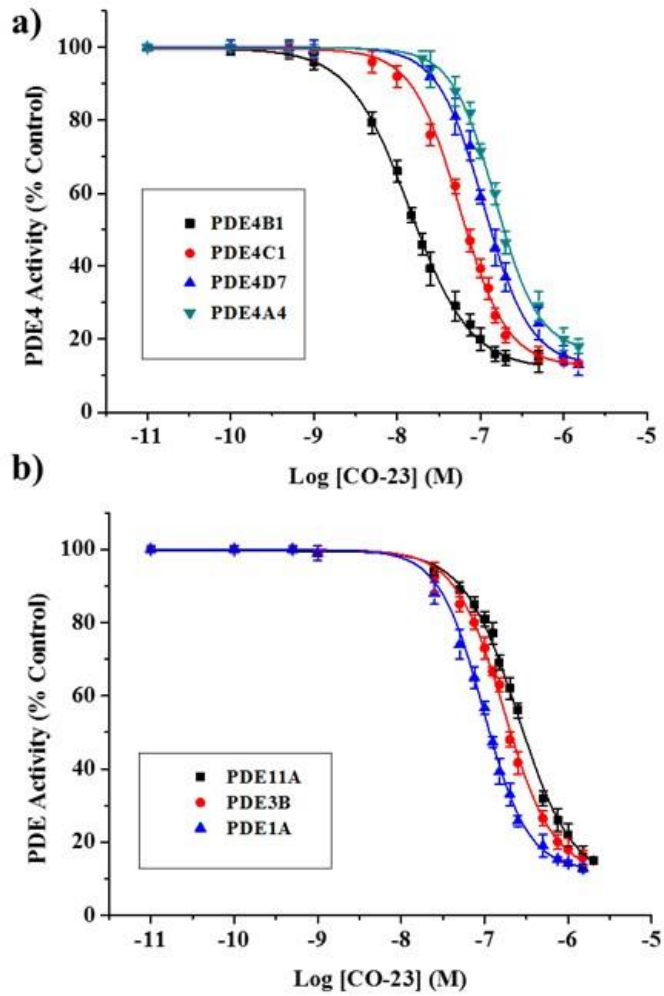

Figure 9. (a) Dose dependent inhibition of PDE4 isoenzymes activity by compound **23**. (b) Dose dependent inhibition of PDE11A, PDE3B, and PDE1A by compound **23**. Values were compared with control. (mean±SD; n=3).

Table 3. The IC_{50} values of selected compounds on various PDEs.

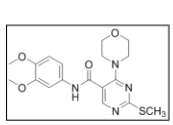
Compound 1

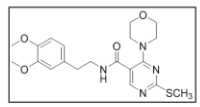
Compound 5

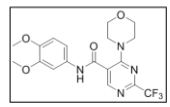
Compound 8

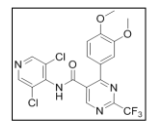
Compound 18

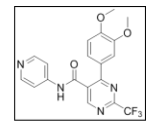
Compound 23

	PDEs, IC_{50}(nM)[a]						
Compounds	**PDE1A**	**PDE3B**	**PDE11A**	**PDE4A4**	**PDE4B1**	**PDE4C1**	**PDE4D7**
1	756±58.98	800±45.78	480±35.07	45±3.54	31±7.17	77±8.8	220±16.3
5	NT[b]	NT[b]	659±12.40	284±3.60	61±2.65	326±5.60	136±8.70
8	678±5.0	950±1.5	1500±6.4	100±4.6	67±3.0	156±7.65	385±2.30
18	281±10.60	321±7.50	245±9.0	89±2.80	44±2.50	39±4.45	360±1.50
23	98± 8.45	169±3.78	250±8.56	152±1.33	15± 0.4	57±4.87	108±3.78
Rolipram (IC_{50}, µM)	NT[b]	NT[b]	NT[b]	1.95±0.25	1.27±0.05	1.68±0.10	1.05±0.30

[a]Data reported are the mean of three independent experiments.

[b] NT = not tested.

2.3.3. Molecular docking study of active compound 23

A molecular docking study was performed in order to obtain further insight into the binding modes of the most active compound **23** into the cAMP binding site of PDE4A, B, C and D enzymes. The reference compound rolipram, a well-known inhibitor of PDE4, was also docked with PDE4B to compare with compound **23** (Figure 10 and 11). PDEs are mainly constituted of three domains: An N-terminal regulatory domain, a catalytic domain, and a C-terminal domain. The most conserved catalytic domain usually consists of 17 α-helices [72-74] and forms a deep pocket located at the junction of the three subdomains. It consists of a metal binding pocket (M pocket) containing bivalent (Zn^{2+}, Mg^{2+}) metals which form a complex with phosphate moiety of cAMP, and a (Q pocket) containing glutamine, which forms hydrogen bonds with the nucleotide moiety of cAMP and a solvent pocket (S pocket). The crystal structure of the 3,4-dialkoxyphenyl (catechol) functionalized compounds bound to PDE4B active site has revealed that the hydrophobic interactions with residues in the M pocket and Q pocket are very important for their PDE4 inhibition activity [75]. Molecular docking of compound **23** and reference compound rolipram were performed on a binding model based on the PDE4B crystal structure (PDB: 1F0J) by the CDOCKER protocol. The docking score of compound **23** and rolipram were -4.10 and -3.31,

respectively. This computer simulated docking scores support the affinity and biological activity of the compound **23**. The 3D optimal conformation and schematic 2D diagram of compound **23** and rolipram in the PDE4B active site and the corresponding amino acids responsible for all of the major interactions are shown in Figure 10. From the docking study it has been shown that the amino acid residues which are mostly responsible for binding with cAMP in PDE4B (Asp 392, Ile 410, Tyr 233, Cys 499) are present in both compound **23** as well as in rolipram. However, compound **23** shows more binding interaction with other amino acid residues (Phe 414, Pro 396, Leu 393 His 234, Thr 345) which constitute strong affinity. From these interactions it is confirmed that compound **23** is deeply embedded into the active site of PDE4B than rolipram. From the docking result, it can be seen that the fluorine molecule (-CF_3, F_a) within 3.23 Å of Gln 500 generates a strong halogen bond, and another fluorine atom (-CF_3, F_b) forms a strong halogen bond with His 234 within 3.71 Å. The –CF_3 group in compound **23** itself exhibits a very important hydrophobic interaction with His 234 and Phe 414 residue (Phe 414 is highly conserved among PDE family). The -CF_3 group which has tremendous influence in medicinal chemistry is absent and responsible for very limited interaction in the reference compound rolipram compared to compound **23**. In halogen bonding, a fluorine atom is the donor

and can establish conventional hydrogen bonding and other halogen bonds, with the protein molecule providing additional stability. The $–CF_3$ group on an aryl system increases lipophilicity, whereas fluorination of saturated alkyl groups results in decreased lipophilicity [76]. The $-CF_3$ group also polarizes the compound and increases the positive intermolecular interaction between the receptor and fluorine atom [77]. The halogen bonds between fluorine atom of the $–CF_3$ group with Gln 500 and His 234 constitute important parameter to the PDE4 inhibition. This was also in agreement with PDE4B enzyme assay. In contrast to the binding mode of rolipram, it is observed that Asp 346 forms a strong hydrogen bond with catechol methoxy group with the distance 3.22 Å, and Pro 396 forms another strong–hydrogen bond with pyridine nitrogen with the distance 3.69 Å in compound **23**. These seem to be the reason for the stability and improvement of the biological activity and selectivity within the binding pocket of the target protein PDE4B (Figure 10a and 10b). The hydrophobic interactions are also superior in compound **23** compared to the reference compound rolipram in the hydrophobic pocket. The other two hydrogen bonds with Glu 304 and Asp 346 are also vital for the stabilization of the binding mode. On the other hand, Leu 393, His 234, Phe 414, and Met 347 form strong hydrophobic interactions with ligand atoms (compound **23**), making the ligand more stable in the hydrophobic pocket of

the protein (Figure. 10a and 10b). The hydrophobic interactions constitute critically important structural parameters, and exhibit a direct correlation with binding free energy in the thermodynamics of the protein-ligand interaction. The interactions between the ligand and the hydrophobic side chains of the protein molecule contribute significantly to the binding free energy in a receptor ligand association [78, 79]. The hydrophobic residues in the protein molecule usually repel water and other polar groups, thereby increasing a net attraction of non-polar groups of the ligand [80]. Hydrophobic amino acid residue, such as phenyl alanine, serves to affix the ligand within the active site of PDE4B. In addition, the aromatic ring of phenyl alanine in PDE4B may also participate in the stacking interaction with the aromatic moieties of the ligand. The Figure. 12 results also suggest that the compound is deeply embedded into the active site of PDE4B. We also successfully docked compound **23** with PDE4 A, C, and D enzymes with respective PDB ID 2QYK, 2QYM, and 3G4K to validate the selectivity of our synthesized compound **23** towards these enzymes with the docking score -8.85, -4.26, and -7.06. In all cases, however, interactions of compound **23** with these PDE4 subtypes were limited (Figure 12). The 3D optimal conformation of compound **23** in the active site of PDE4 A, C, and D and their comparative study of all major interactions are shown in Figure.12. From these

computational studies, we have confirmed that the compound **23** is selective towards PDE4B. Thus, compound **23** could constitute a potential inhibitor of PDE4B with potent anti-inflammatory activity.

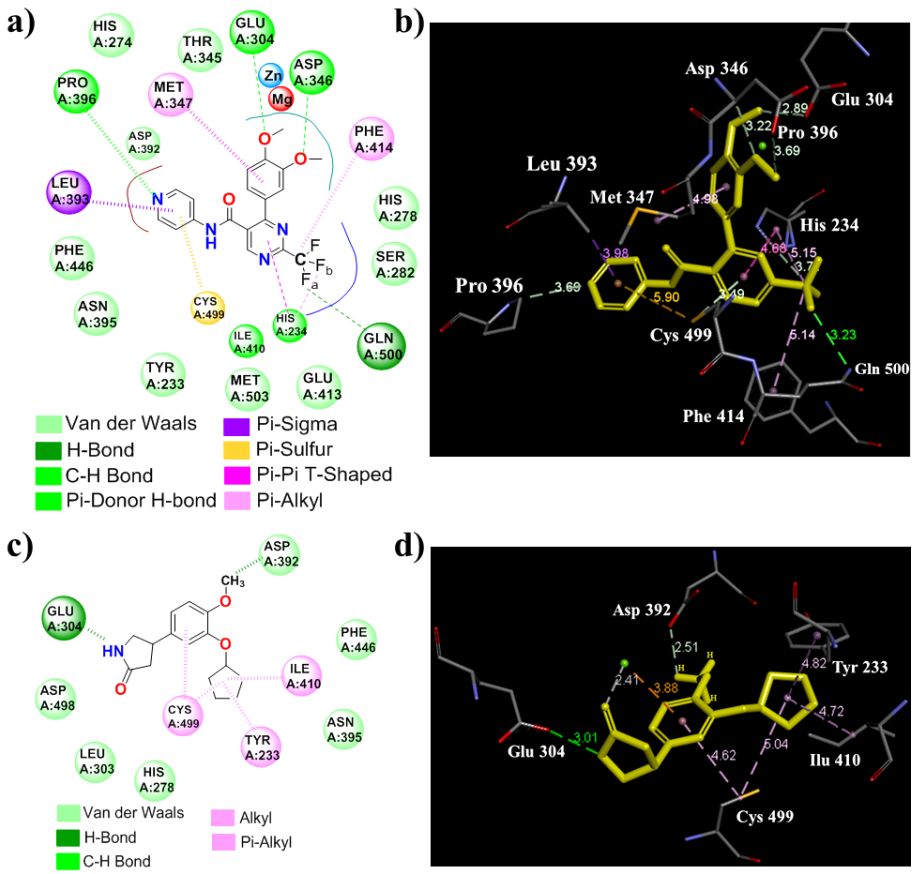

Figure 10. Binding mode of compound **23** and rolipram in the catalytic domain of PDE4B. Schematic 2D and 3D diagram of compound **23** (a, b) and rolipram (c, d) in catalytic pocket of PDE4B. (Compound **23** and rolipram are colored in yellow in 3D diagram (b, d)).

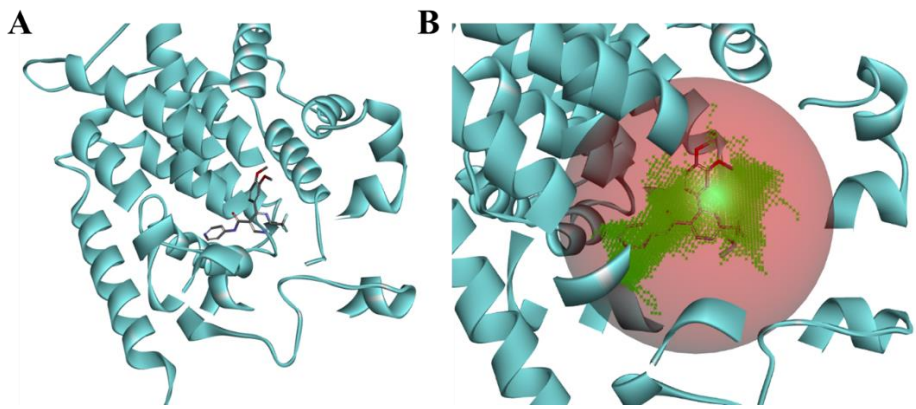

Figure 11. Binding mode between the compound **23** and PDE4B catalytic binding site.

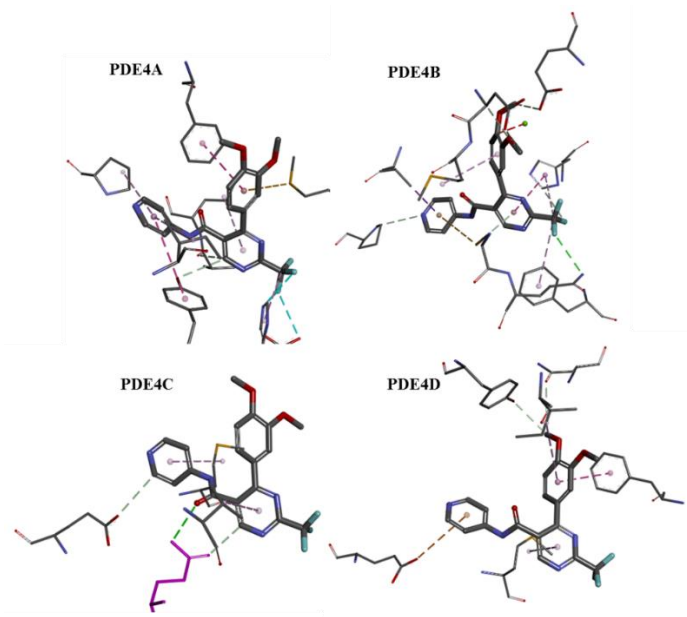

Figure 12. Molecular docking of compound **23** with PDE4 A, B, C, and D enzymes.

2.3.4. X-ray crystal structure of active compound 23

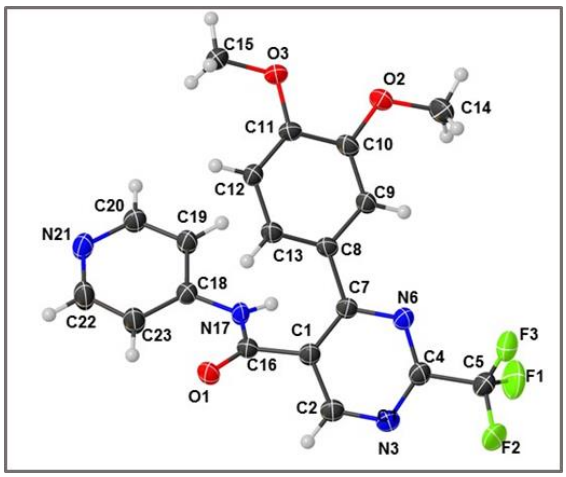

Figure 13. The ORTEP diagram of compound **23**. Ellipsoids are drawn at 50% probability level.

Crystallization of compound **23** was attempted by using different solvent systems through changing the polarity, boiling point, and temperature conditions (0˚-30˚C). Finally, single crystals of compound **23** were obtained by slow evaporation of chloroform and hexane solvent mixture in 1:1 volume ratio at 4˚C. Compound **23** crystallized in the monoclinic form with space group $P2_1/n$. All C-C bond lengths in the structure are almost similar (~ 1.3 to 1.4Å), except amide carbon (C16, 1.50 Å) and $–CF_3$ carbon (C5, 1.51 Å), and are typical sp^2 hybridized carbon-carbon bonds. Unfavorable H-H, N-H, and O-H interactions are not found within the molecule. The aminopyridine

ring in compound **23** is bifurcated by C1 and C16 through amide bond (C16, N17, and O1), and orient near perpendicularly to the pyrimidine nucleus. The bond lengths and bond angles of the fluorine atoms attached to carbon in the $–CF_3$ group are almost similar (F1, F2, F3 ~1.3Å and 107°). The planes of catechol moiety attached to pyrimidine nucleus (i.e., catecholopyrimidine) were slightly twisted by 123°and 117° dihedral angle (C1-C7-C8 and N6-C7-C8), which may be due to two methoxy groups attached in C11 and C10 position in the catechol structure. The ORTEP representation of compound **23** is shown in Figure 13, and the solvent is omitted for clarity. The crystal data for compound **23** shown in table 3.

2.4. The in vivo animal study of active compounds 1 and 23

2.4.1. Compound 23 treatment alleviates AD-like symptoms in BALB/c mice

Based on the IC_{50} values and the molecular docking analysis, compound **23** was chosen for *in vivo* analysis. DNCB was used to induce AD-like symptoms on the dorsal skin of Balb/c mice (Figure. 14A). AD-like skin features were confirmed by evaluating the dryness of the skin, erosion, erythema, and hemorrhage. AD symptoms was progressively increased in response to the periodic doses of DNCB in Balb-c mice. The compound **23** treatment clearly

reversed these DNCB-induced AD symptoms in experimental mice (Figure. 14A). To evaluate the degree of clinical response to the inhibitor treatment, dermatitis score was calculated. Skin features of dermatitis, such as erythema/hemorrhage, edema, excoriation/erosion, and scaling/dryness were considered in the evaluation. Dermatitis scores were significantly very high and progressive in DNCB treated mice as compared to the control group of mice ($p<0.001$). However, topical application of compound **23** daily once to the AD-induced mice remarkably relieved the mice from the AD like symptoms. The dermatitis score significantly reversed after the second week of drug treatment compared to the DNCB-alone treated mice (Figure. 14B and 14C). Itching is the major clinical outcome in AD. Scratching frequency was monitored to determine the efficacy of the synthesized compounds against itching behavior in the experimental mice. The observed results clearly indicated that the DNCB-induced scratching frequency was significantly reduced in compound **23** ($p<0.01$) treated AD-induced experimental mice (Figure. 14D).

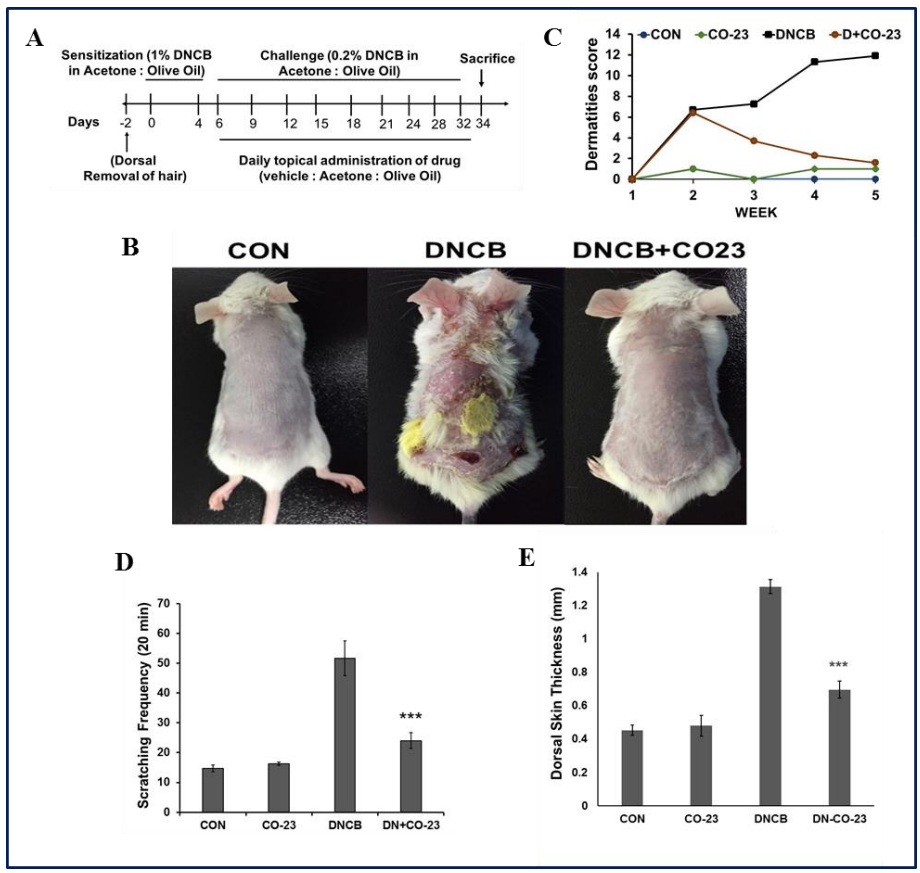

Figure 14. (A) Experimental scheme for the DNCB-induced AD model in Balb/c mice. (B) Image represent the AD in experimental groups, which were taken before sacrifice. (C) Epidermal skin score of compound 23 (CO-23) treated AD induced mice were compared with control and DNCB-treated mice. (D) Scratching frequency in experimental animals. (E) Epidermal thickness of the dorsal skin of experimental mice. Data represent the mean ± SEM (n=6). *** $p < 0.001$ vs. DNCB.

2.4.2. Histological observation of compound 23 treated BALB/c mice

Physical features of the skin of experimental mice were carefully examined. Marked hypertrophy and edematous features were observed in the skin of the DNCB-treated mice. In contrast, skin features of compound **23** treated atopic mice exhibited less hypertrophy and no signs of edema compared to the DNCB-treated mice. Compound **23** alone treated mice exhibited normal skin feature, no sign of allergy was observed. Furthermore, significantly increased dorsal skin thickness was observed in DNCB-treated mice (1.19 mm, $p<0.001$) as compared to that of the control group (0.45 mm). Treatment of compound **23** (0.71 mm, $p<0.01$) markedly reduced the DNCB-induced dorsal skin thickness (Figure. 14E). Histopathological observation of tissue sections obtained from the experimental mice of control, compound **23** alone treated mice shows normal skin architecture. However, dorsal skin of the DNCB–treated experimental mice exhibited severe epidermal hyperplasia, (acanthosis) hyperkeratosis, and dense infiltration of inflammatory cells into both the epidermal and dermal region of the skin. Treatment of compound **23** significantly reversed the DNCB-induced alterations. H&E stained sections of DNCB-induced mice showed thickened epidermis compared to the control groups. However, reduced epidermal thickness was observed in compound

23-treated AD-induced mice, as compared to the DNCB-alone treated mice (Figure. 15A).

2.4.3. Compound 23 treatment suppress the inflammatory mediators

Serum IgE level is directly co-related to the severity of AD. IgE is crucially involved in the activation of mast cell and subsequently the secretion of pruritus factor such as histamine and prostaglandins. Moreover, activated mast cell releases chemokines and cytokines such as IL-4, IL-13, and TNF-α which collectively promote the mobilization and sensitization of Th2 cells [81, 82]. The observed result in the present study show that serum IgE level in the DNCB-treated mice were significantly increased ($p<0.001$), as compared to the normal and drug control mice. However, the DNCB-induced Immunoglobulin-E (Ig-E) synthesis was significantly reduced in the compound **23** ($p<0.001$) treated mice (Figure. 15B). Reduced levels of serum IgE can be co-related to the reduced scratching behavior among the compound **23** treated AD affected mice. Similarly, pro-inflammatory mediator, TNF-α level was also measured in the tissue extracts of experimental mice. The observed result show that compound **23** treatment significantly reduced the DNCB–induced TNF-α levels in the experimental mice (Figure. 15C). Suppression of TNF-α is highly beneficial in the

treatment AD since the TNF-α is a well-known activator of pro-inflammatory transcription factor NF-kB in lymphocytes.

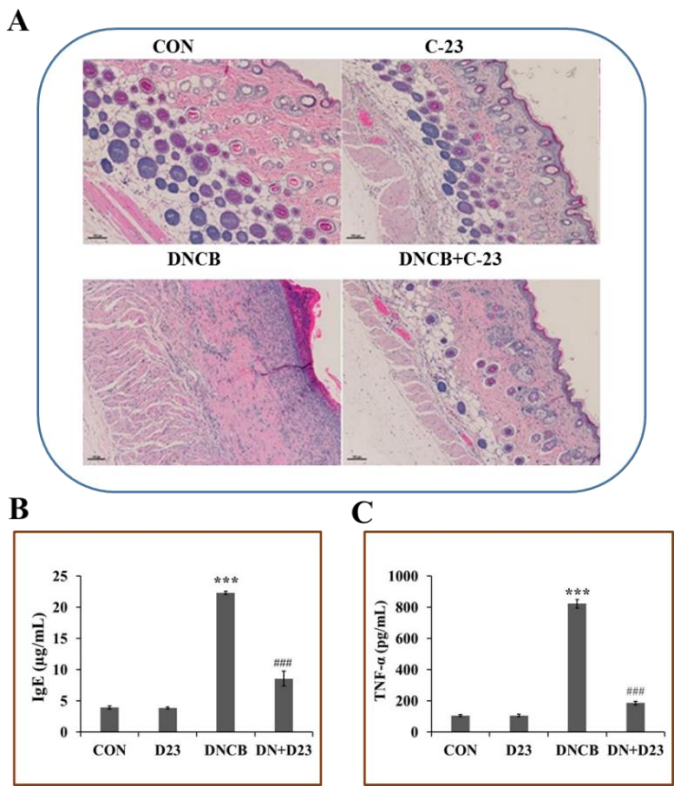

Figure 15. (A) H&E staining of dorsal skin of experimental animals (scale bar =100 μm; magnification: x 400). (B) Bar graph represent the serum IgE and (C) the tissue TNF-α levels in control, DNCB, compound **23** (D23) and DNCB+compound **23** co-treated experimental mice. Data represent the mean ± SEM (n=6). * p < 0.5 ,*** p < .001 vs. control; # p < 0.5, ## p < 0.01 vs. DNCB.

2.4.4. Compounds 1 and 23 alleviates AD-like Symptoms in NC/Nga Mice

Figure 16A shows the structure of compound **1** and **23**. Scheme used to develop AD-like symptoms in NC/Nga mice is depicted in Figure 16C. All the experimental mice exhibited AD-like skin features after sensitization with 1% DNCB. AD-like symptoms such as itching, dry skin, erythema and hemorrhage were progressively accumulated in DNCB treated mice. Compounds **1** and **23** treated AD induced mice showed reduced levels of erythema and hemorrhage and dry skin compared to DNCB alone induced mice. Compounds **1** and **23** alone treated mice exhibited normal skin feature, no sign of allergy was observed (Figure 16B). Efficacy of the drug was analyzed through dermatitis score. Dermatitis scores were significantly very high and progressive in DNCB-alone treated mice as compared to the control group of mice ($p<0.001$). A significant reduction ($p<0.01$) in dermatitis score was observed after the third and second week, respectively for the compounds **1** and **23** treatments (Figure 17A and 17B). Scratching frequency was observed to monitor the itching behavior of the experimental mice. Compounds **1** and **2** treatments significantly ($p<0.01$) inhibited the DNCB – induced itching sensation in the experimental mice group (Figure 17C). At the end of the experiment, dorsal skin was peeled off and the skin thickness was measured. A pronounced increase in the dorsal skin thickness was

observed (1.19 mm, $p<0.001$) in DNCB-treated mice as compared to that of the control group (0.45 mm). Skin thickness of 0.78 mm and 0.64 mm were observed in compounds **1** and **23** treated experimental mice (Figure 17D). During inflammatory stress, lymph node size will increase. We observed a significant increase in the size and weight of the subiliac lymph node in DNCB-alone treated mice, as compared to the control mice. The size and weight of the lymph node are drastically reduced in both compounds **1** and **23** treated DNCB-induced mice, as compared to the DNCB-alone treated mice (Figure 18A and 18B). In addition, spleen weight was measured to assess the general health and immunological status of mice. It was found that topical application of DNCB markedly alters spleen weight, as compared to the vehicle alone-treated and drug-alone treated mice ($p<0.001$). However, compounds **1** and **23**-treated atopic mice exhibited significantly reduced spleen weight ($p<0.5$), as compared to that of DNCB-alone treated mice (Figure 18C).

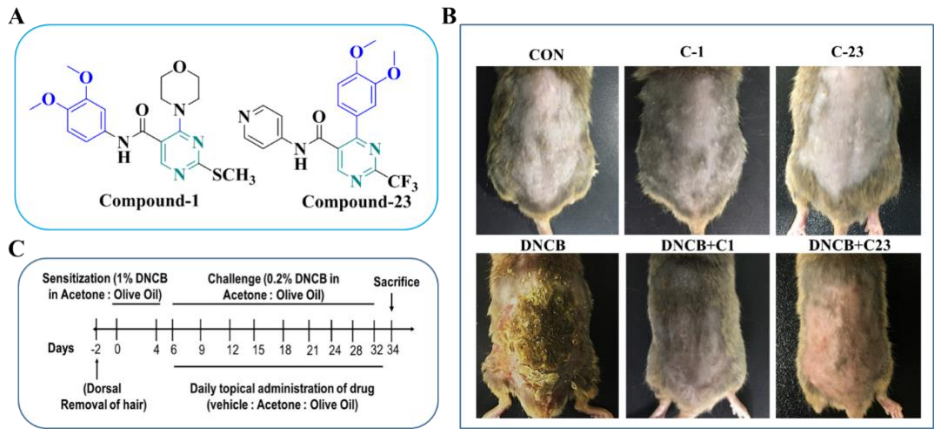

Figure 16. (A) Structure of compound **1** and compound **23.** (B) Experimental scheme for the DNCB-induced AD model. On day 0 and day 4, the mice were sensitized with 150 µL of 1% DNCB or vehicle at their shaved back. From day 6 onwards 150 µL of 0.2% of DNCB or vehicle was applied to challenge the dorsal skin twice-a-week for 4weeks. Atopic dermatitis-induced mice were co-treated with either compound-**1** or compound-**23** once daily from day six onwards until the end of the experiments. (C) Image represent the AD in experimental groups, which were taken before sacrifice. (Con- Control; C1- Compound **1**; C23- compound **23**; D+C1- DNCB+ Compound **1**; D+C23- DNCB+ Compound **23**).

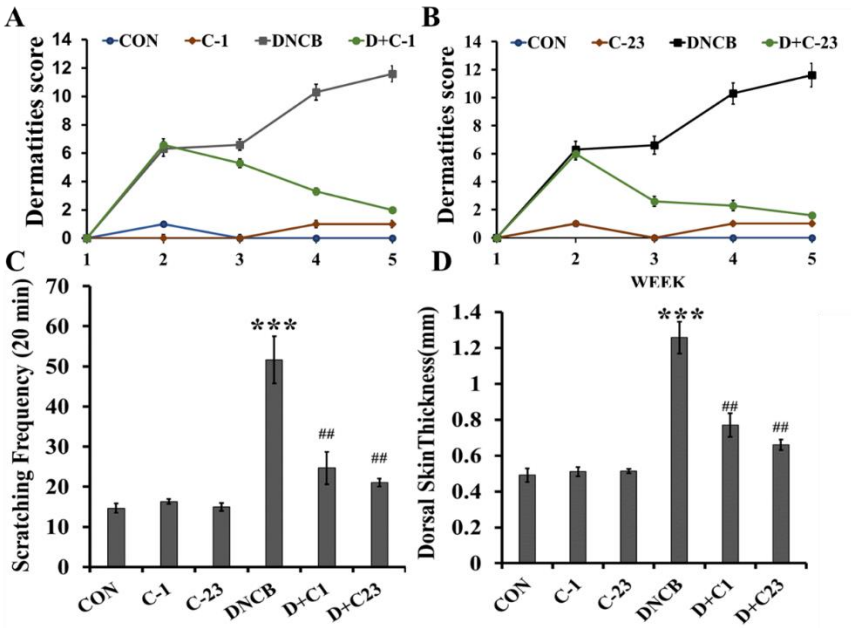

Figure 17. (A, B) Clinical skin severity was assessed through the epidermal skin score. Criteria for the skin score was described in materials and method. Epidermal skin score of compound **1** and **23** treated AD induced mice were compared with control and DNCB-treated mice. (C) Scratching frequency in experimental animals. The frequency of scratching around the dorsal skin lesions, and nose was counted during a 20-minute period. Scratching frequency was measured once-a-week for five weeks. (D) Thickness of the dorsal skin of experimental mice.

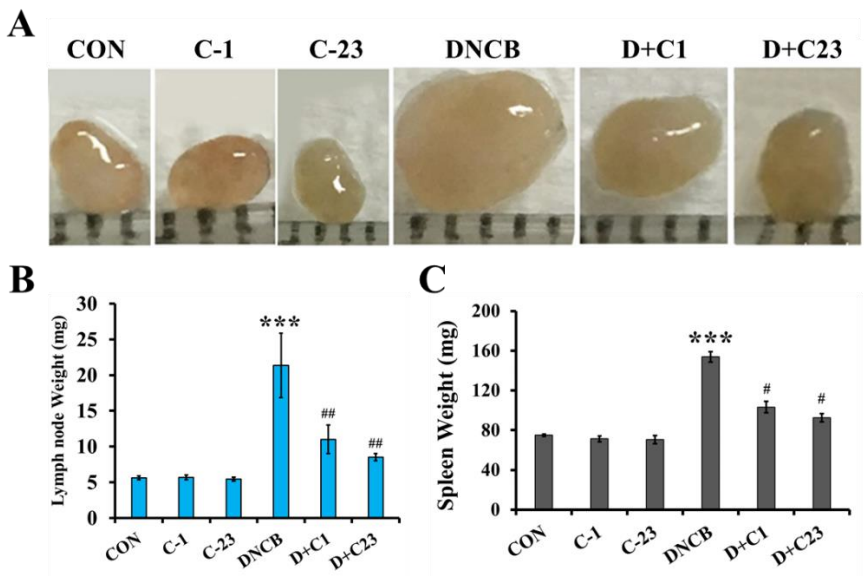

Figure 18. (A) Subiliac lymph node size. (B) Subiliac lymph node weight. (C) Spleen weight in experimental animals. (Con- Control; C1- Compound **1**; C23- compound **23**; D+C1- DNCB+ Compound 1; D+C23- DNCB+ Compound **23**). Data represent the mean ± SEM (n=6). *** p>0.001 vs. control; # p>0.5, ## p>0.01 vs. DNCB.

2.4.5. Histological observation of the NC/Nga mice skin

H&E stained sections indicate dense infiltration of inflammatory cells into both epidermis and dermis region in DNCB–treated mice. In contrast, reduced levels of inflammatory cells were observed in compound **1** and **23** treated atopic mice. In addition, reduced epidermal thickening was observed in compounds **1** and **23** treated atopic mice as compared to the DNCB-alone treated mice (Figure 19A). Immunohistochemical staining of CD4+ T cells revealed increased infiltration of CD4+ T cells in the DNCB-treated mice, as compared to the control, drug control, and treatment group of mice (Figure 19B). Similarly, increased levels of mast cell infiltration were observed in the epidermis region of DNCB-treated mice (97 ± 10.58, $p \leq 0.001$), as compared to the control group (13 ± 2). However, significantly decreased mast cell infiltration was observed in compound **1** (56 ± 11, $p \leq 0.01$) and compound **23** (29.41 ± 6, $p \leq 0.001$) treated atopic mice (Figure. 20A and 20B). IgE plays a key role in the degranulation of mast cell. Serum IgE level in the DNCB-treated mice was significantly increased (seven-fold, $p<0.001$), as compared to the normal and drug control mice. However, the DNCB-induced synthesis of IgE was significantly reduced in the compound **1** ($p<0.01$) and compound **23** ($p<0.01$) treated mice (Figure. 20C).

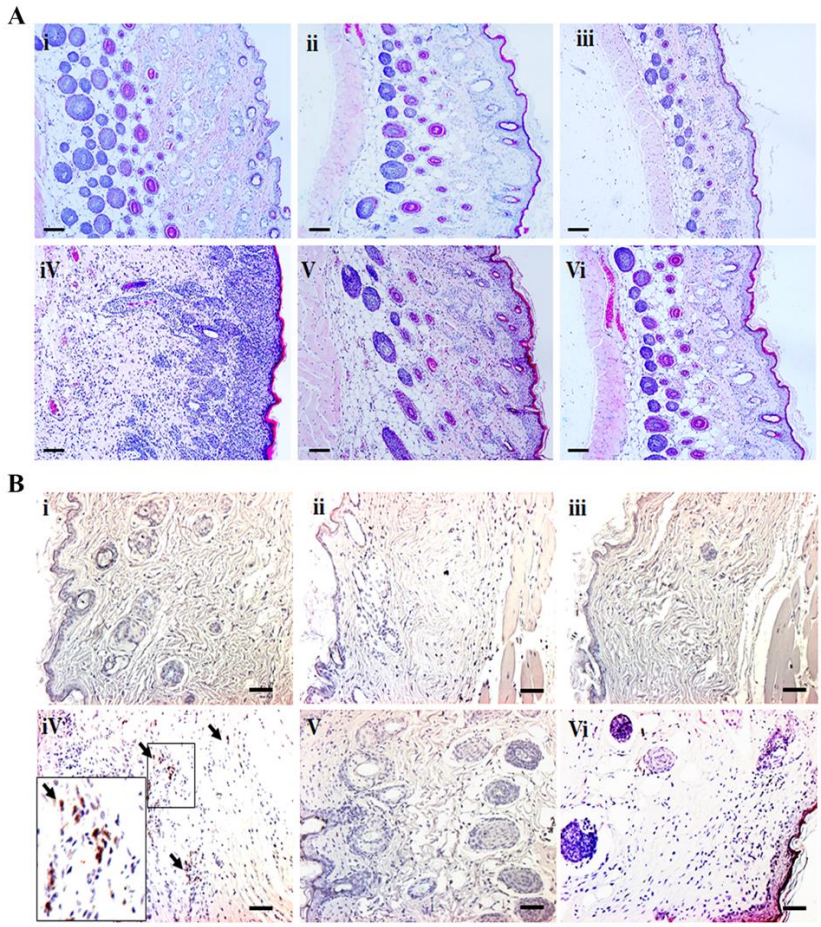

Figure 19. (A) H&E staining of dorsal skin of experimental animals (scale bar =100 μm; magnification: x 400). (B) Representative images depicting the immunohistochemical staining of CD4+ cells. The arrows indicate CD4+ cells. (i- Control, ii- Compound **1** alone, iii- Compound **23** alone, iv- DNCB, v- DNCB+Compound **1**, vi- DNCB+ Compound **23**)

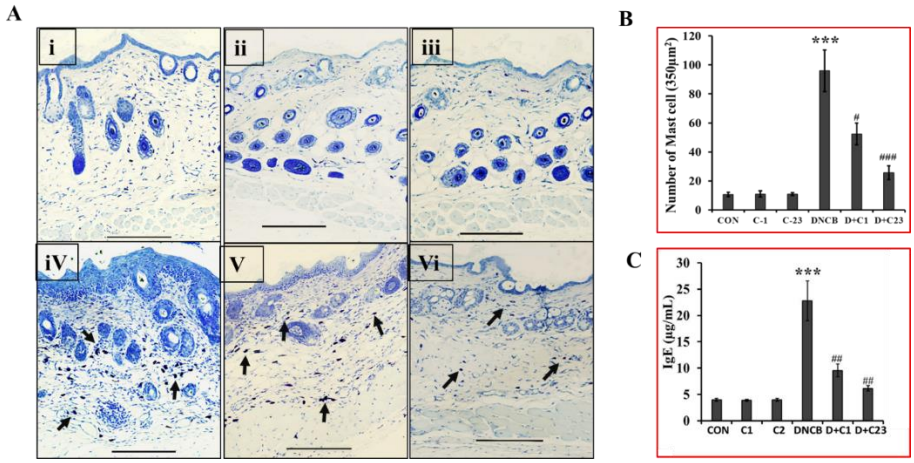

Figure 20. (A) Toluidine blue staining of mast cells. The arrows indicate mast cells. (B) Bar graph represent the number of mast cells counted per 350µm^2 at a magnification of x 400 in the epidermis region were counted. (C) Serum IgE (i- Control, ii- Compound **1** alone, iii- Compound **23** alone, iv- DNCB, v- DNCB+Compound **1**, vi- DNCB+ Compound **23**) Data represent the mean ± SEM (n=3). *** p>.001 vs. control; # p>0.5, ## p>0.01 vs. DNCB.

2.4.6. PDE4B Inhibitors Improves Intracellular cAMP Levels in Macrophage

The macrophage cell line, Raw 264.7 was pre-treated with compounds**1** and **23** and then induced with lipopolysaccharide (LPS). The observed result in figure 21A shows that cAMP levels were not significantly differed between control and LPS treated cells. However, cells treated with compounds**1** and **23** significantly improved the intracellular levels of cAMP in macrophage cell line. Furthermore, much difference in the levels of cAMP was not observed between compounds**1** and **23** treated cells. It clearly implicates that PDE4B specific inhibition plays an important role in the maintenance of intracellular cAMP level in the macrophage. In a similar set of experiment, TNF-α levels were monitored. The PDE4 inhibitor treatment showed that both compound **1** and **23** effectively inhibited the LPS-induced TNF-α synthesis in macrophage cell culture (Figure 21B).

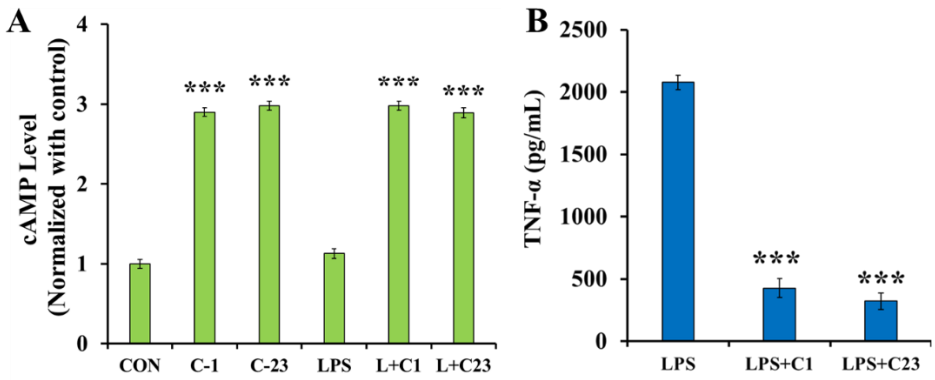

Figure 21. (A) cAMP levels in the cell lysate of compound **1** and **23** treated LPS stimulated Raw 264.7 cells. Cells were pretreated with 30nM of compound **1** and 15nM of compound **23** for 1h, then stimulated with 1µM of LPS for 30 min. cAMP levels were normalized with control. **(B)** TNF-α level in LPS-treated Raw 264.7 cells of control, compound **1** and **23.** 30 nM of compound **1** and 15nM of compound **23** treated cells were stimulated with 1µM of LPS for 30 min.

2.4.7. Effect of Novel PDE4 Inhibitors on DNCB-Induced Inflammatory Mediators

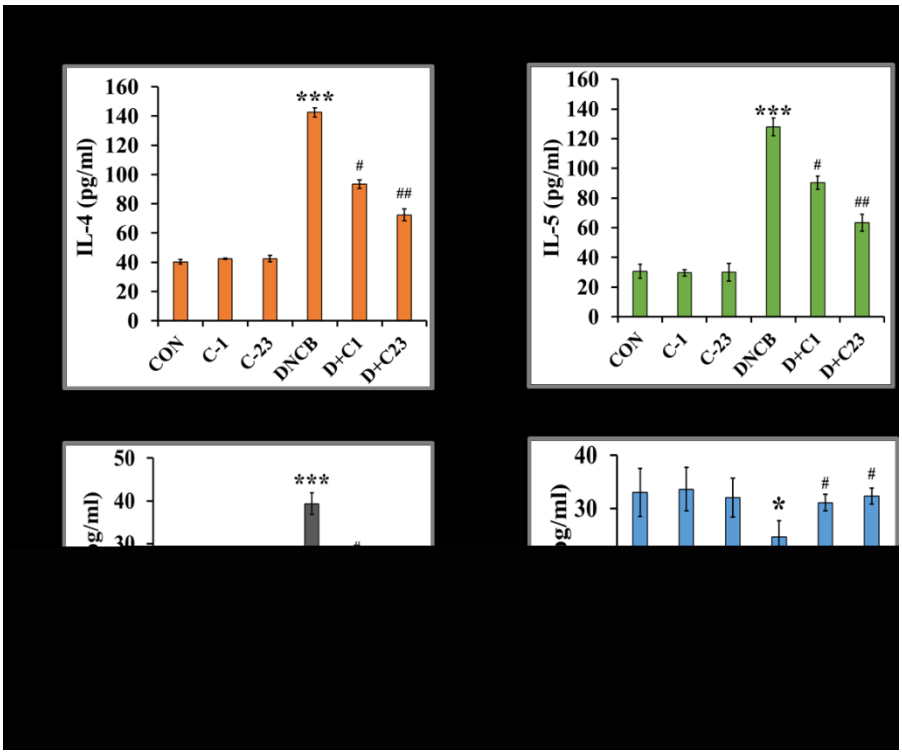

Figure 22. Serum cytokines level in experimental mice were quantified by ELISA: **(A)** Expression of serum IL-4. **(B)** Serum IL-5. **(C)** Serum IL-17. **(D)** Serum IFN-γ. Data represent the mean ± SEM (n=6). * p>0.5,*** p>.001 vs. control; # p>0.5, ## p>0.01 vs. DNCB.

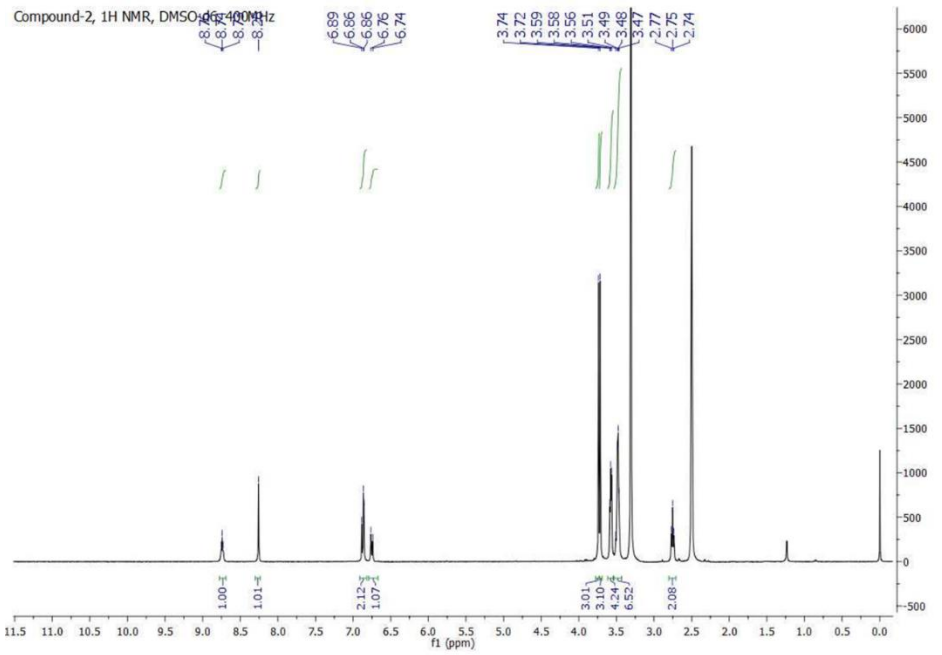
Compound-2, 1H NMR, DMSO-d6, 400MHz
8.77
8.75
8.21
8.19
6.89
6.86
6.86
6.76
6.74
3.74
3.72
3.59
3.58
3.56
3.51
3.49
3.48
3.47
2.77
2.75
2.74
1.00
1.01
2.12
1.07
3.01
3.10
4.24
6.52
2.08
f1 (ppm)

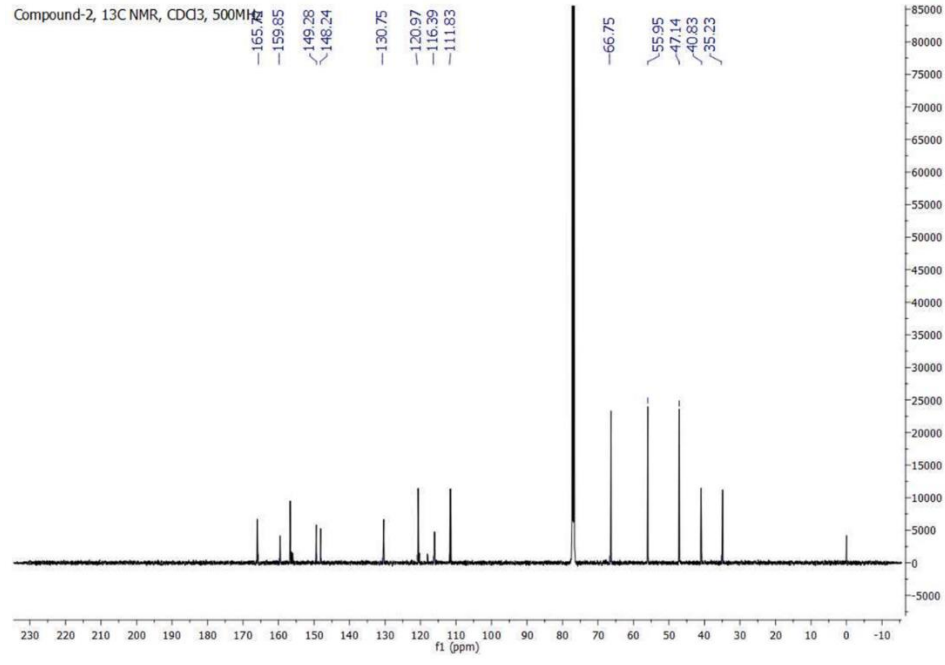
Compound-2, 13C NMR, CDCl3, 500MHz
165.72
159.85
149.28
148.24
130.75
120.97
116.39
111.83
66.75
55.95
47.14
40.83
35.23
f1 (ppm)

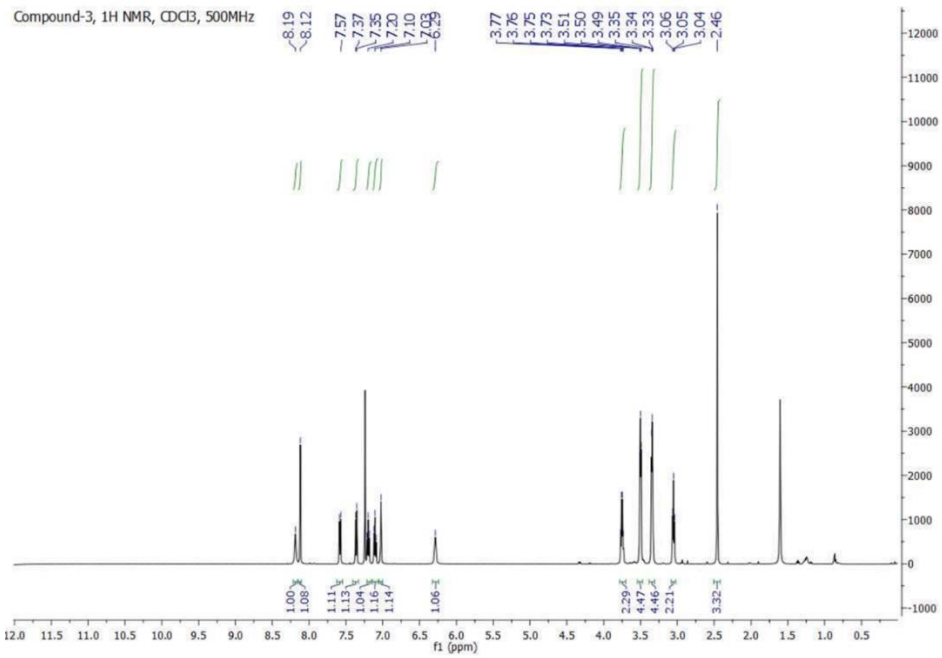
Compound-3, 1H NMR, CDCl3, 500MHz
8.19
8.12
7.57
7.37
7.35
7.20
7.10
7.08
6.29
3.77
3.76
3.75
3.73
3.51
3.50
3.49
3.35
3.34
3.33
3.06
3.05
3.04
2.46
1.00
1.08
1.11
1.13
1.04
1.16
1.14
1.06
2.29
4.47
4.46
2.21
3.32
f1 (ppm)

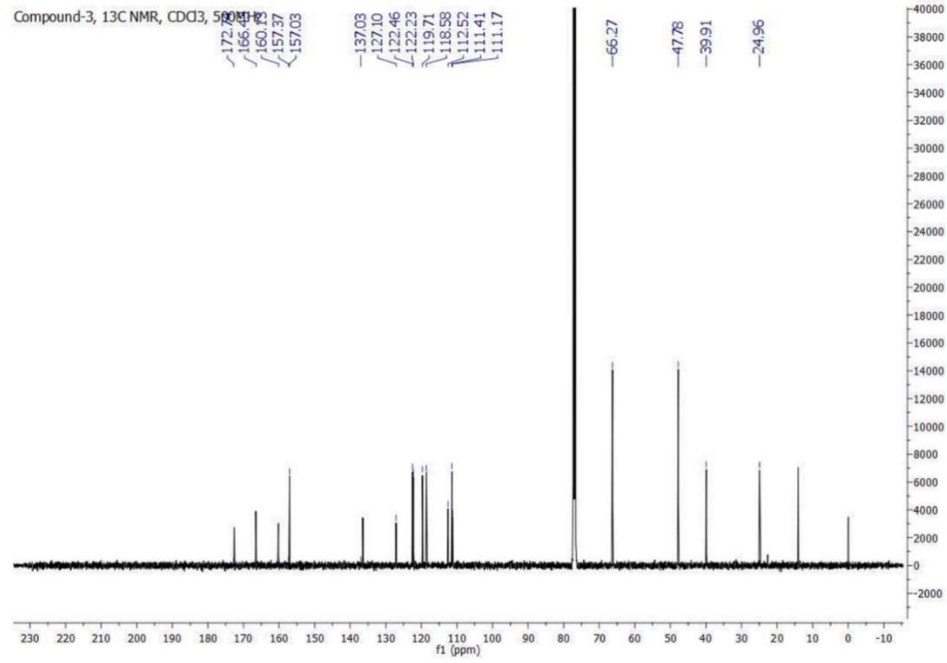
Compound-3, 13C NMR, CDCl3, 500MHz
172.70
166.47
160.13
157.37
157.03
137.03
127.10
122.46
122.23
119.71
118.58
112.52
111.41
111.17
66.27
47.78
39.91
24.96
f1 (ppm)

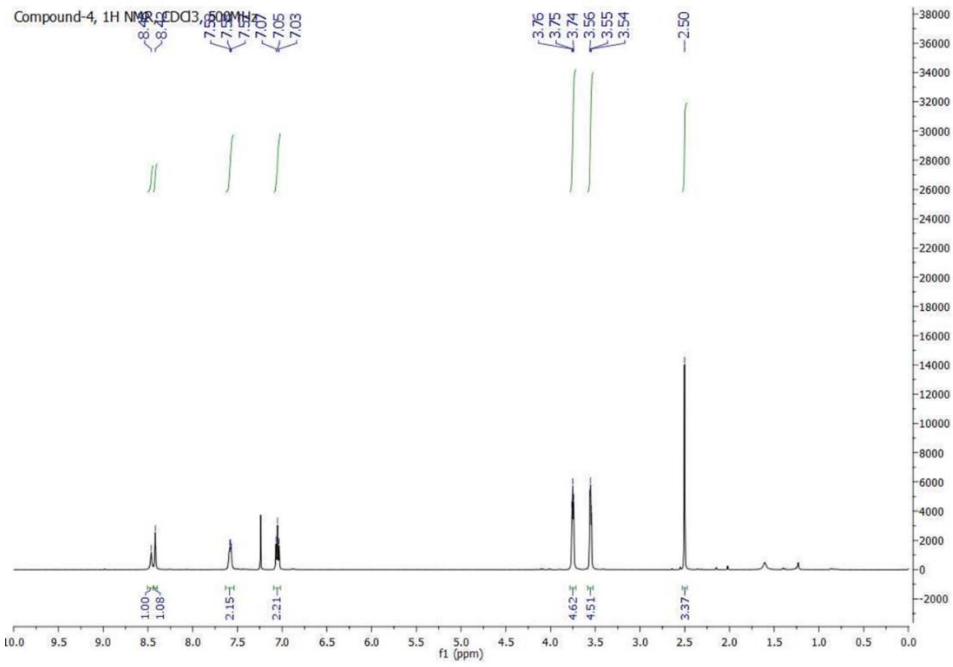
Compound-4, 1H NMR, CDCl3, 500MHz
8.41
8.40
7.55
7.54
7.53
7.07
7.05
7.03
3.76
3.75
3.74
3.56
3.55
3.54
2.50
1.00
1.08
2.15
2.21
4.62
4.51
3.37
f1 (ppm)

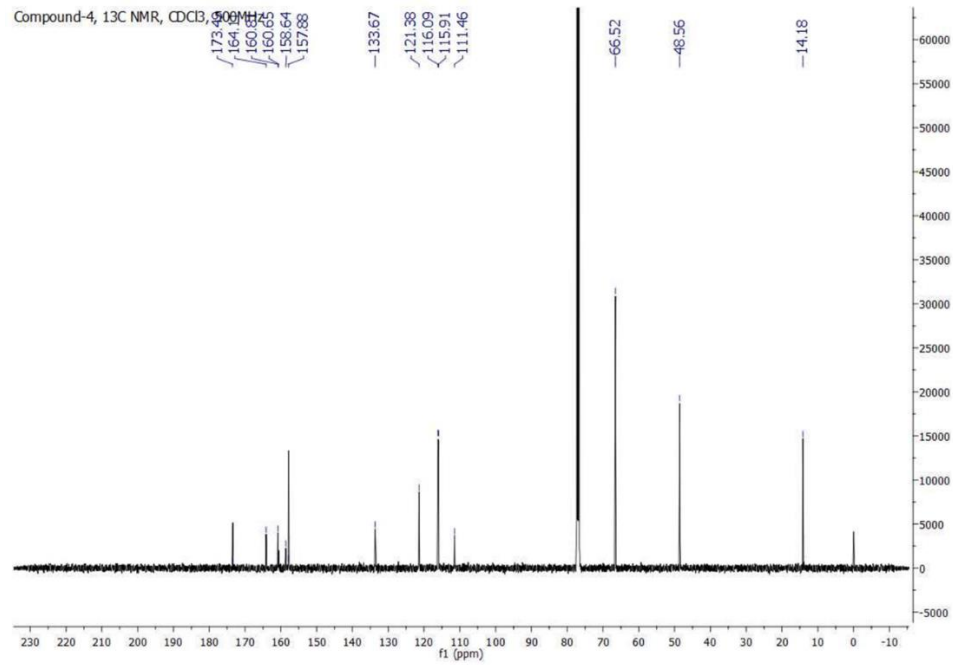
Compound-4, 13C NMR, CDCl3, 500MHz
173.46
164.15
160.85
160.65
158.64
157.88
133.67
121.38
116.09
115.91
111.46
66.52
48.56
14.18
f1 (ppm)

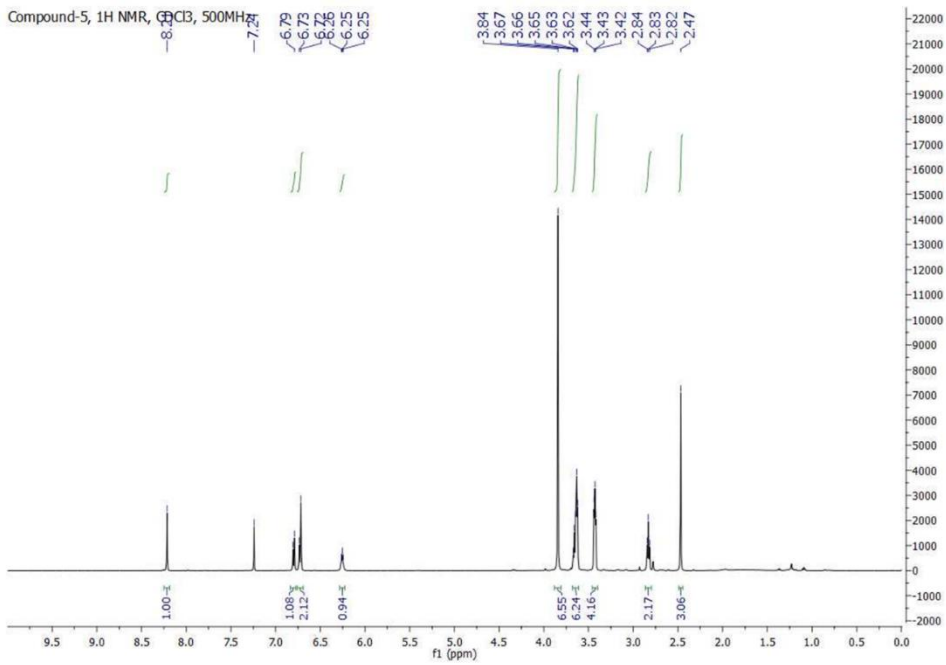
Compound-5, 1H NMR, CDCl3, 500MHz
8.21
7.24
6.79
6.73
6.26
6.25
6.25
3.84
3.67
3.66
3.65
3.63
3.62
3.44
3.43
3.42
2.84
2.83
2.82
2.47
1.00
1.08
2.12
0.94
6.55
6.24
4.16
2.17
3.06
f1 (ppm)

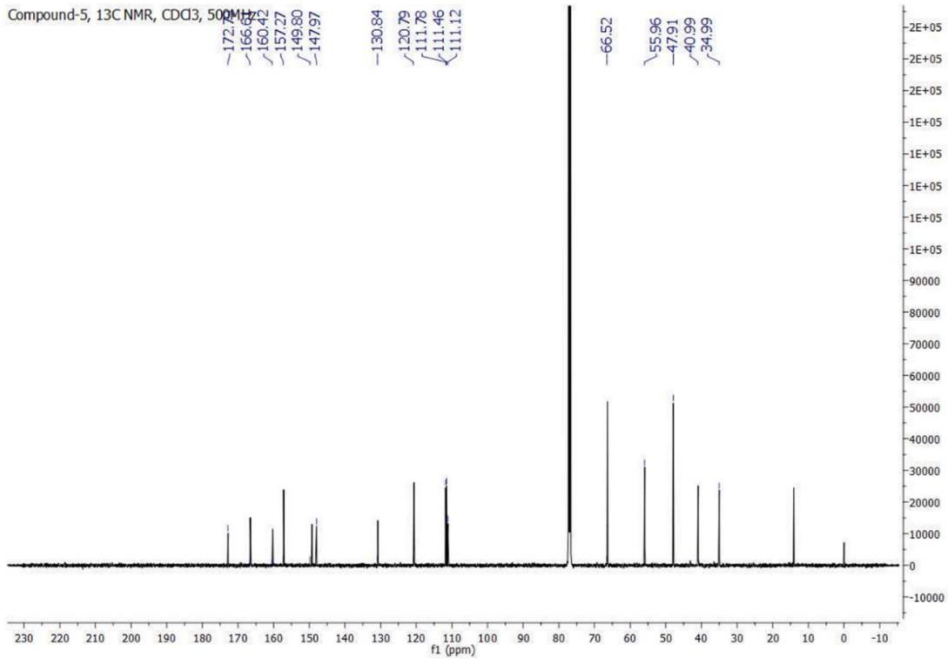
Compound-5, 13C NMR, CDCl3, 500MHz
172.76
166.62
160.42
157.27
149.80
147.97
130.84
120.79
111.78
111.46
111.12
66.52
55.96
47.91
40.99
34.99
f1 (ppm)

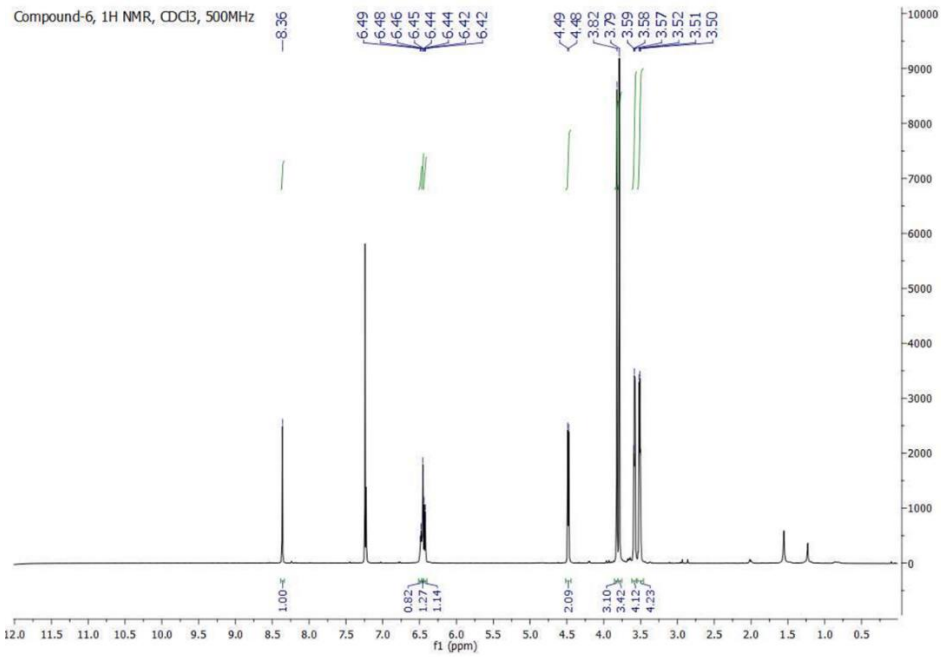
Compound-6, 1H NMR, CDCl3, 500MHz
8.36
6.49
6.48
6.46
6.45
6.44
6.44
6.42
6.42
4.49
4.48
3.82
3.79
3.59
3.58
3.57
3.52
3.51
3.50
1.00
0.82
1.27
1.14
2.09
3.10
3.42
4.12
4.23
f1 (ppm)

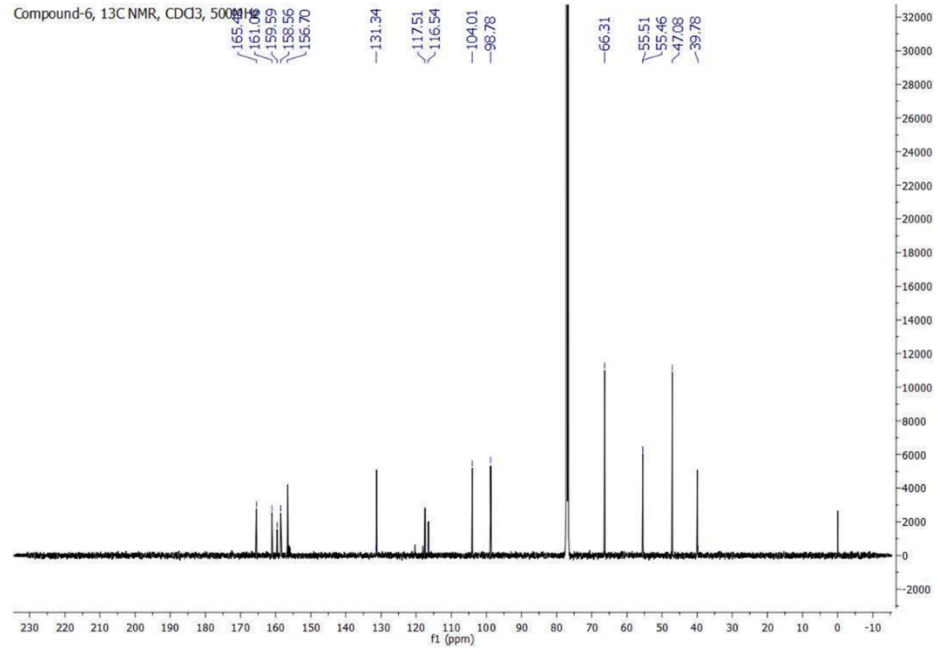
Compound-6, 13C NMR, CDCl3, 500MHz
165.48
161.08
159.59
158.56
156.70
131.34
117.51
116.54
104.01
98.78
66.31
55.51
55.46
47.08
39.78
f1 (ppm)

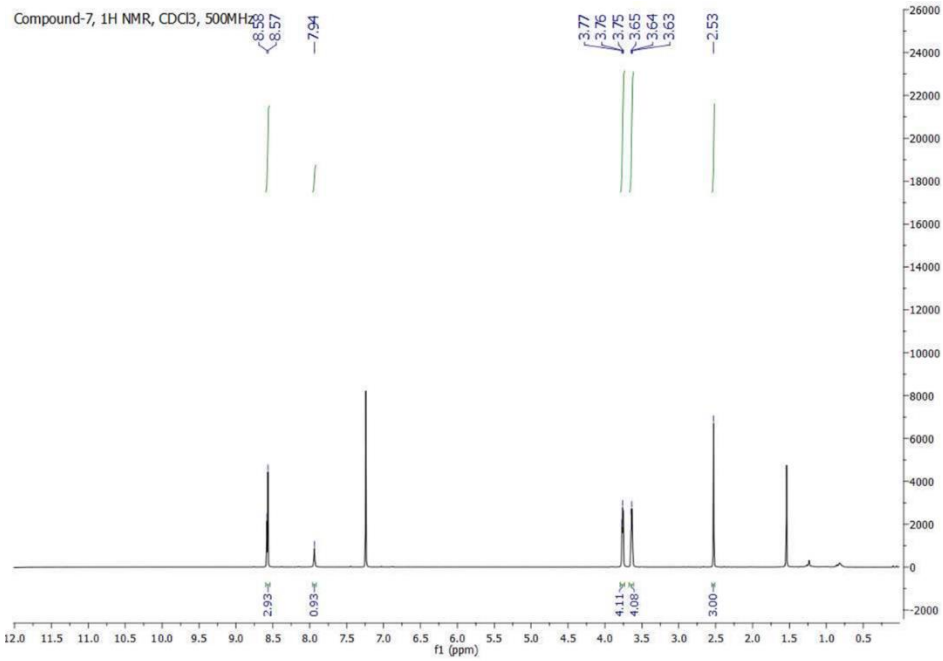
Compound-7, 1H NMR, CDCl3, 500MHz
8.58
8.57
7.94
3.77
3.76
3.75
3.65
3.64
3.63
2.53
2.93
0.93
4.11
4.08
3.00
f1 (ppm)

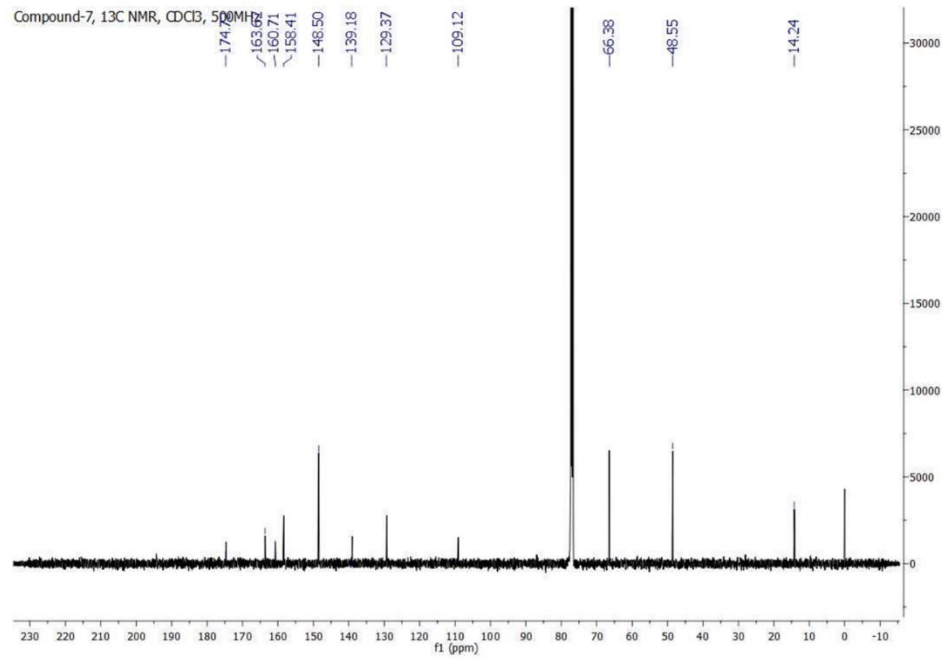
Compound-7, 13C NMR, CDCl3, 500MHz
174.72
163.07
160.71
158.41
148.50
139.18
129.37
109.12
66.38
48.55
14.24
f1 (ppm)

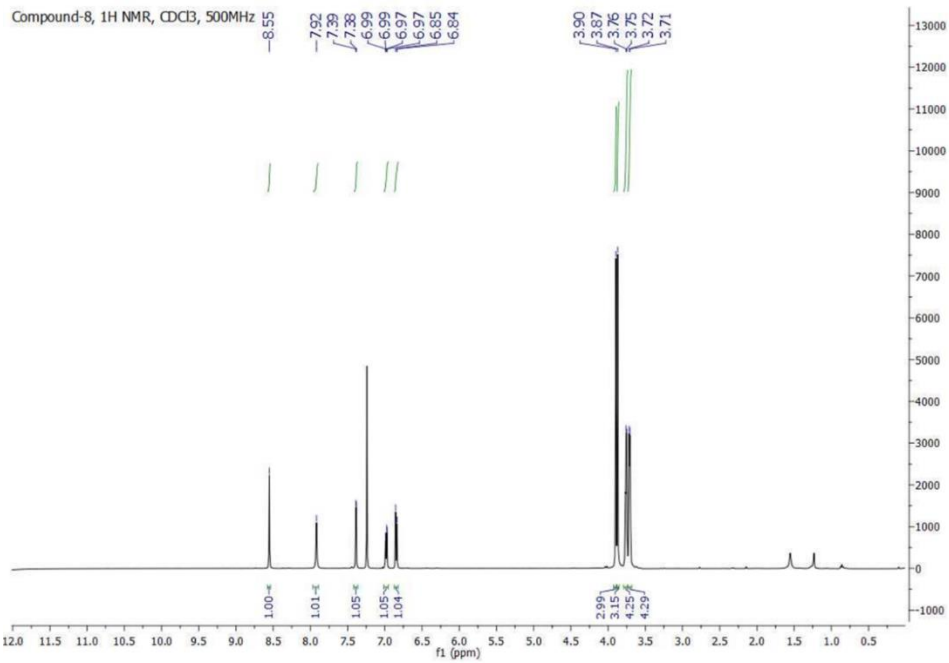
Compound-8, 1H NMR, CDCl3, 500MHz
8.55
7.92
7.39
7.38
6.99
6.99
6.97
6.97
6.85
6.84
3.90
3.87
3.76
3.75
3.72
3.71
1.00
1.01
1.05
1.05
1.04
2.99
3.15
4.25
4.29
f1 (ppm)

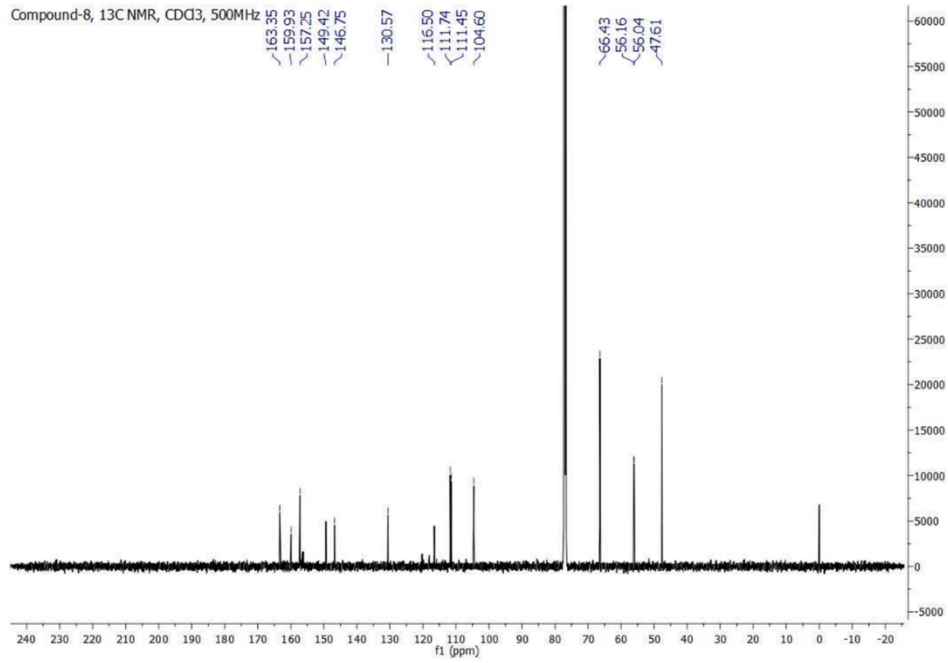
Compound-8, 13C NMR, CDCl3, 500MHz
163.35
159.93
157.25
149.42
146.75
130.57
116.50
111.74
111.45
104.60
66.43
56.16
56.04
47.61
f1 (ppm)

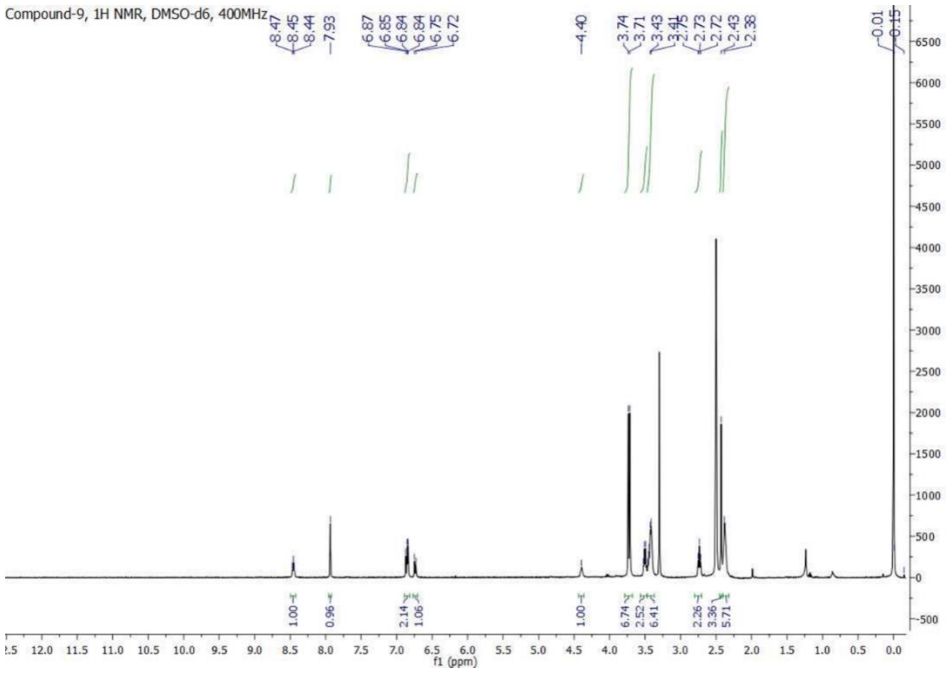
Compound-9, 1H NMR, DMSO-d6, 400MHz
8.47
8.45
8.44
7.93
6.87
6.85
6.84
6.84
6.75
6.72
4.40
3.74
3.71
3.43
3.41
2.75
2.73
2.72
2.43
2.38
0.01
0.15
1.00
0.98
2.14
1.06
1.00
6.74
2.52
6.41
2.26
3.36
5.71
f1 (ppm)

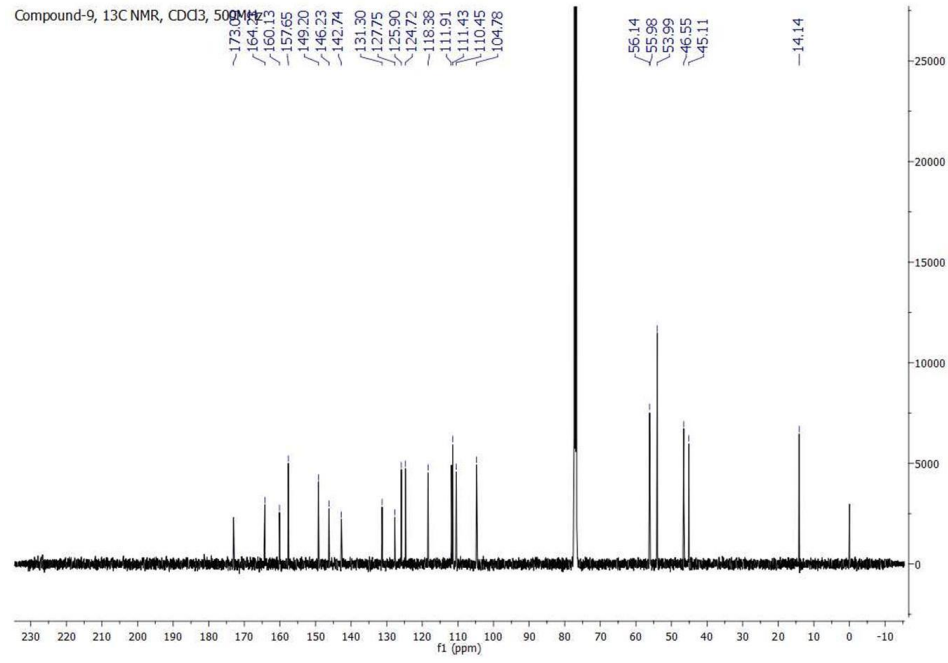
Compound-9, 13C NMR, CDCl3, 500MHz
173.01
164.14
160.13
157.65
149.20
146.23
142.74
131.30
127.75
125.90
124.72
118.38
111.91
111.43
110.45
104.78
56.14
55.98
53.99
46.55
45.11
14.14
f1 (ppm)

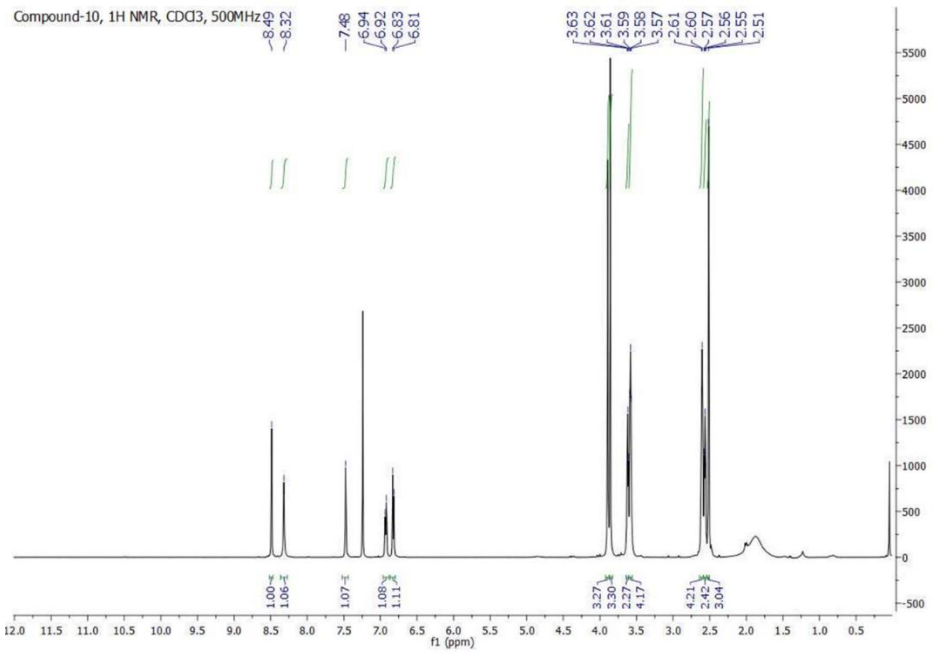
Compound-10, 1H NMR, CDCl3, 500MHz
8.49
8.32
7.48
6.94
6.92
6.83
6.81
3.63
3.62
3.61
3.59
3.58
3.57
2.61
2.60
2.57
2.56
2.55
2.51
1.00
1.06
1.07
1.08
1.11
3.27
3.30
2.27
4.17
4.21
2.42
3.04
f1 (ppm)

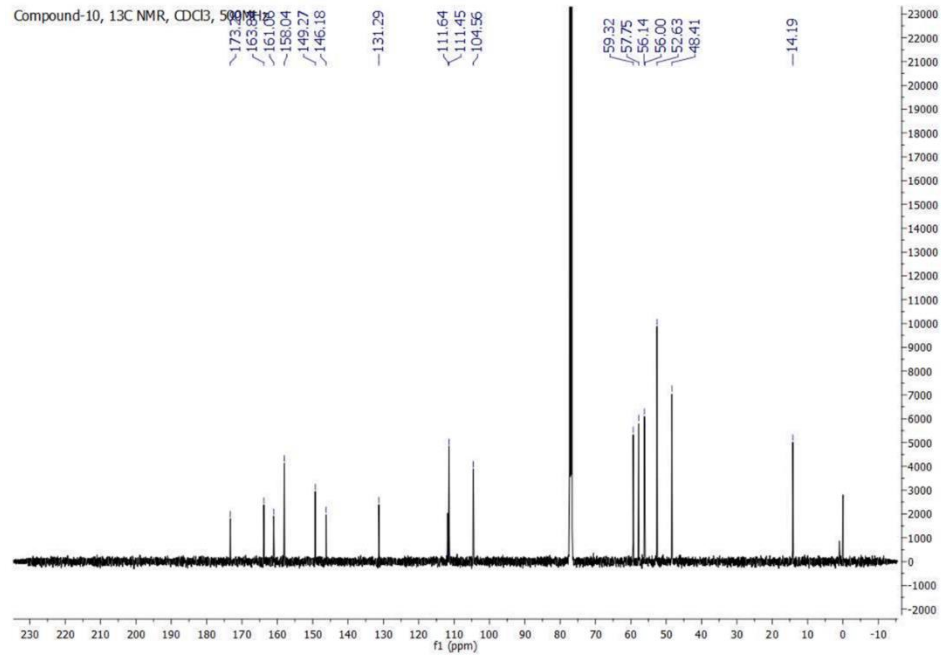
Compound-10, 13C NMR, CDCl3, 500MHz
173.25
163.88
161.08
158.04
149.27
146.18
131.29
111.64
111.45
104.56
59.32
57.75
56.14
56.00
52.63
48.41
14.19
f1 (ppm)

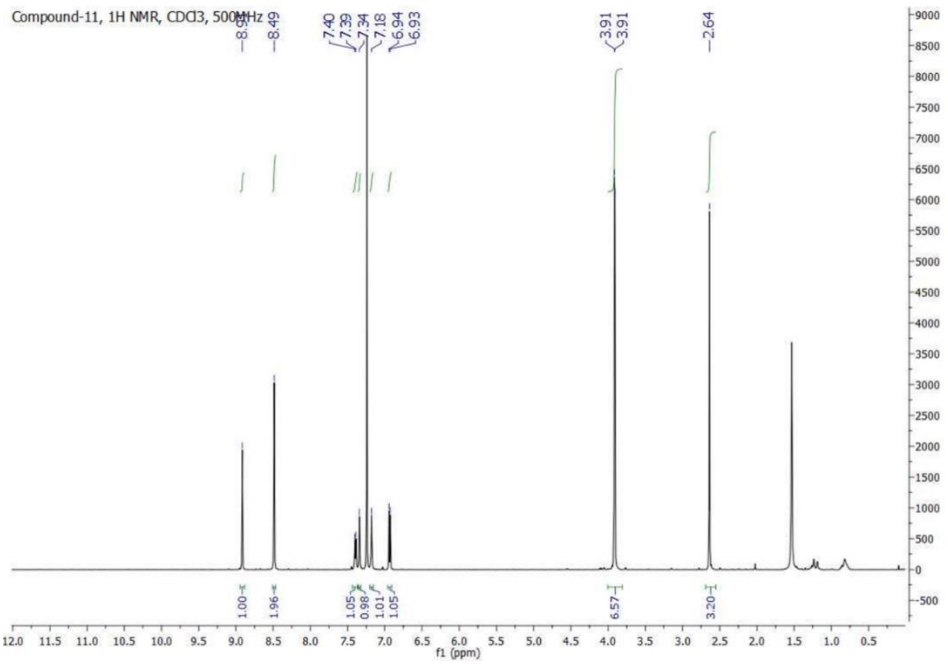
Compound-11, 1H NMR, CDCl3, 500MHz
8.49
7.40
7.39
7.34
7.18
6.94
6.93
3.91
3.91
2.64
1.00
1.96
1.05
0.98
1.01
1.05
6.57
3.20
f1 (ppm)

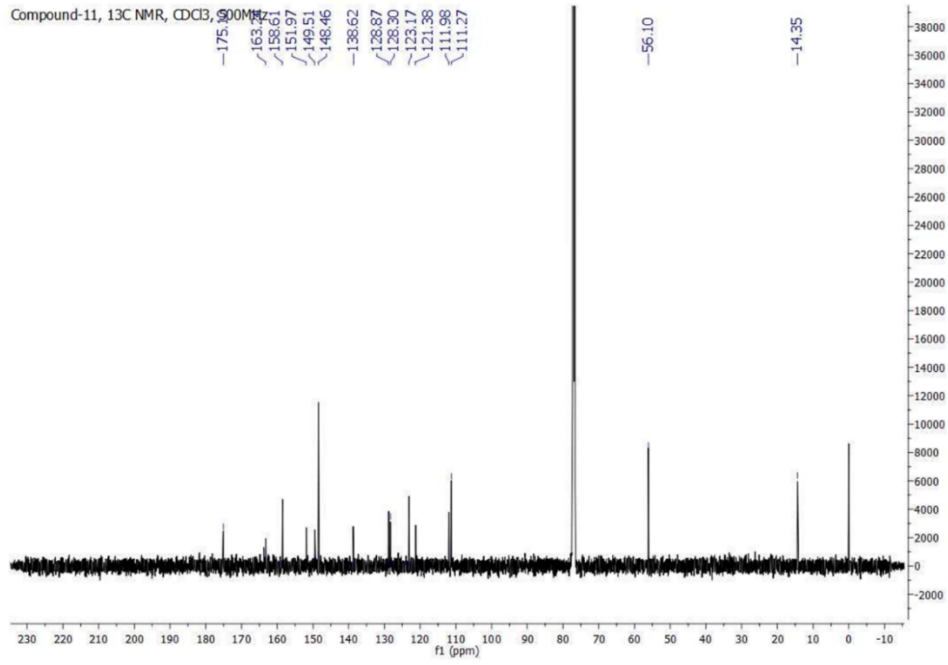
Compound-11, 13C NMR, CDCl3, 500MHz
175.1
163.4
158.61
151.97
149.51
148.46
138.62
128.87
128.30
123.17
121.38
111.98
111.27
56.10
14.35
f1 (ppm)

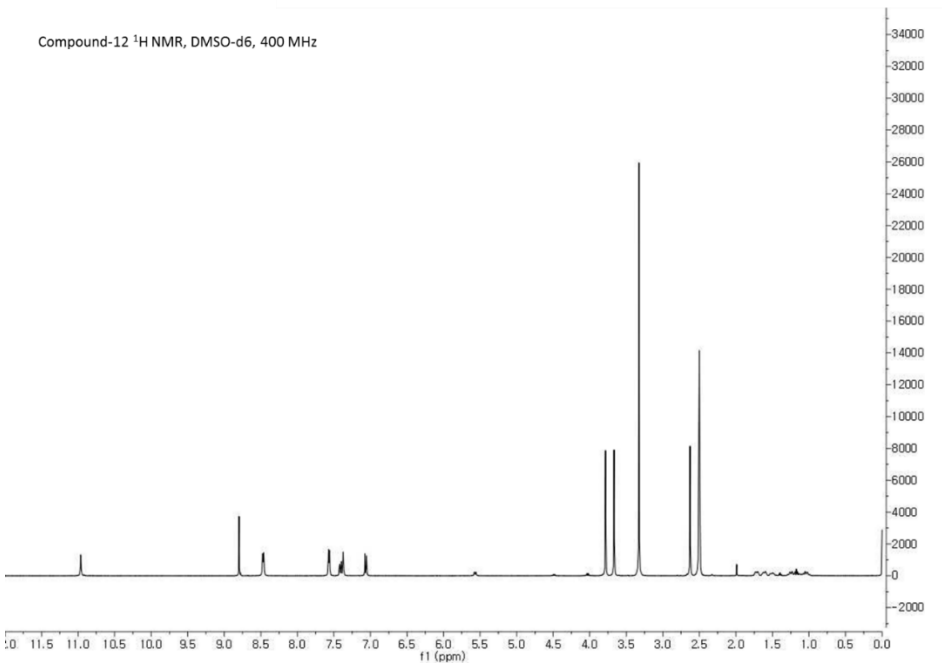
Compound-12 ¹H NMR, DMSO-d6, 400 MHz
f1 (ppm)

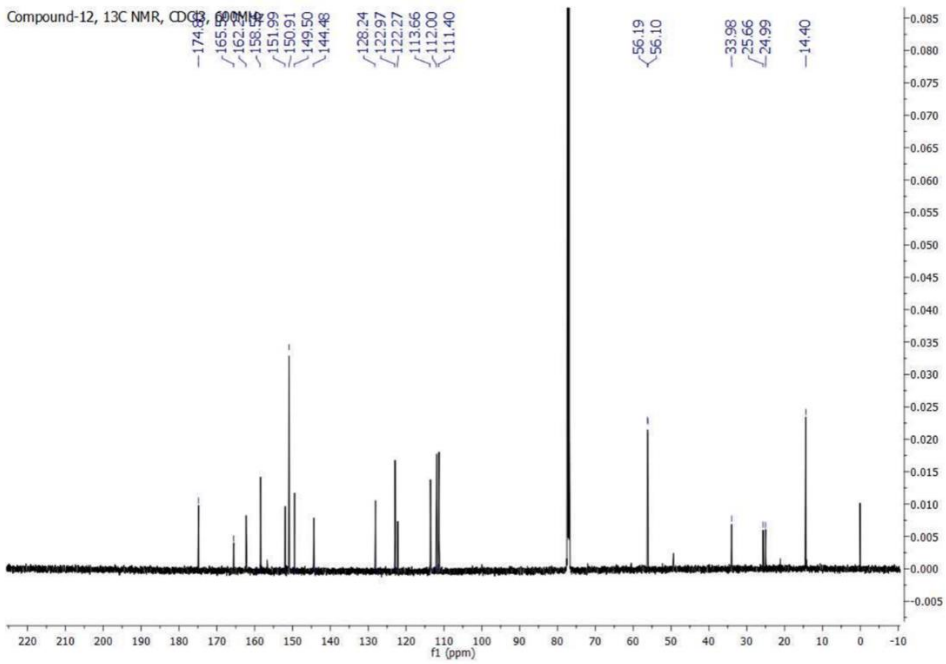
Compound-12, 13C NMR, CDCl3, 600MHz
174.68
165.57
162.45
158.56
151.99
150.91
149.50
144.48
128.24
122.97
122.27
113.66
112.00
111.40
56.19
56.10
33.98
25.66
24.99
14.40
f1 (ppm)

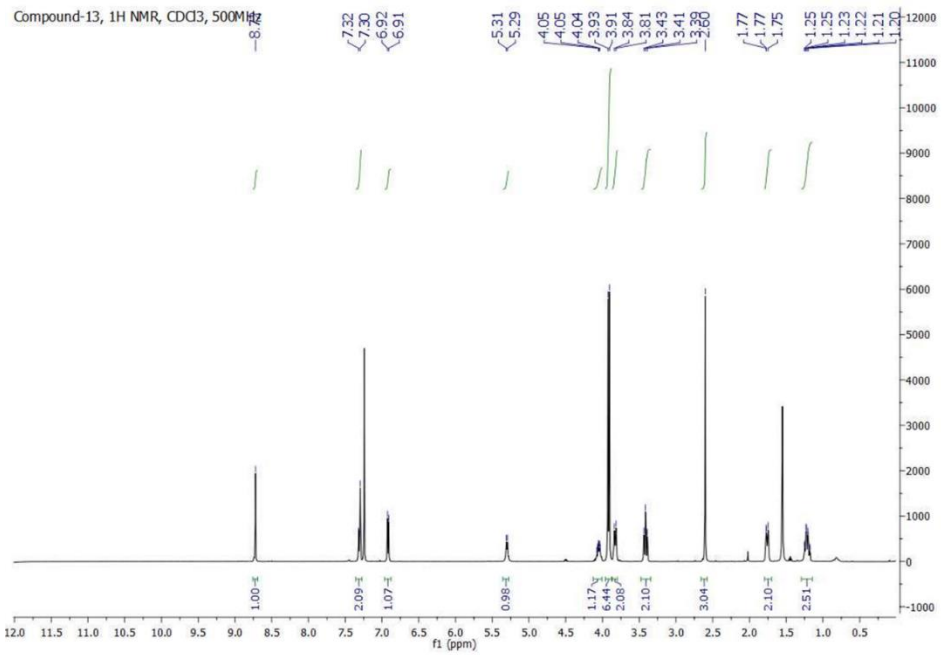
Compound-13, 1H NMR, CDCl3, 500MHz
8.77
7.32
7.30
6.92
6.91
5.31
5.29
4.05
4.05
4.04
3.93
3.91
3.84
3.81
3.43
3.41
3.39
2.60
1.77
1.77
1.75
1.25
1.25
1.23
1.22
1.21
1.20
1.00
2.09
1.07
0.98
1.17
6.44
2.08
2.10
3.04
2.10
2.51
f1 (ppm)

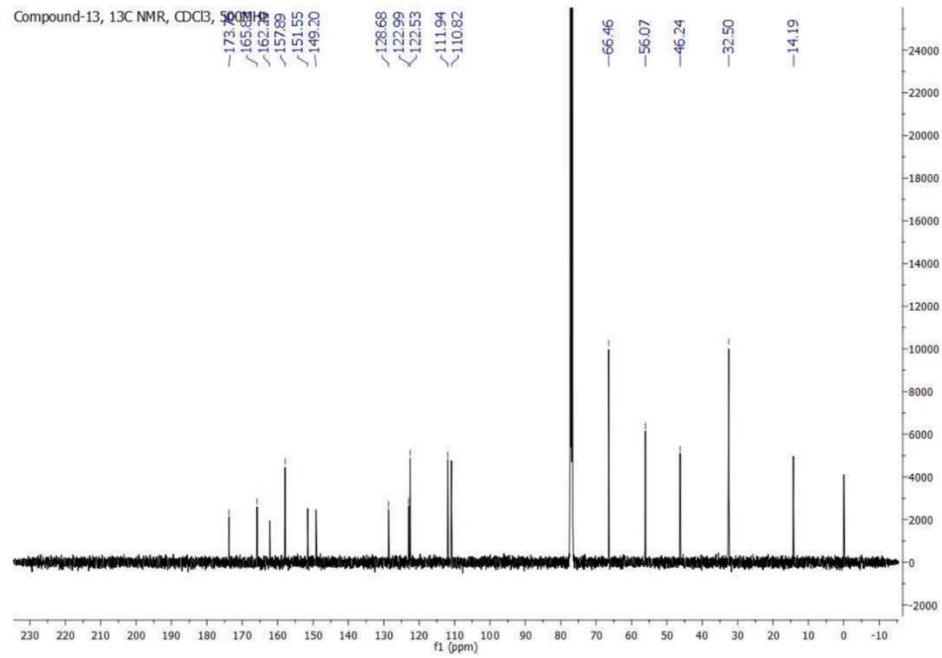
Compound-13, 13C NMR, CDCl3, 500MHz
173.74
165.68
162.26
157.89
151.55
149.20
128.68
122.99
122.53
111.94
110.82
66.46
56.07
46.24
32.50
14.19
f1 (ppm)

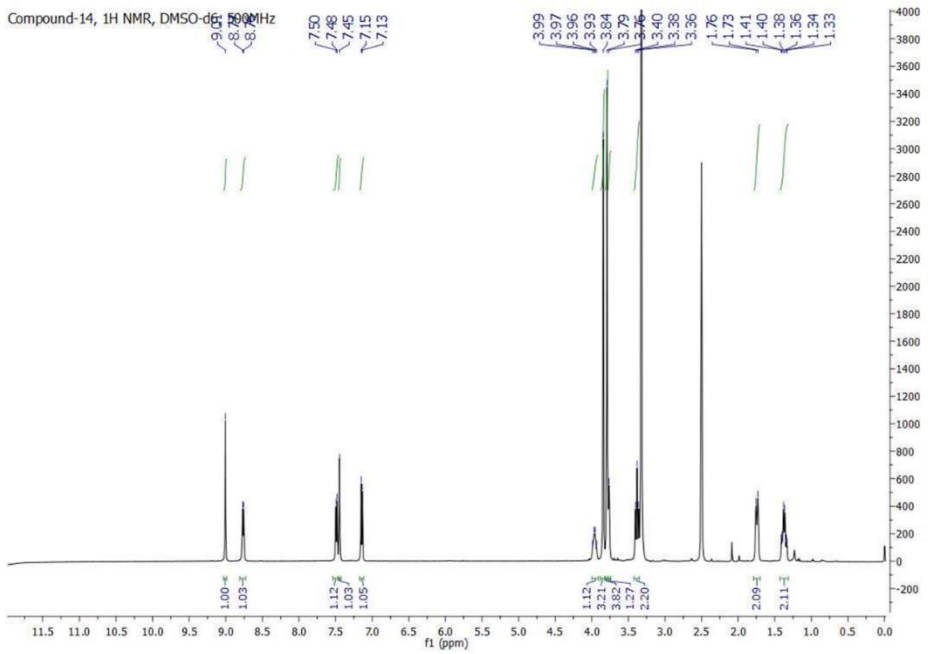
Compound-14, 1H NMR, DMSO-d6, 500MHz
9.07
8.78
8.77
7.50
7.48
7.45
7.15
7.13
3.99
3.97
3.96
3.93
3.84
3.79
3.76
3.40
3.38
3.36
1.76
1.73
1.41
1.40
1.38
1.36
1.34
1.33
1.00
1.03
1.12
1.03
1.05
1.12
3.21
3.82
1.27
2.20
2.09
2.11
f1 (ppm)

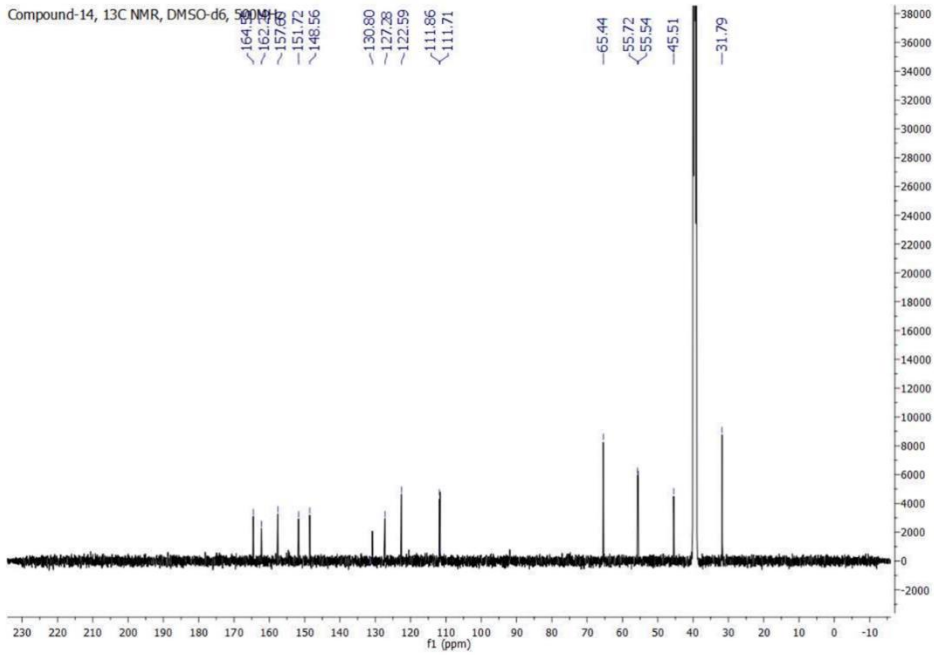
Compound-14, 13C NMR, DMSO-d6, 500MHz
164.59
162.48
157.68
151.72
148.56
130.80
127.28
122.59
111.86
111.71
65.44
55.72
55.54
45.51
31.79
f1 (ppm)

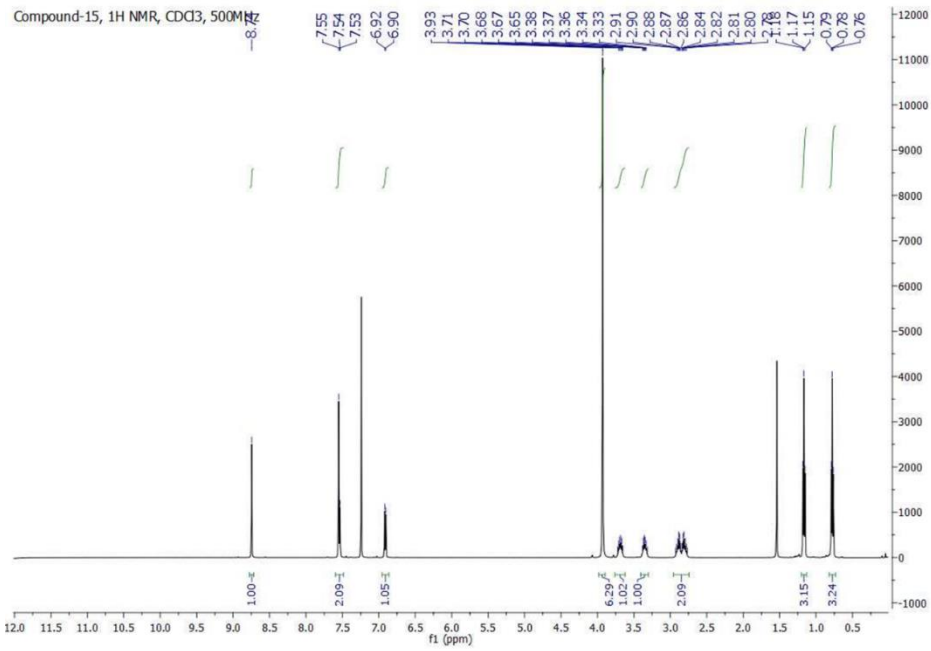
Compound-15, 1H NMR, CDCl3, 500MHz
8.74
7.55
7.54
7.53
6.92
6.90
3.93
3.71
3.70
3.68
3.67
3.65
3.38
3.37
3.36
3.34
3.33
2.91
2.90
2.88
2.87
2.86
2.84
2.82
2.81
2.80
2.78
1.18
1.17
1.15
0.79
0.78
0.76
1.00
2.09
1.05
6.29
1.02
1.00
2.09
3.15
3.24
f1 (ppm)

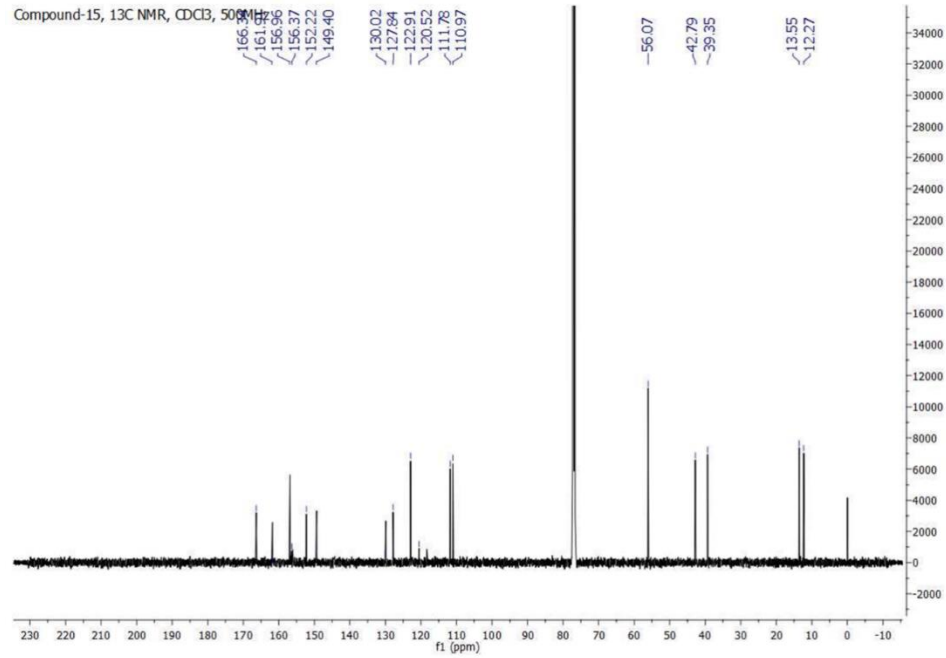
Compound-15, 13C NMR, CDCl3, 500MHz
166.32
161.92
156.96
156.37
152.22
149.40
130.02
127.84
122.91
120.52
111.78
110.97
56.07
42.79
39.35
13.55
12.27
f1 (ppm)

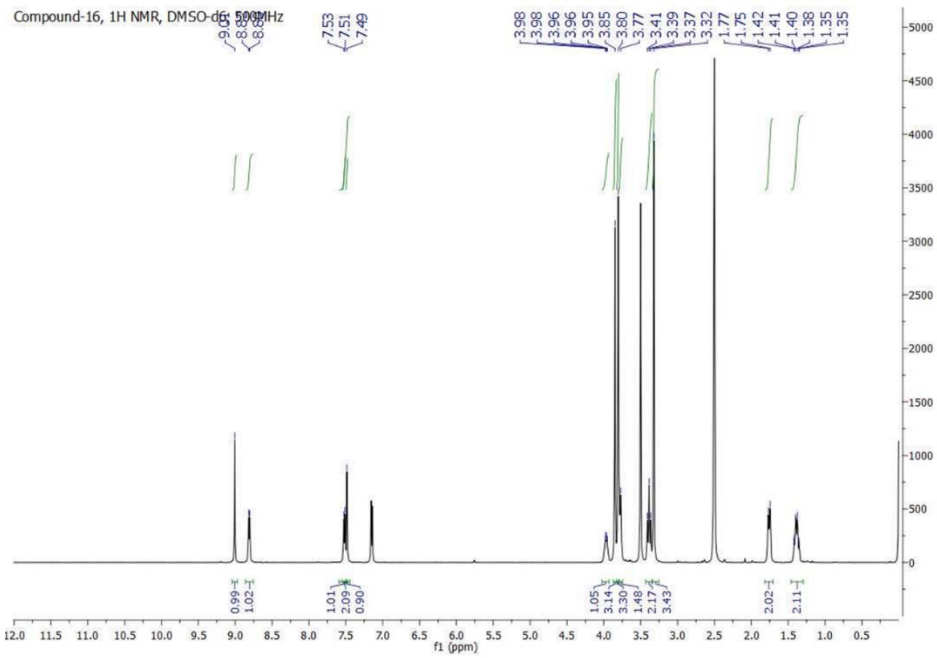
Compound-16, 1H NMR, DMSO-d6, 500MHz
9.01
8.99
8.82
8.80
7.53
7.51
7.49
3.98
3.98
3.96
3.96
3.95
3.85
3.80
3.77
3.41
3.39
3.37
3.32
1.77
1.75
1.42
1.41
1.40
1.38
1.35
1.35
0.99
1.02
1.01
2.09
0.90
1.05
3.14
3.30
1.48
2.17
3.43
2.02
2.11
f1 (ppm)

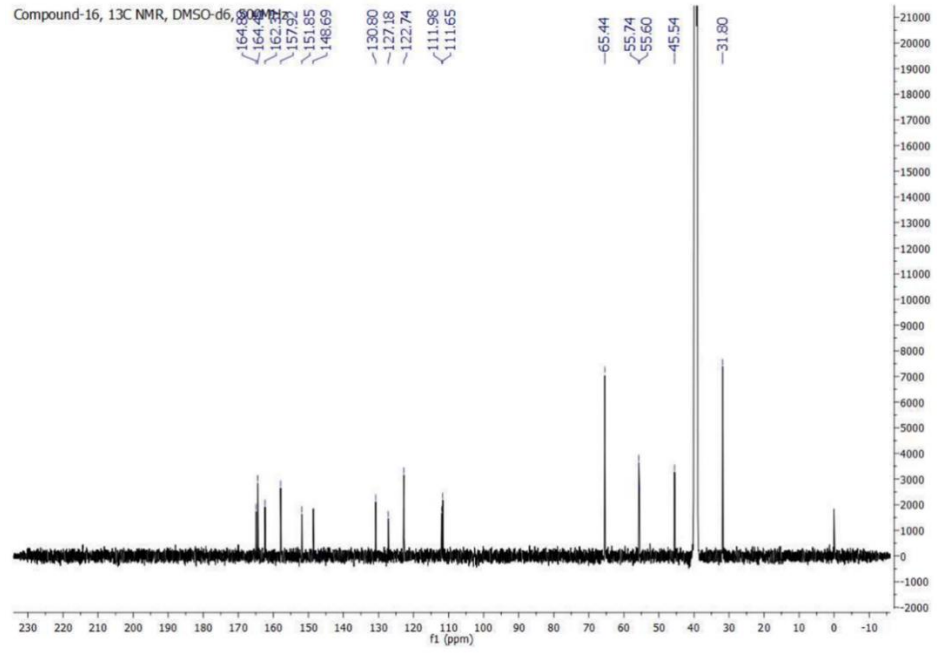
Compound-16, 13C NMR, DMSO-d6, 800MHz
164.88
164.47
162.53
157.92
151.85
148.69
130.80
127.18
122.74
111.98
111.65
65.44
55.74
55.60
45.54
31.80
f1 (ppm)

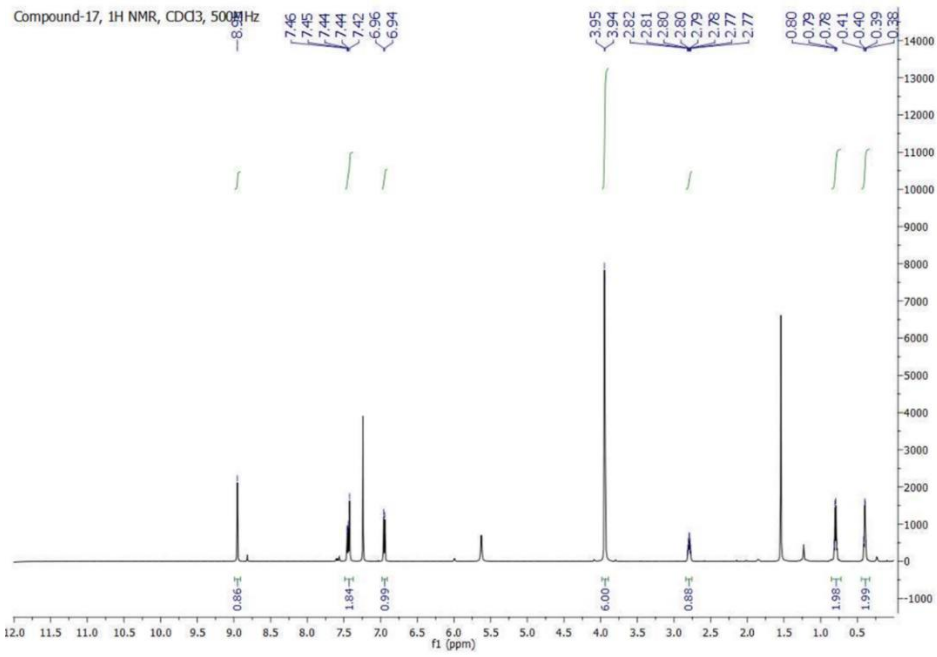
Compound-17, 1H NMR, CDCl3, 500MHz
8.99
7.46
7.45
7.44
7.44
7.42
6.96
6.94
3.95
3.94
2.82
2.81
2.80
2.80
2.79
2.78
2.77
2.77
0.80
0.79
0.78
0.41
0.40
0.39
0.38
0.86
1.84
0.99
6.00
0.88
1.98
1.99
f1 (ppm)

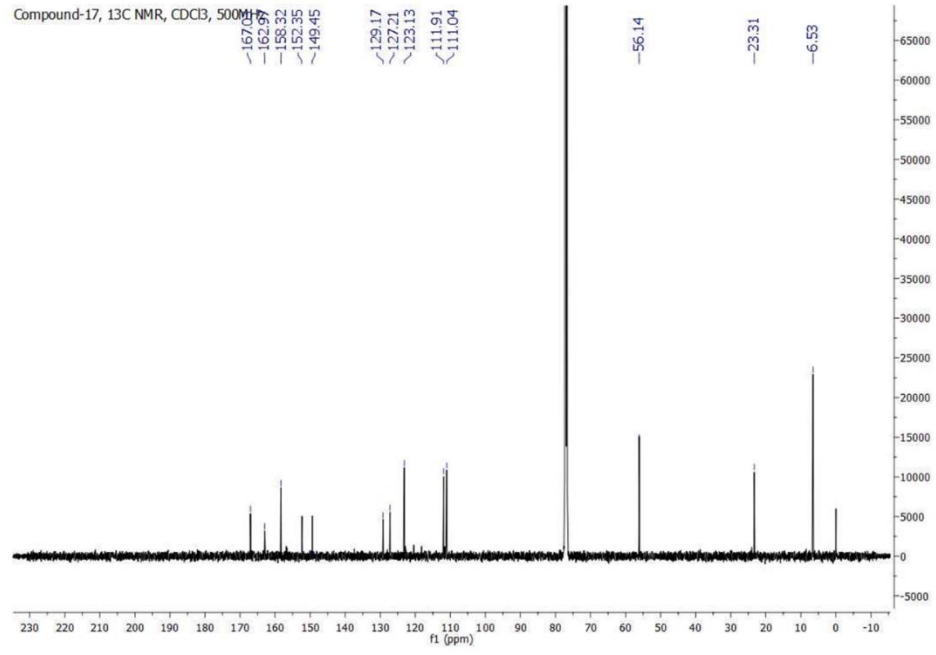
Compound-17, 13C NMR, CDCl3, 500MHz
167.03
162.97
158.32
152.35
149.45
129.17
127.21
123.13
111.91
111.04
56.14
23.31
6.53
f1 (ppm)

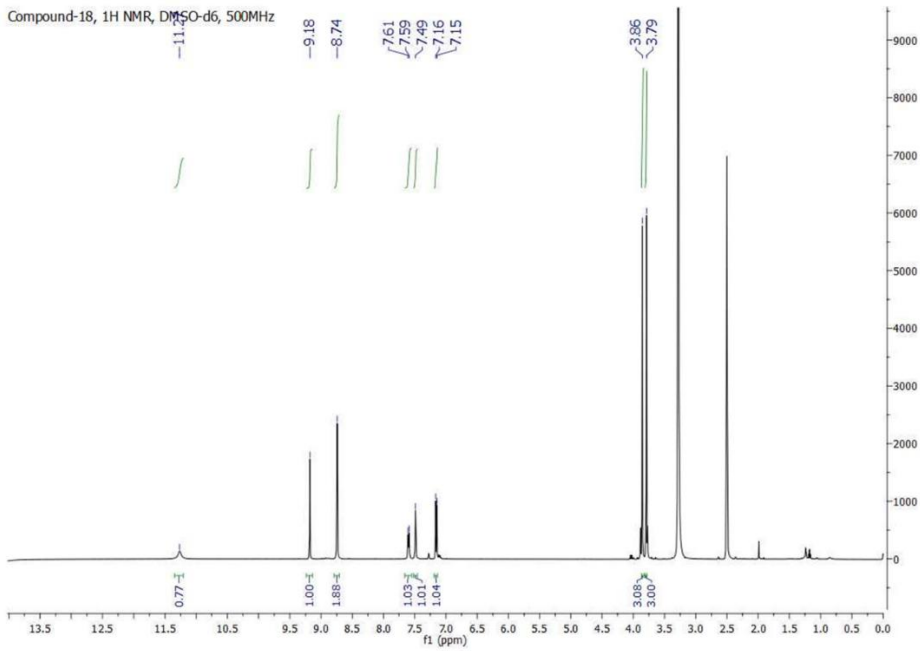
Compound-18, 1H NMR, DMSO-d6, 500MHz
11.15
9.18
8.74
7.61
7.59
7.49
7.16
7.15
3.86
3.79
0.77
1.00
1.88
1.03
1.01
1.04
3.08
3.00
f1 (ppm)

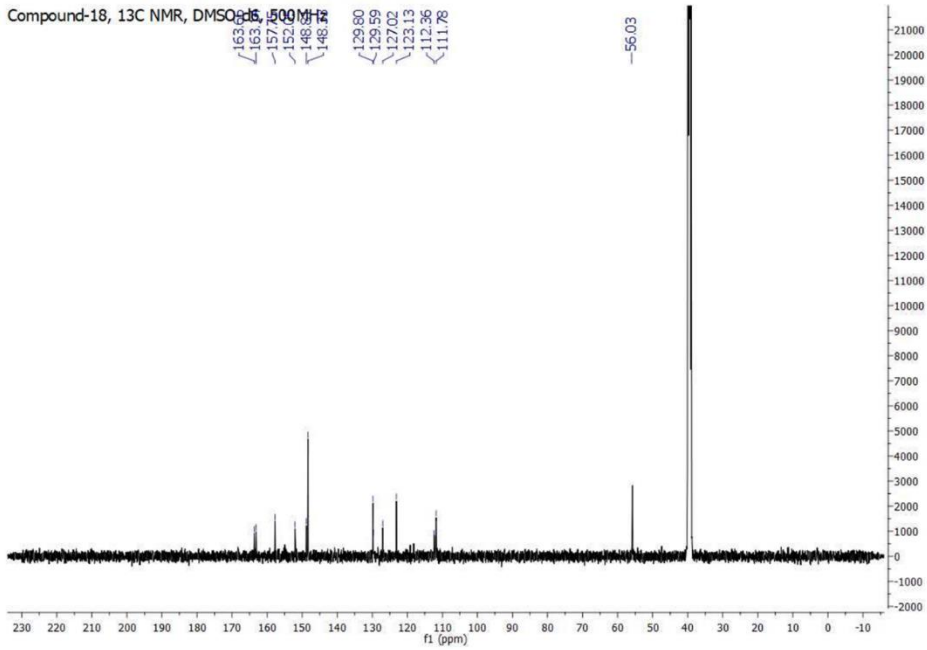
Compound-18, 13C NMR, DMSO-d6, 500MHz
163.61
163.37
157.74
152.62
148.68
148.42
129.80
129.59
127.02
123.13
112.36
111.78
56.03
f1 (ppm)

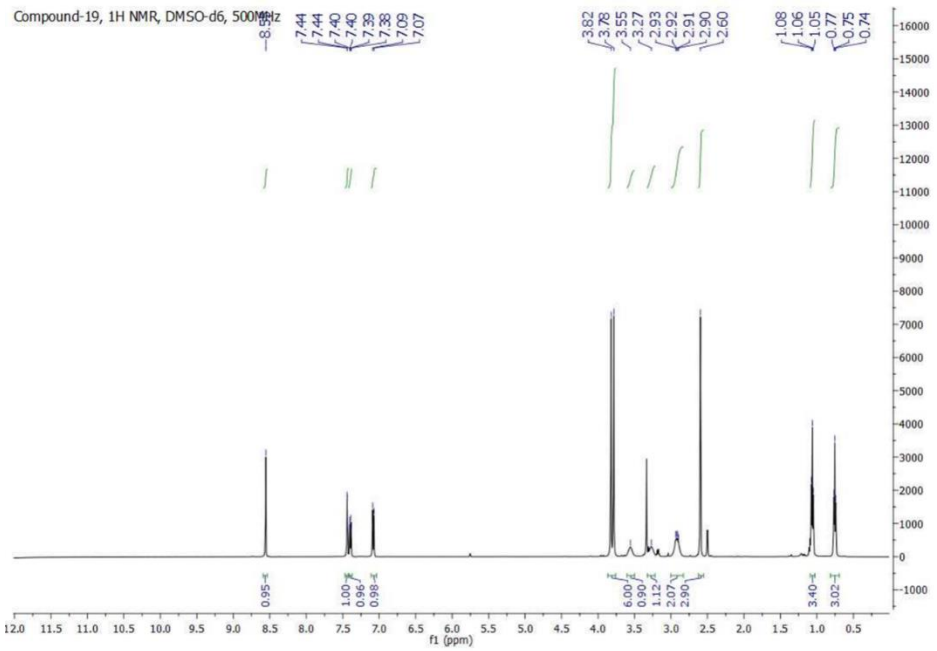
Compound-19, 1H NMR, DMSO-d6, 500MHz
8.58
7.44
7.44
7.40
7.40
7.39
7.38
7.09
7.07
3.82
3.78
3.55
3.27
2.93
2.92
2.91
2.90
2.60
1.08
1.06
1.05
0.77
0.75
0.74
0.95
1.00
0.96
0.98
6.00
0.90
1.12
2.07
2.90
3.40
3.02
f1 (ppm)

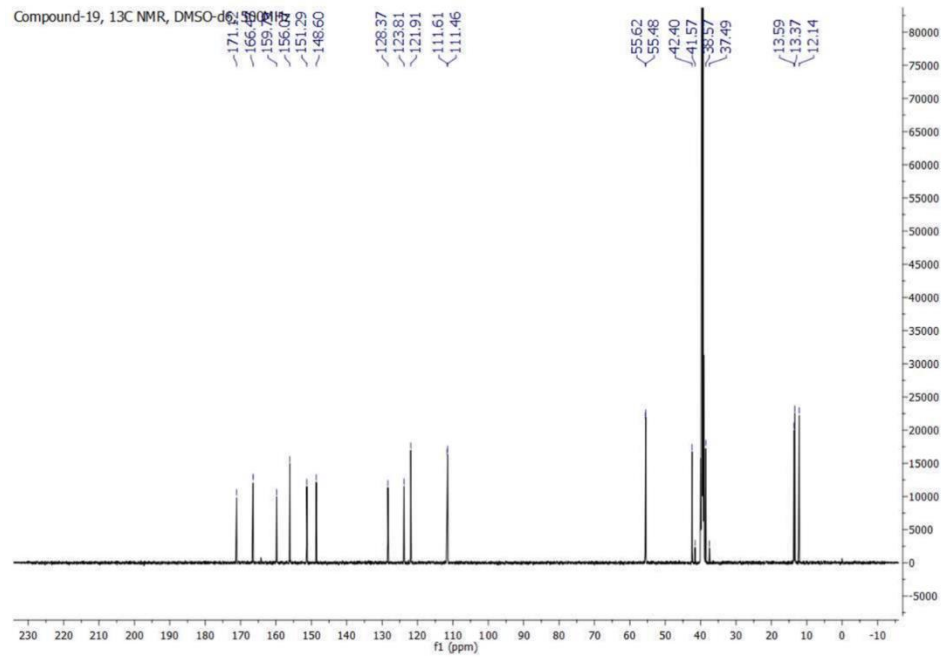
Compound-19, 13C NMR, DMSO-d6, 500MHz
171.83
166.49
159.72
156.04
151.29
148.60
128.37
123.81
121.91
111.61
111.46
55.62
55.48
42.40
41.57
38.57
37.49
13.59
13.37
12.14
f1 (ppm)

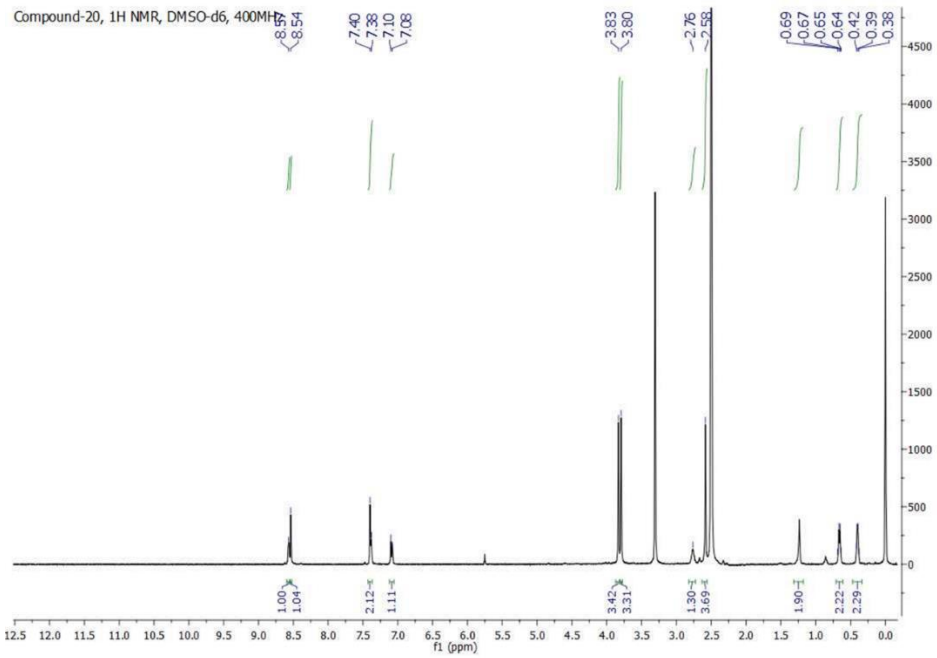
Compound-20, 1H NMR, DMSO-d6, 400MHz
8.57
8.54
7.40
7.38
7.10
7.08
3.83
3.80
2.76
2.58
0.69
0.67
0.65
0.64
0.42
0.39
0.38
1.00
1.04
2.12
1.11
3.42
3.31
1.30
3.69
1.90
2.22
2.29
f1 (ppm)

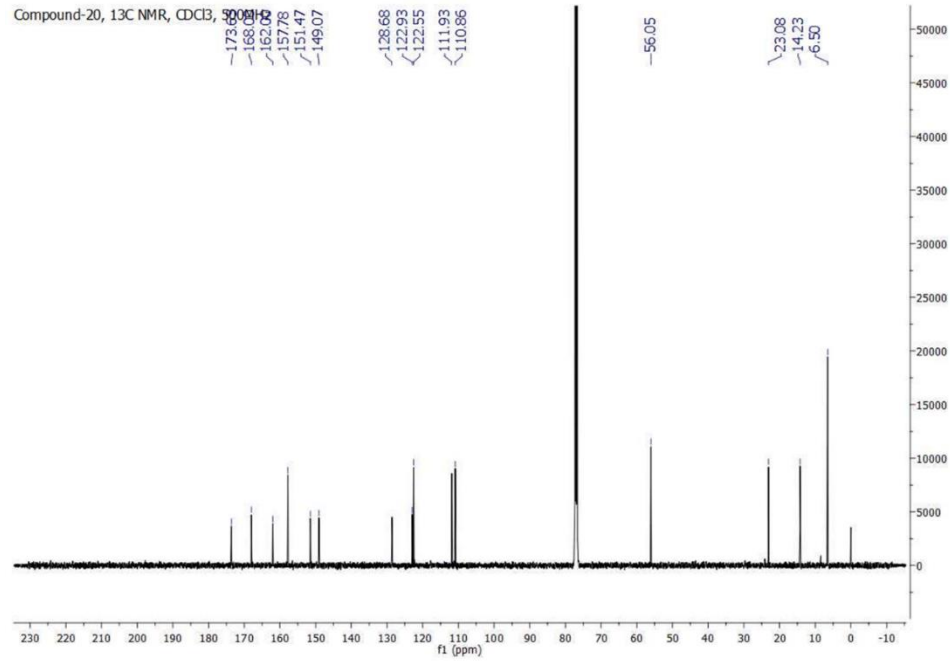
Compound-20, 13C NMR, CDCl3, 100MHz
173.65
168.05
162.05
157.78
151.47
149.07
128.68
122.93
122.55
111.93
110.86
56.05
23.08
14.23
6.50
f1 (ppm)

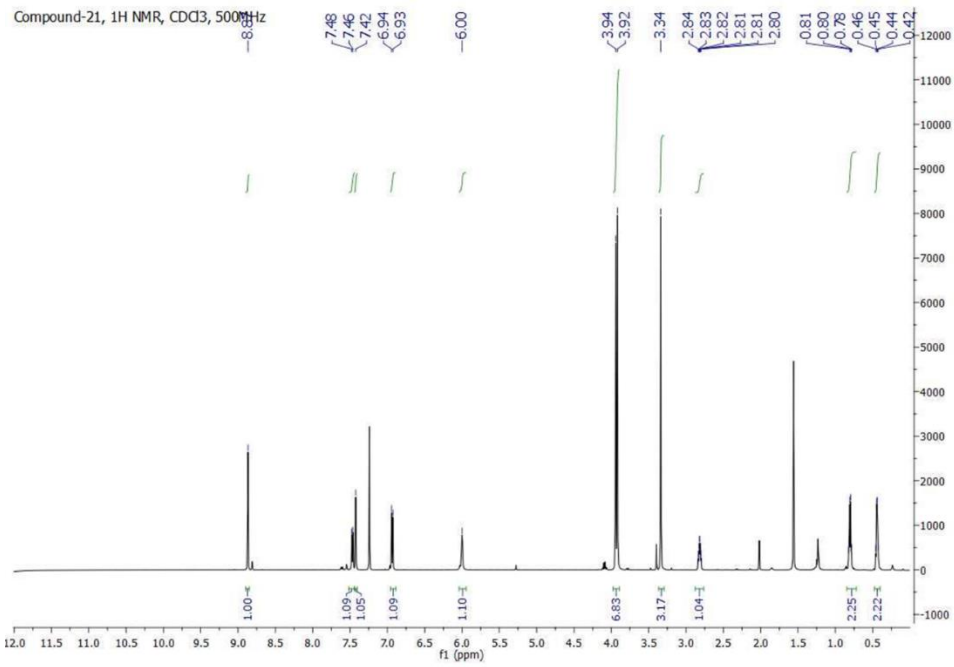
Compound-21, 1H NMR, CDCl3, 500MHz
8.83
7.48
7.46
7.42
6.94
6.93
6.00
3.94
3.92
3.34
2.84
2.83
2.82
2.81
2.81
2.80
0.81
0.80
0.78
0.46
0.45
0.44
0.42
1.00
1.09
1.05
1.09
1.10
6.83
3.17
1.04
2.25
2.22
f1 (ppm)

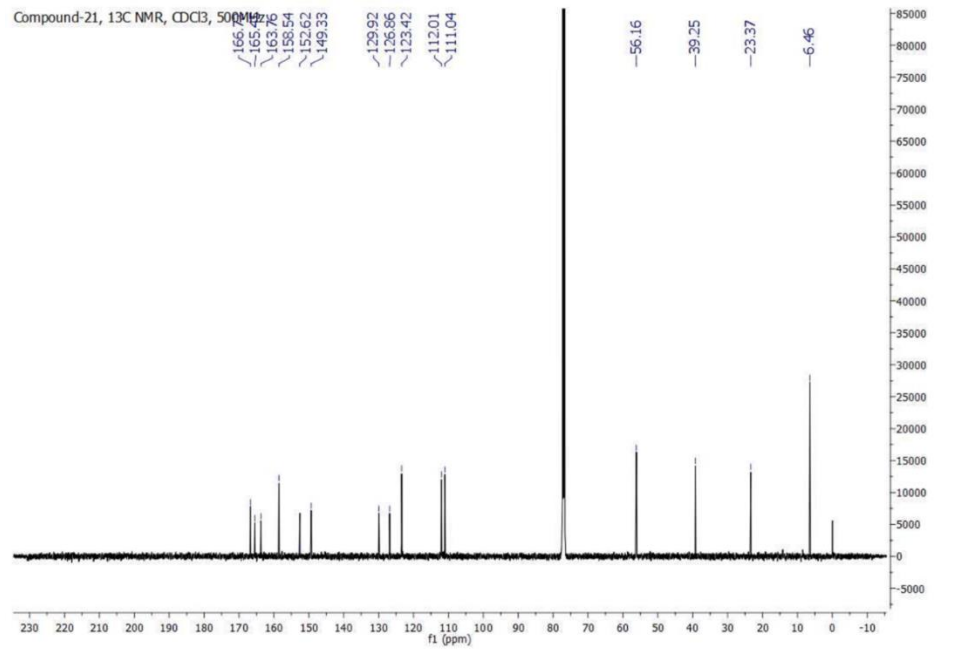
Compound-21, 13C NMR, CDCl3, 500MHz
166.74
165.42
163.76
158.54
152.62
149.33
129.92
126.86
123.42
112.01
111.04
56.16
39.25
23.37
6.46
f1 (ppm)

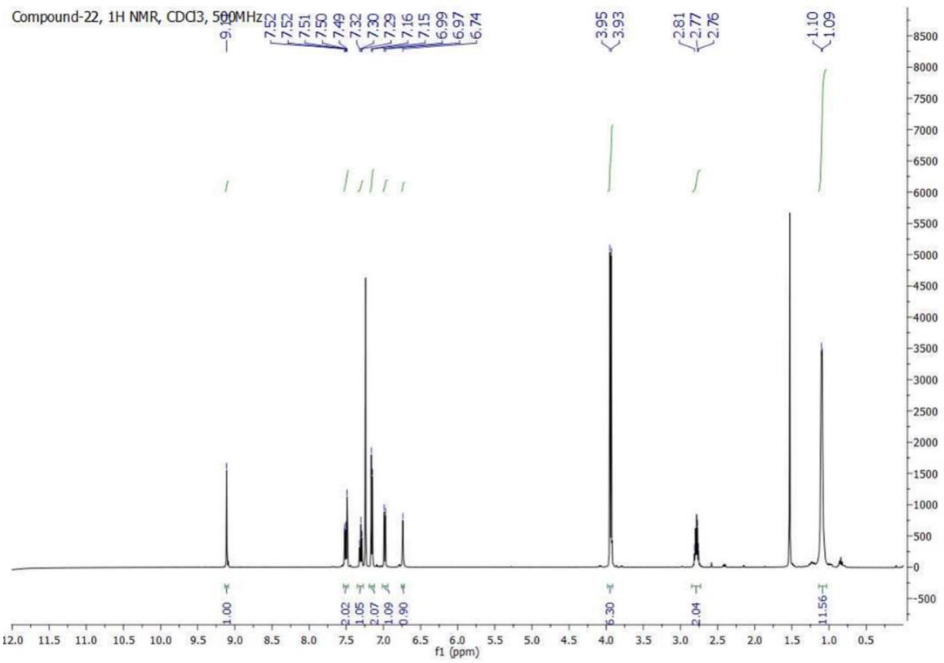
Compound-22, 1H NMR, CDCl3, 500MHz
9.10
7.52
7.52
7.51
7.50
7.49
7.32
7.30
7.29
7.16
7.15
6.99
6.97
6.74
3.95
3.93
2.81
2.77
2.76
1.10
1.09
1.00
2.02
1.05
2.07
1.09
0.90
6.30
2.04
11.56
f1 (ppm)

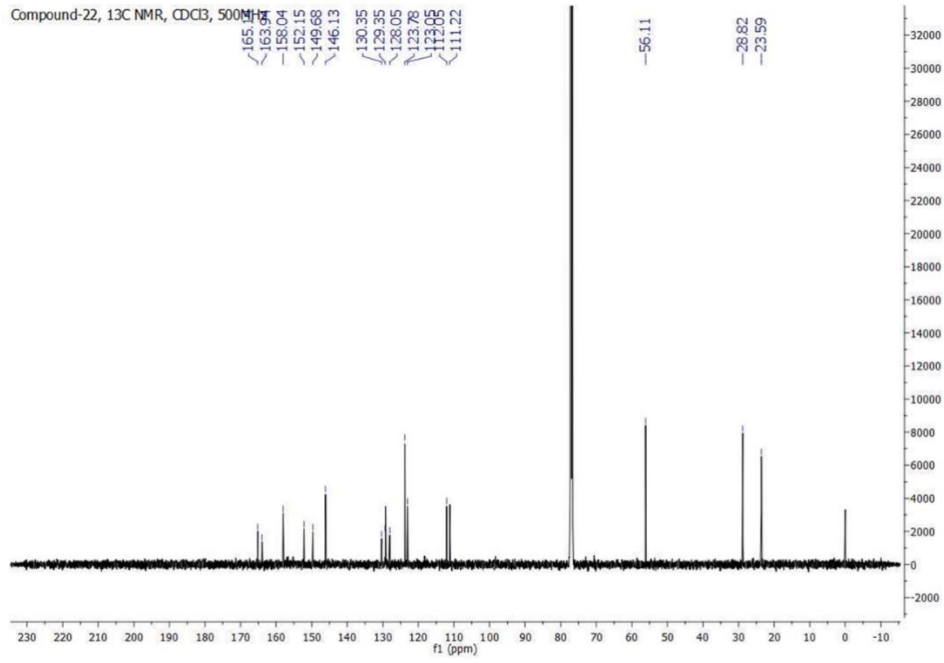
Compound-22, 13C NMR, CDCl3, 500MHz
165.51
163.94
158.04
152.15
149.68
146.13
130.35
129.35
128.05
123.78
123.05
112.05
111.22
56.11
28.82
23.59
f1 (ppm)

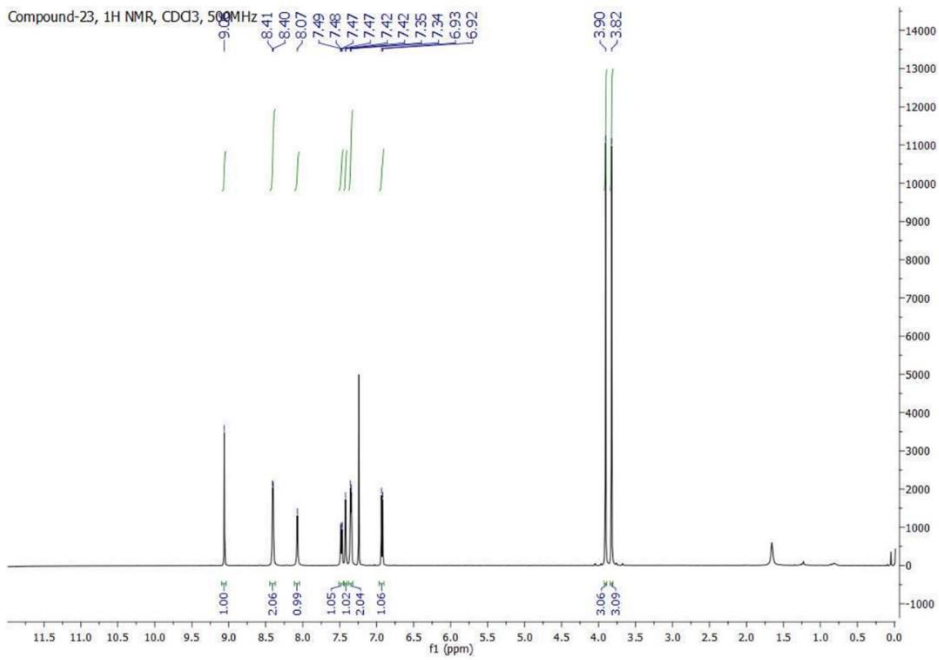
Compound-23, 1H NMR, CDCl3, 500MHz
9.08
8.41
8.40
8.07
7.49
7.48
7.47
7.47
7.42
7.42
7.35
7.34
6.93
6.92
3.90
3.82
1.00
2.06
0.99
1.05
1.02
2.04
1.06
3.06
3.09
f1 (ppm)

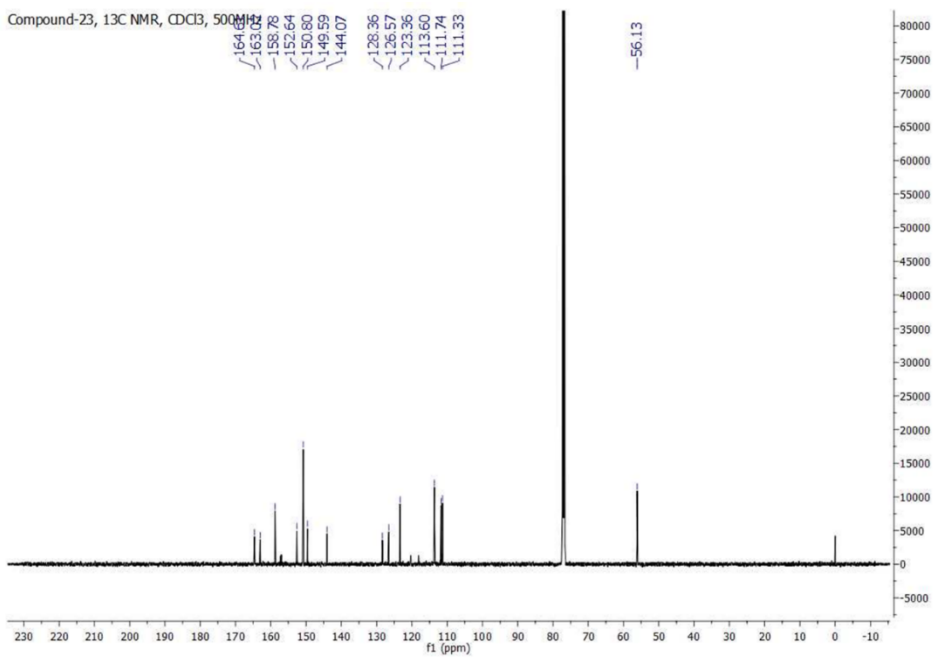
Compound-23, 13C NMR, CDCl3, 500MHz
164.64
163.04
158.78
152.64
150.80
149.59
144.07
128.36
126.57
123.36
113.60
111.74
111.33
56.13
f1 (ppm)

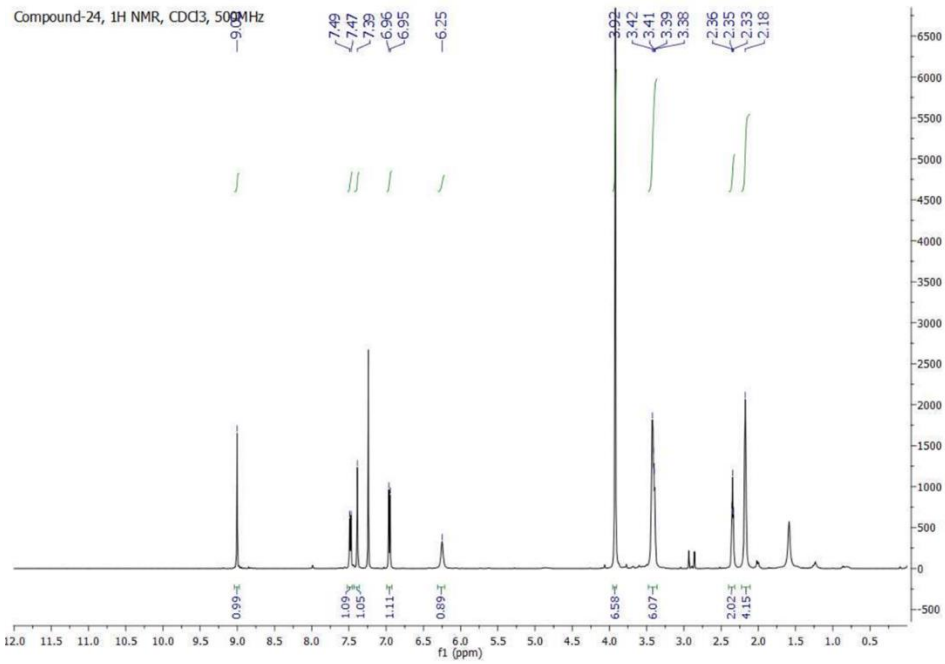
Compound-24, 1H NMR, CDCl3, 500MHz
9.00
7.49
7.47
7.39
6.96
6.95
6.25
3.92
3.42
3.41
3.39
3.38
2.36
2.35
2.33
2.18
0.99
1.09
1.05
1.11
0.89
6.58
6.07
2.02
4.15
f1 (ppm)

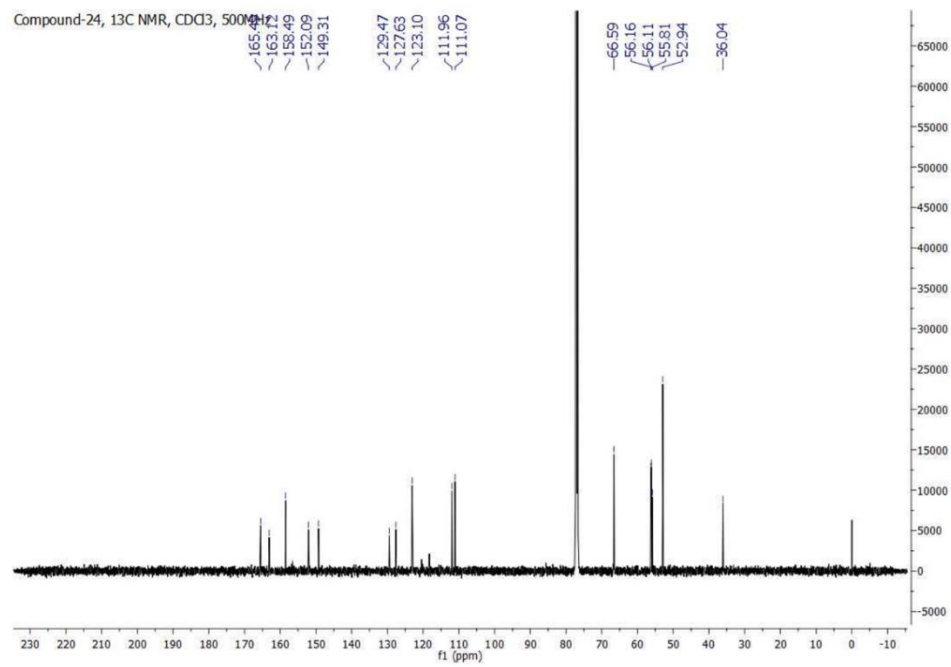
Compound-24, 13C NMR, CDCl3, 500MHz
165.47
163.72
158.49
152.09
149.31
129.47
127.63
123.10
111.96
111.07
66.59
56.16
56.11
55.81
52.94
36.04
f1 (ppm)

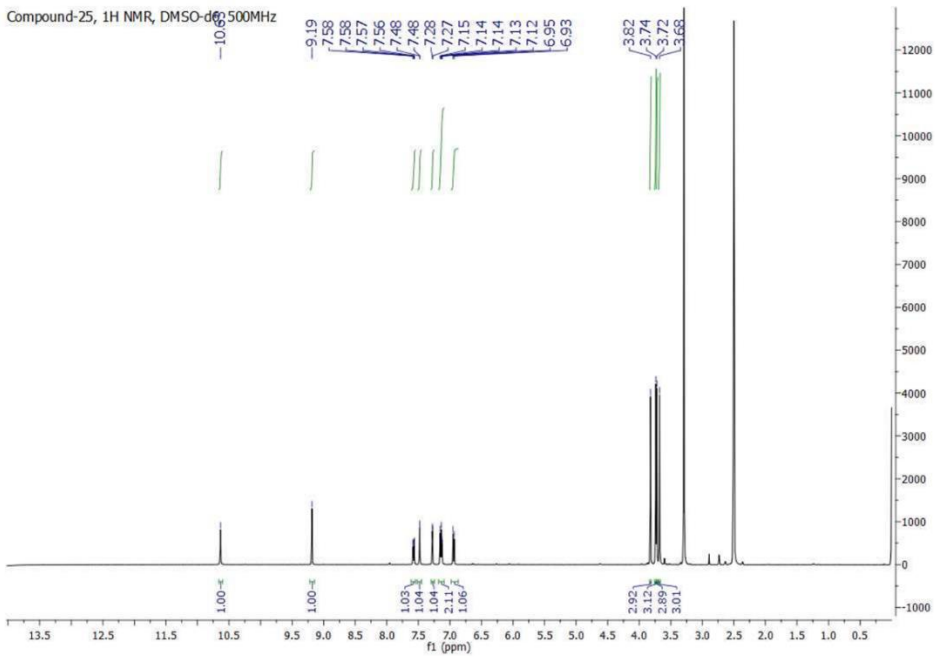
Compound-25, 1H NMR, DMSO-d6 500MHz
10.48
9.19
7.58
7.58
7.57
7.56
7.48
7.48
7.28
7.27
7.15
7.14
7.14
7.13
7.12
6.95
6.93
3.82
3.74
3.72
3.68
1.00
1.00
1.03
1.04
1.04
2.11
1.06
2.92
3.12
2.89
3.01
f1 (ppm)

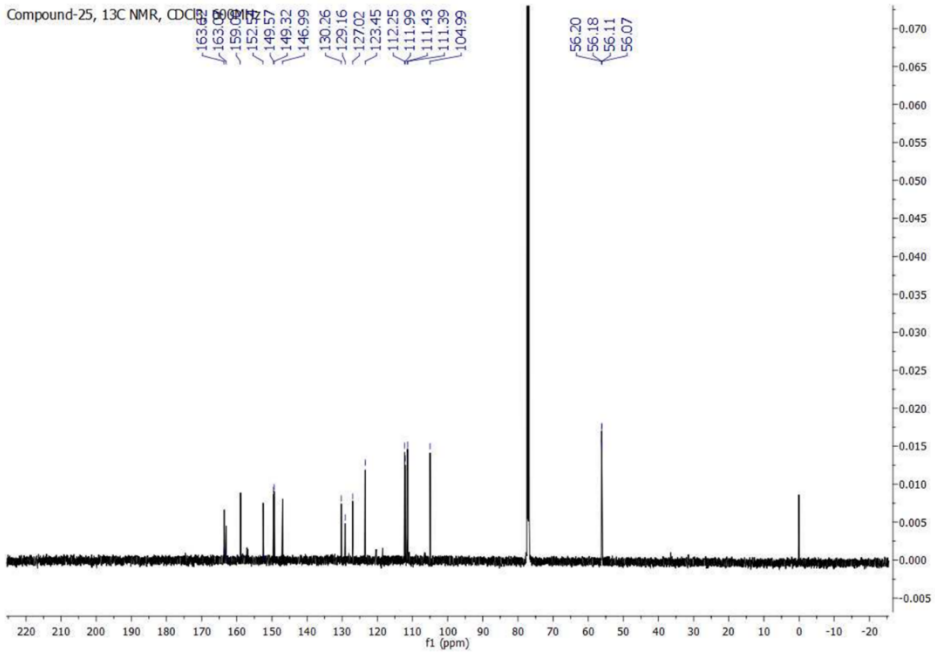
Compound-25, 13C NMR, CDCl3 500MHz
163.62
163.09
159.06
152.52
149.57
149.32
146.99
130.26
129.16
127.02
123.45
112.25
111.99
111.43
111.39
104.99
56.20
56.18
56.11
56.07
f1 (ppm)

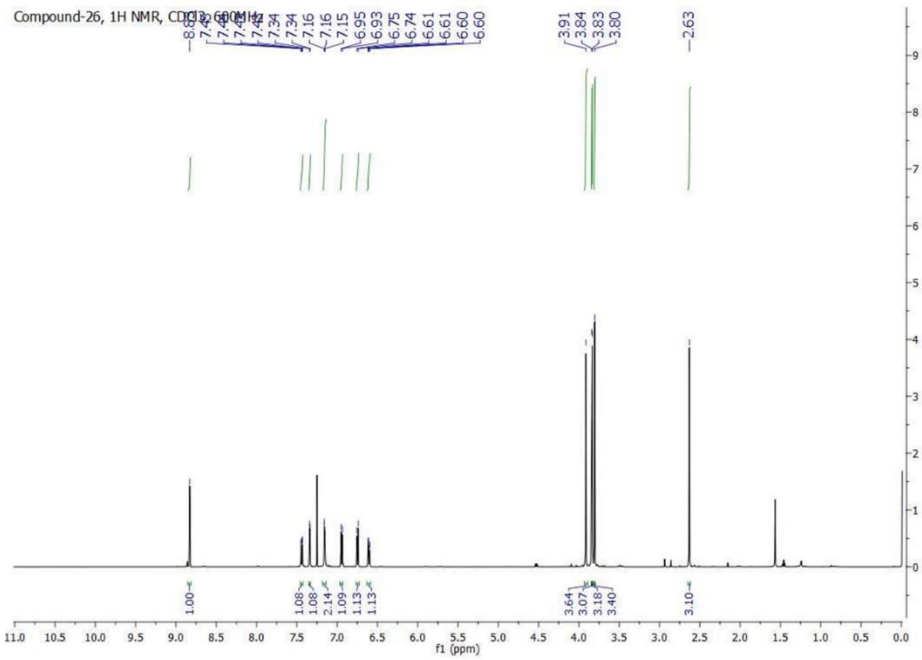
Compound-26, 1H NMR, CDCl3, 600MHz
8.89
7.36
7.34
7.16
7.15
6.95
6.93
6.75
6.74
6.61
6.60
3.91
3.84
3.83
3.80
2.63
1.00
1.08
1.08
2.14
1.09
1.13
1.13
3.64
3.07
3.18
3.40
3.10
f1 (ppm)

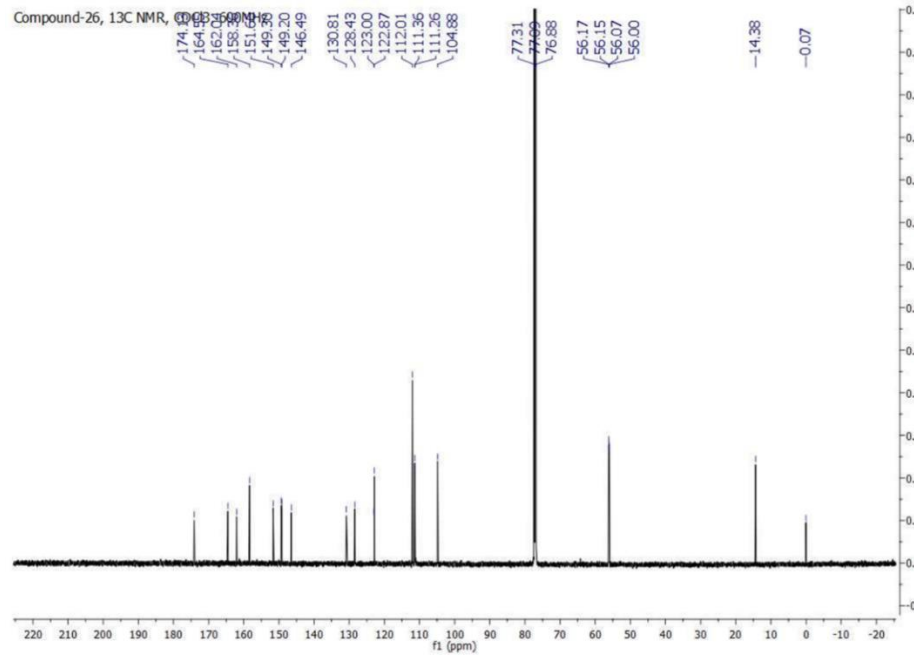
Compound-26, 13C NMR, CDCl3, 600MHz
174.14
164.15
162.50
158.38
151.82
149.36
149.20
146.49
130.81
128.43
123.00
122.87
112.01
111.36
111.26
104.88
77.31
77.09
76.88
56.17
56.15
56.07
56.00
14.38
0.07
f1 (ppm)

Figure 25. ^{1}H-^{1}H COSY and HMBC NMR spectrum of compound-**23**

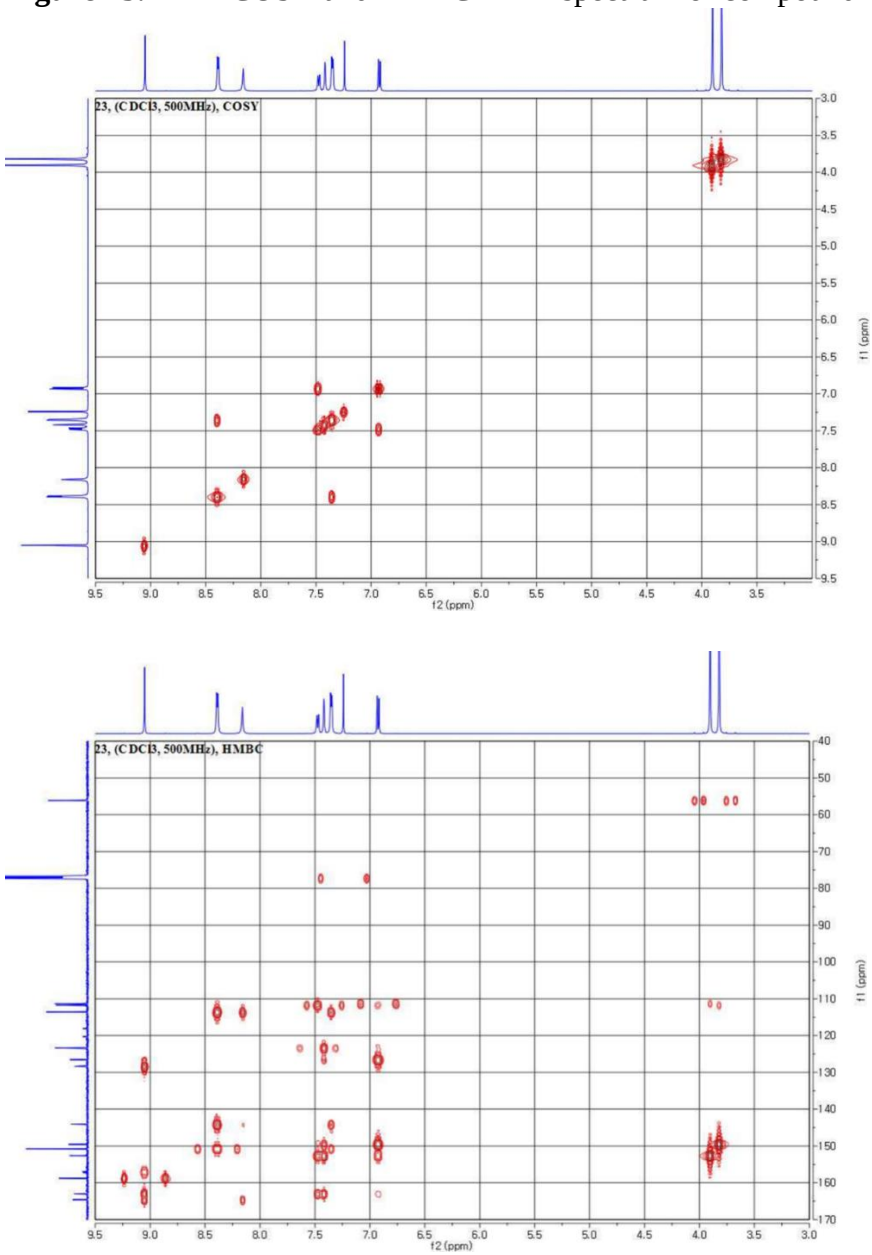

Figure 26. NOESY and HSQC spectrum of compound-**23**

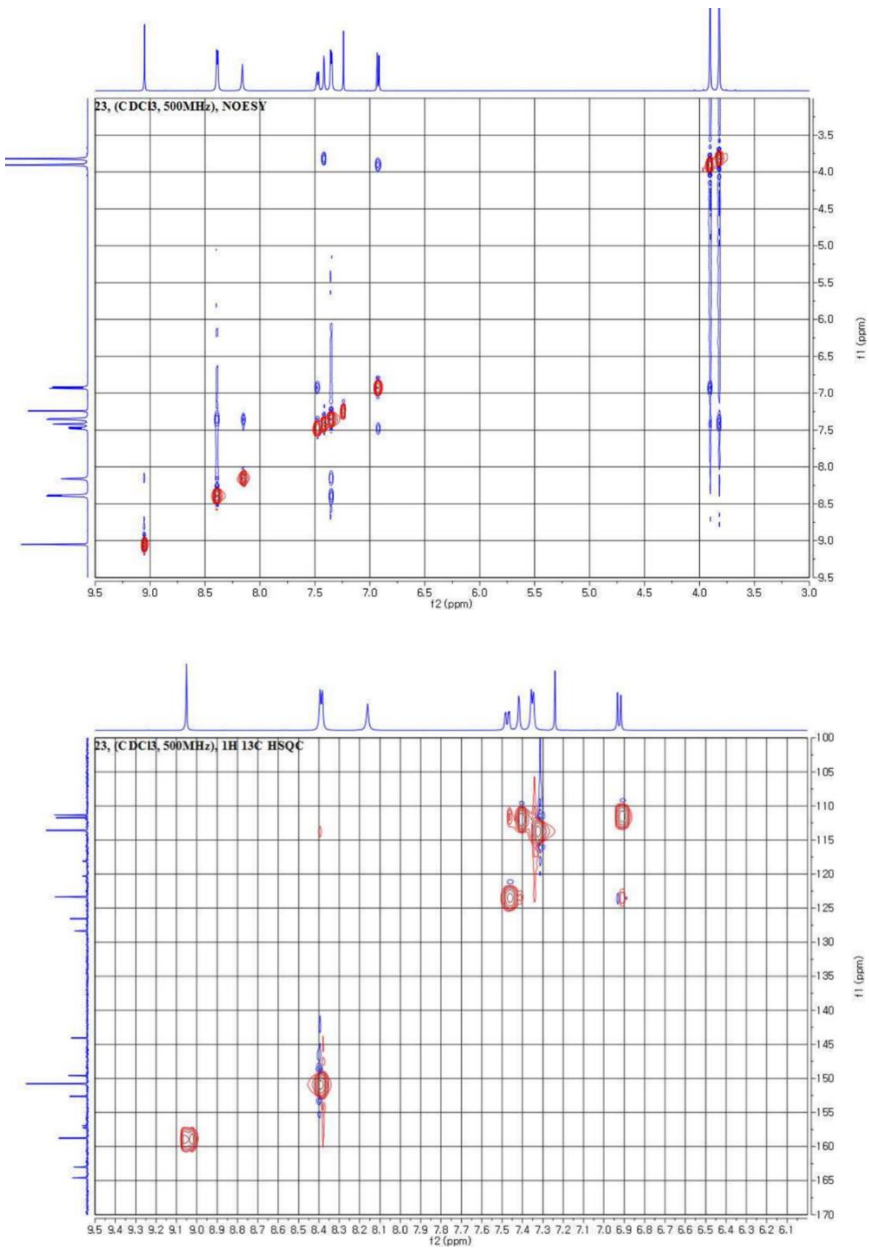

6. REFERENCES

[1] R. Beasley, T.I.S. of Asthma, Worldwide variation in prevalence of symptoms of asthma, allergic rhino conjunctivitis, and atopic eczema: ISAAC, The Lancet, 351 (1998) 1225-1232.

[2] J.A. Odhiambo, H.C. Williams, T.O. Clayton, C.F. Robertson, M.I. Asher, I.P.T.S. Group, Global variations in prevalence of eczema symptoms in children from ISAAC Phase Three, J. Allergy. Clin. Immunol. 124 (2009) 1251-1258. e1223.

[3] D.Y. Leung, M.Boguniewicz, M.D. Howell, I. Nomura, Q.A. Hamid. New insights into atopic dermatitis. J. Clin. Invest. 113(5), (2004) 651-657.

[4] C. J. Apfelbacher, T. L.Diepgen,J.Schmitt, Determinants of eczema: population-based cross-sectional study in Germany. Allergy 66, (2011) 206–213.

[5] N.Wadonda-Kabondoet al. Association of parental eczema, hay fever, and asthma with atopic dermatitis in infancy: birth cohort study. Arch. Dis. Child 89, 917–921 (2004).

[6] X. Wu, H. Chen, H. Xu, The genomic landscape of human immune-mediated diseases, J. Hum. Genet. 60 (2015) 675-681.

[7] E.L. Simpson, T. Bieber, L. Eckert, R. Wu, M. Ardeleanu, N.M. Graham, G. Pirozzi, V. Mastey, Patient burden of moderate to severe atopic dermatitis

(AD): Insights from a phase 2b clinical trial of dupilumab in adults, J. Am. Acad. Dermatol. 74 (2016) 491-498.

[8] M. Boguniewicz, D.Y. Leung, Atopic dermatitis: a disease of altered skin barrier and immune dysregulation, Immunol. Rev. 242 (2011) 233-246.

[9] M.J. Gooderham, H.C. Hong, P. Eshtiaghi, K.A. Papp, Dupilumab: A review of its use in the treatment of atopic dermatitis. J. Am. Acad. Dermatol. 78(3) (2018) S28-36.

[10] J.M. Oldhoff, U. Darsow, T. Werfel, I.C. Bihari, K. Katzer, J. Laifaoui, S. Plötz, A. E.F. Kapp, Knol, C.A. Bruijnzeel-Koomen, J. Ring, No effect of anti-interleukin-5 therapy (mepolizumab) on the atopy patch test in atopic dermatitis patients. Int. Arch. Allergy Immunol. 141 (2006) 290-294.

[11] a) A. Wollenberg, M.D. Howell, E. Guttman-Yassky, J.I. Silverberg, C. Kell, K. Ranade, R. Moate, R. van der Merwe, Treatment of Atopic Dermatitis with Tralokinumab, an Anti–IL-13 Monoclonal Antibody.J. Allergy Clin. Immunol. 2018 Jun 12. b) E.L. Simpson, C. Flohr, L.F. Eichenfield, T. Bieber, H. Sofen, A. Taïeb, R. Owen, W. Putnam, M. Castro, K. DeBusk, C.Y. Lin, Efficacy and safety of lebrikizumab (an anti-IL-13 monoclonal antibody) in adults with moderate-to-severe atopic dermatitis inadequately controlled by topical corticosteroids: A randomized, placebo-

controlled phase II trial (TREBLE). J. Am. Acad. Dermatol. 78 (2018) 863-871.

[12] https://clinicaltrials.gov/ct2/show/NCT03568136

[13] M. Londei, B. Kenney, G. Los, M.H. Marino, A Phase 1 Study of ANB020, an anti-IL-33 monoclonal Antibody in Healthy Volunteers. J. Allergy Clin. Immunol. 139(2) (2017) AB73.

[14] E. Guttman-Yassky, P.M. Brunner, A.U. Neumann, S. Khattri, A.B. Pavel, K. Malik, G.K. Singer, D. Baum, P. Gilleaudeau, M. Sullivan-Whalen, S. Rose, Efficacy and safety of fezakinumab (an IL-22 monoclonal antibody) in adults with moderate-to-severe atopic dermatitis inadequately controlled by conventional treatments: A randomized, double-blind, phase 2a trial. J. Am. Acad. Dermatol. 78(5) (2018) 872-881.

[15] T. Ruzicka, J.M. Hanifin, M. Furue, G. Pulka, I. Mlynarczyk, A. Wollenberg, R. Galus, T. Etoh, R. Mihara, H. Yoshida, J. Stewart, Anti–interleukin-31 receptor A antibody for atopic dermatitis. N. Engl. J. Med. 376(9) (2017) 826-835.

[16] https://clinicaltrials.gov/ct2/show/NCT01614756

[17] Vanda Pharmaceuticals Inc. Vanda's tradipitant improves itch and disease severity in patients with atopic dermatitis. CISION https://www.prnewswire.com/news-releases/vandas-tradipitant-improvesitch-and-disease-severity-in-patients-with-atopicdermatitis-300519177.html

[18] G.M. Gauvreau, J.P. Arm, L.P. Boulet, R. Leigh, D.W. Cockcroft, B.E. Davis, I. Mayers, J.M. FitzGerald, B. Dahlen, K.J. Killian, M. Laviolette, Efficacy and safety of multiple doses of QGE031 (ligelizumab) versus omalizumab and placebo in inhibiting allergen-induced early asthmatic responses. J. Allergy Clin. Immunol. 138 (2016) 1051-1059.

[19] E. Guttman-Yassky, J.I. Silverberg, O. Nemoto, S.B. Forman, A. Wilke, R. Prescilla, A. de la Peña, F.P. Nunes, J. Janes, M. Gamalo, D. Donley, Baricitinib in adult patients with moderate-to-severe atopic dermatitis: a phase 2 parallel, double-blinded, randomized placebo-controlled multiple-dose study.J. Am. Acad. Dermatol. 2018 Feb 2.

[20] Abbvie. AbbVie's Upadacitinib (ABT-494) Meets Primary Endpoint in Phase 2b Study in Atopic Dermatitis. AbbVie Newsroom https://news.abbvie.com/news/abbvies-upadacitinib-abt-494-meets-primary-endpointin-phase-2b-study-in-atopic-dermatitis.htm (2018).

[21] E. Guttman-Yassky, A.B. Pavel, T. Song, H. Kim, D. Zammit, S. Toker, Rao N. 559 ASN002 a dual oral inhibitor of JAK/SYK signaling improves clinical outcomes and associated cutaneous inflammation in moderate-to-severe atopic dermatitis patients. J. Investig. Dermatol. 138(5) (2018) S95.

[22] R. Bissonnette, K.A. Papp, Y. Poulin, M. Gooderham, M. Raman, L. Mallbris, C. Wang, V. Purohit, C. Mamolo, J. Papacharalambous, W.C. Ports. Topical tofacitinib for atopic dermatitis: a phase II a randomized trial. Br. J. Dermatol. 175(5) (2016) 902-911.

[23] H. Nakagawa, O. Nemoto, A. Igarashi, T. Nagata, Efficacy and safety of topical JTE-052, a Janus kinase inhibitor, in Japanese adult patients with moderate-to-severe atopic dermatitis: a phase II, multicentre, randomized, vehicle-controlled clinical study. Br. J. Dermatol. 178(2) (2018) 424-432.

[24] https://clinicaltrials.gov/ct2/show/NCT03011892.

[25] Novartis. Ziarco Pharma Announces Positive Top Line Results from Phase 2a Study in Moderate to Severe Atopic Dermatitis with its Oral Lead Compound ZPL-389. Lundbeckfonden https://www.lundbeckfonden.com/en/ziarco-pharma-announces-positive-topline-results-from-phase-2a-study-in-moderateto-severe-atopic-dermatitis-with-its-oral-leadcompound-zpl-389/(2016).

[26] G. Castelli, M. Schaffer Crisaborole (Eucrisa) for Mild to Moderate Atopic Dermatitis. American family physician. 98(6) (2018) 379.

[27] https://clinicaltrials.gov/ct2/show/NCT01856764.

[28] https://clinicaltrials.gov/ct2/show/NCT03394677.

[29] M. Abrouk, B. Farahnik, T.H. Zhu, M. Nakamura, R. Singh, K. Lee, S.M. Lucking, J. Blossom, W. Liao, J. Koo, T. Bhutani, Apremilast treatment of atopic dermatitis and other chronic eczematous dermatoses. J. Am. Acad. Dermatol. 77 (2017) 177-180.

[30] https://clinicaltrials.gov/ct2/show/NCT01037881.

[31] R. Mosenden, K. Taskén, Cyclic AMP-mediated immune regulation—overview of mechanisms of action in T cells, Cell. Signal. 23 (2011) 1009-1016.

[32] J.L. Jimenez, C. Punzón, J.n. Navarro, M.A. Muñoz-Fernández, M. Fresno, Phosphodiesterase 4 inhibitors prevent cytokine secretion by T lymphocytes by inhibiting nuclear factor-κB and nuclear factor of activated T cells activation, J. Pharmacol. Exp. Ther. 299 (2001) 753-759.

[33] J. Arp, M. G.Kirchhof, M. L.Baroja, S. H. Nazarian, T. A. Chau, C. A.Strathdee et al. Regulation of T-cell activation by phosphodiesterase4B2

requires its dynamic redistribution during immunological synapseformation. Mol. Cell. Biol. 23(2003) 8042-8057.

[34] A. L. Asirvatham, S. G.Galligan, R. V. Schillace,M. P. Davey, V.Vasta, J. A. Beavoet al.. A-kinase anchoring proteins interact with phosphodiesterasesin T lymphocyte cell lines. J. Immunol. 173(2004) 4806–4814.

[35] D.H. Maurice, H. Ke, F. Ahmad, Y. Wang, J. Chung, V.C. Manganiello, Advances in targeting cyclic nucleotide phosphodiesterases, Nat. Rev. Drug Discov. 13 (2014) 290.

[36] K. Omori, J. Kotera, Overview of PDEs and their regulation, Circulation research, 100 (2007) 309-327.

[37] A. Kodimuthali, S.S.L. Jabaris, M. Pal, Recent advances on phosphodiesterase 4 inhibitors for the treatment of asthma and chronic obstructive pulmonary disease, J. Med. Chem. 51 (2008) 5471-5489.

[38] P. Wang, P. Wu, K.M. Ohleth, R.W. Egan, M.M. Billah, Phosphodiesterase 4B2 is the predominant phosphodiesterase species and undergoes differential regulation of gene expression in human monocytes and neutrophils, Mol. Pharmacol. 56 (1999) 170-174.

[39] A. Robichaud, P.B. Stamatiou, S.-L.C. Jin, N. Lachance, D. MacDonald, F. Laliberté, S. Liu, Z. Huang, M. Conti, C.-C. Chan, Deletion of phosphodiesterase 4D in mice shortens α2-adrenoceptor–mediated anesthesia, a behavioral correlate of emesis, J. Clin. Invest. 110 (2002) 1045.

[40] D.R. Gorja, S. Mukherjee, C.L.T. Meda, G.S. Deora, K.L. Kumar, A. Jain, G.H. Chaudhari, K.S. Chennubhotla, R.K. Banote, P. Kulkarni, K.V. L. Parsa, K. Mukkantib and M. Pal Novel N-indolylmethyl substituted olanzapine derivatives: their design, synthesis and evaluation as PDE4B inhibitors, Org. Biomol. Chem. 11 (2013) 2075-2079.

[41] K. Naganuma, A. Omura, N. Maekawara, M. Saitoh, N. Ohkawa, T. Kubota, H. Nagumo, T. Kodama, M. Takemura, Y. Ohtsuka, Discovery of selective PDE4B inhibitors, Bioorganic Med. Chem. Lett. 19 (2009) 3174-3176.

[42] T. Goto, A. Shiina, T. Murata, M. Tomii, T. Yamazaki, K.-i. Yoshida, T. Yoshino, O. Suzuki, Y. Sogawa, K. Mizukami, Identification of the 5, 5-dioxo-7, 8-dihydro-6H-thiopyrano [3, 2-d] pyrimidine derivatives as highly selective PDE4B inhibitors, Bioorganic Med. Chem. Lett. 24 (2014) 893-899.

[43] M. Kranz, M. Wall, B. Evans, A. Miah, S. Ballantine, C. Delves, B. Dombroski, J. Gross, J. Schneck, J.P. Villa, Identification of PDE4B Over 4D

subtype-selective inhibitors revealing an unprecedented binding mode, Bioorganic Med. Chem. 17 (2009) 5336-5341.

[44] M. Wittmann, P.S. Helliwell, Phosphodiesterase 4 inhibition in the treatment of psoriasis, psoriatic arthritis and other chronic inflammatory diseases, DermatolTher, 3 (2013) 1-15.

[45] A.L. Buchman, Side effects of corticosteroid therapy, J. Clin. Gastroentero. 33 (2001) 289-294.

[46] N. Bordag, S. Klie, K. Jürchott, J. Vierheller, H. Schiewe, V. Albrecht, J.-C. Tonn, C. Schwartz, C. Schichor, J. Selbig, Glucocorticoid (dexamethasone)-induced metabolome changes in healthy males suggest prediction of response and side effects, Sci. Rep. 5 (2015)15954.

[47] N. Parikh, A. K Chakraborti, Phosphodiesterase 4 (PDE4) inhibitors in the treatment of COPD: promising drug candidates and future directions, Curr. Med. Chem. 23 (2016) 129-141.

[48] S. Contreras, J. Milara, E. Morcillo, J. Cortijo, Selective Inhibition of Phosphodiesterases 4A, B, C and D Isoforms in Chronic Respiratory Diseases: Current and Future Evidences, Curr. Pharm. Des. 23 (2017) 2073-2083.

[49] J. Arp, M.G. Kirchhof, M.L. Baroja, S.H. Nazarian, T.A. Chau, C.A. Strathdee, E.H. Ball, J. Madrenas, Regulation of T-cell activation by phosphodiesterase 4B2 requires its dynamic redistribution during immunological synapse formation, Mol. Cell. Biol. 23 (2003) 8042-8057.

[50] A.L. Asirvatham, S.G. Galligan, R.V. Schillace, M.P. Davey, V. Vasta, J.A. Beavo, D.W. Carr, A-kinase anchoring proteins interact with phosphodiesterases in T lymphocyte cell lines, J. Immunol. 173 (2004) 4806-4814.

[51] A.L. Small-Howard, L.M. Shimoda, H. TURNER, Anti-inflammatory potential of CB1-mediated cAMP elevation in mast cells, Biochem. J. 388 (2005) 465-473.

[52] D. Spina, PDE4 inhibitors: current status, Br. J. Pharmacol. 155 (2008) 308-315.

[53] F.M. Konrad, A. Bury, M.A. Schick, K.-C. Ngamsri, J. Reutershan, The unrecognized effects of phosphodiesterase 4 on epithelial cells in pulmonary inflammation, PloS one, 10 (2015) e0121725.

[54] P.M. Calverley, F. Sanchez-Toril, A. McIvor, P. Teichmann, D. Bredenbroeker, L.M. Fabbri, Effect of 1-year treatment with roflumilast in

severe chronic obstructive pulmonary disease, Am. J. Respir. Crit. Care. Med. 176 (2007) 154-161.

[55] K.F. Rabe, Update on roflumilast, a phosphodiesterase 4 inhibitor for the treatment of chronic obstructive pulmonary disease, Br. J. Pharmacol. 163 (2011) 53-67.

[56] P.C. Gray, J.D. Scott, W.A. Catterall, Regulation of ion channels by cAMP-dependent protein kinase and A-kinase anchoring proteins, Curr. Opin. Neurobiol. 8 (1998) 330-334.

[57] J.A. Carvajal, A.M. Germain, J.P. Huidobro-Toro, C.P. Weiner, Molecular mechanism of cGMP-mediated smooth muscle relaxation, J. Cell. Physiol. 184 (2000) 409-420.

[58] S.H. Carroll, K. Ravid, Differentiation of mesenchymal stem cells to osteoblasts and chondrocytes: a focus on adenosine receptors, Expert. Rev. Mol. Med. 15 (2013) e1.

[59] M.M. Khan, D. Lustrino, W.A. Silveira, F. Wild, T. Straka, Y. Issop, E. O'Connor, D. Cox, M. Reischl, T. Marquardt, Sympathetic innervation controls homeostasis of neuromuscular junctions in health and disease, Proc. Natl. Acad. Sci. U.S.A. 113 (2016) 746-750.

[60] Y. Wang, J. Viscarra, S.-J. Kim, H.S. Sul, Transcriptional regulation of hepatic lipogenesis, Nat. Rev. Mol. Cell. Biol. 16 (2015) 678-689.

[61] Z. Wang, D. Liu, A. Varin, V. Nicolas, D. Courilleau, P. Mateo, C. Caubere, P. Rouet, A. Gomez, G. Vandecasteele, A cardiac mitochondrial cAMP signaling pathway regulates calcium accumulation, permeability transition and cell death, Cell. Death. Dis. 7 (2016) e2198.

[62] R. Bissonnette, D.M. Pariser, N.R. Wasel, J. Goncalves, R.M. Day, R. Chen, M. Sebastian, Apremilast, an oral phosphodiesterase-4 inhibitor, in the treatment of palmoplantar psoriasis: Results of a pooled analysis from phase II PSOR-005 and phase III Efficacy and Safety Trial Evaluating the Effects of Apremilast in Psoriasis (ESTEEM) clinical trials in patients with moderate to severe psoriasis, J. Am. Acad. Dermatol. 75 (2016) 99-105.

[63] J. Felding, M.D. Sørensen, T.D. Poulsen, J. Larsen, C. Andersson, P. Refer, K. Engell, L.G. Ladefoged, T. Thormann, A.M. Vinggaard, Discovery and early clinical development of 2-{6-[2-(3, 5-dichloro-4-pyridyl) acetyl]-2, 3-dimethoxyphenoxy}-N-propylacetamide (LEO 29102), a soft-drug inhibitor of phosphodiesterase 4 for topical treatment of atopic dermatitis, J. Med. Chem. 57 (2014) 5893–5903.

[64] S. Cherukupalli, R. Karpoormath, B. Chandrasekaran, G.A. Hampannavar, N. Thapliyal, V.N. Palakollu, An insight on synthetic and medicinal aspects of pyrazolo[1, 5-a]pyrimidine scaffold, Eur. J. Med. Chem. 126 (2017) 298-352.

[65] J. Taltavull, J. Serrat, J. Gràcia, A. Gavaldà, M. Córdoba, E. Calama, J.L. Montero, M. Andrés, M. Miralpeix, D. Vilella, Synthesis and biological activity of pyrido[3′, 2′: 4, 5] furo [3, 2-d] pyrimidine derivatives as novel and potent phosphodiesterase type 4 inhibitors, Eur. J. Med. Chem. 46 (2011) 4946-4956.

[66] P. D'Ursi, S. Guariento, G. Trombetti, A. Orro, E. Cichero, L. Milanesi, P. Fossa, O. Bruno, Further Insights in the Binding Mode of Selective Inhibitors to Human PDE4D Enzyme Combining Docking and Molecular Dynamics, Mol. Inform. 35 (2016) 369-381.

[67] A.F. Donnell, P.J. Dollings, J.A. Butera, A.J. Dietrich, K.K. Lipinski, A. Ghavami, W.D. Hirst, Identification of pyridazino [4, 5-b] indolizines as selective PDE4B inhibitors, Bioorganic Med. Chem. Lett. 20 (2010) 2163-2167.

[68] E.P. Gillis, K.J. Eastman, M.D. Hill, D.J. Donnelly, N.A. Meanwell, Applications of fluorine in medicinal chemistry, J. Med. Chem. 58 (2015) 8315-8359.

[69] W.K. Hagmann, The many roles for fluorine in medicinal chemistry, J. Med. Chem. 51 (2008) 4359-4369.

[70] A.F. Littke, C. Dai, G.C. Fu, Versatile catalysts for the Suzuki cross-coupling of arylboronic acids with aryl and vinyl halides and triflates under mild conditions, J. Am. Chem. Soc. 122 (2000) 4020-4028.

[71] B. Gopalan, L.A. Gharat, B. Chandrasekhar, B.G. Pillai, Process for the preparation of n-(3, 5-dichloropyrid-4-yl)-4-difluoromethoxy-8-methanesulfonamido-dibenzo [b, d] furan-1-carboxamide, in, Google Patents, 2009.

[72] O. Dym, I. Xenarios, H. Ke, J. Colicelli, Molecular docking of competitive phosphodiesterase inhibitors, Mol. Pharmacol. 61 (2002) 20-25.

[73] R.X. Xu, A.M. Hassell, D. Vanderwall, M.H. Lambert, W.D. Holmes, M.A. Luther, W.J. Rocque, M.V. Milburn, Y. Zhao, H. Ke, Atomic structure of PDE4: insights into phosphodiesterase mechanism and specificity, Science, 288 (2000) 1822-1825.

[74] S. Guariento, O. Bruno, P. Fossa, E. Cichero, New insights into PDE4B inhibitor selectivity: CoMFA analyses and molecular docking studies, Molec. Divers. 20 (2016) 77-92.

[75] G.L. Card, B.P. England, Y. Suzuki, D. Fong, B. Powell, B. Lee, C. Luu, M. Tabrizizad, S. Gillette, P.N. Ibrahim, Structural basis for the activity of drugs that inhibit phosphodiesterases, Structure, 12 (2004) 2233-2247.

[76] B.E. Smart, Characteristics of CF systems, in: Organofluorine Chemistry, Springer, 1994, pp. 57-88.

[77] M. Morgenthaler, E. Schweizer, A. Hoffmann-Röder, F. Benini, R.E. Martin, G. Jaeschke, B. Wagner, H. Fischer, S. Bendels, D. Zimmerli, Predicting and tuning physicochemical properties in lead optimization: amine basicities, ChemMedChem, 2 (2007) 1100-1115.

[78] C. Bissantz, B. Kuhn, M. Stahl, A medicinal chemist's guide to molecular interactions, J. Med. Chem. 53 (2010) 5061-5084.

[79] P. Zhou, F. Tian, J. Zou, Z. Shang, Rediscovery of halogen bonds in protein-ligand complexes, Mini. Rev. Med. Chem. 10 (2010) 309-314.

[80] R. Perozzo, G. Folkers, L. Scapozza, Thermodynamics of protein–ligand interactions: history, presence, and future aspects, J. Recept. Signal. Transduct. 24 (2004) 1-52.

[81] K.D. Stone, C. Prussin, D.D. Metcalfe, IgE, mast cells, basophils, and eosinophils, Journal of Allergy and Clinical Immunology, 125 (2010) S73-S80.

[82] N. Parameswaran, S. Patial, Tumor necrosis factor-α signaling in macrophages, Crit. Rev. Eukaryot. Gene Expr. 20 (2010).

[83] E. Y. Zhang, A. Y. Chen, and B. T. Zhu, Mechanism of dinitrochlorobenzene-induced dermatitis in mice: role of specific antibodies in pathogenesis. PLoS One (2009) 4:e7703.

[84] Hertz, A. L., Bender, A. T., Smith, K. C., Gilchrist, M., Amieux, P. S.,Aderem, A., et al.. Elevated cyclic AMP and PDE4 inhibition induce chemokine expression in human monocyte-derived macrophages. Proc. Natl. Acad. Sci. U.S.A. 106, (2009) 21978–21983.

[85] V. K. Raker, C. Becker, and K. Steinbrink, The cAMP pathway as therapeutic target in autoimmune and inflammatory diseases. Front. Immunol. 7 (2016) 123.

[86] S.-L. Jin, L. Lan, M. Zoudilova, and M. Conti, Specific role of phosphodiesterase 4B in lipopolysaccharide-induced signaling in mouse macrophages. J. Immunol. 175, (2005)1523–1531.

[87] E. Reyes-Irisarri, A. J. Sánchez, J. A. García-Merino, and G. Mengod, Selective induction of cAMP phosphodiesterase PDE4B2 expression in experimental autoimmune encephalomyelitis. J. Neuropathol. Exp. Neurol. 66 (2007) 923–931.

[88] M. D. Mannie, D. J. Fraser, and T. J. Mcconnell, IL-4 responsive CD4& plus; T cells specific for myelin basic protein: IL-2 confers a prolonged post activation refractory phase. Immunol. Cell Biol. 81, (2003) 8–19.

[89] J. H. Namkung, J. E. Lee, E. Kim, H. J. Cho, S. Kim, E. S. Shin, IL-5 and IL-5 receptor alpha polymorphisms are associated with atopic dermatitis in Koreans. Allergy, 62, (2007) 934–942.

[90] E. Vakirlis, E. Lazaridou, T. Tzellos, S. Gerou, D. Chatzidimitriou, D. Ioannides, Investigation of cytokine levels and their association with SCORAD index in adults with acute atopic dermatitis. J. Eur. Acad. Dermatol.Venereol. 25, (2011) 409–416.

[91] A. Elbe-Bürger, A. Egyed, S.Olt, R. Klubal, U. Mann, K. Rappersberger, Overexpression of IL-4 alters the homeostasis in the skin. J. Invest. Dermatol. 118, (2002) 767–778.

[92] G.R. Lee, R.A. Flavell, Transgenic mice which overproduce Th2 cytokines develop spontaneous atopic dermatitis and asthma. Int. Immunol. 16(8) (2004) 1155-60.

[93] N. Mikhalkevich, B. Becknell, M.A. Caligiuri, M.D. Bates, R. Harvey, W.P. Zheng, Responsiveness of naive CD4 T cells to polarizing cytokine determines the ratio of Th1 and Th2 cell differentiation. J. Immunol. 176(3) (2006) 1553-1560.

[94] A. Di Cesare, P. Di Meglio, F.O. Nestle. A role for Th17 cells in the immunopathogenesis of atopic dermatitis?. J. Investig. Dermatol. 128(11) (2008) 2569-2571.

[95] A. Chiricozzi, K. E. Nograles, L. M. Johnson-Huang, J. Fuentes-Duculan, I. Cardinale, K. M. Bonifacio, IL-17 induces an expanded range of downstream genes in reconstituted human epidermis model. PLoS One (2014) 9:e90284.

[96] C. L. Weller, S. J. Collington, J. K. Brown, H. R. Miller, A. Al-Kashi, P. Clark, Leukotriene B4, an activation product of mast cells, is a chemoattractant for their progenitors. J. Exp. Med. 201, (2005) 1961–1971.

[97] U. Darsow, and J. Ring, Immunoglobulin e-mediated allergy plays a role in atopic eczema as shown in the atopy patch test. World Allergy Organ. J. (2008) 1:107.

[98] S. G. Tangye, A. Ferguson, D. T. Avery, C. S. Ma, and P. D. Hodgkin, Isotype switching by human B cells is division-associated and regulated by cytokines. J. Immunol. 169, (2002) 4298–4306.

[99] Geha, R. S., Jabara, H. H., and Brodeur, S. R. The regulation of immunoglobulin E class-switch recombination. Nat. Rev. Immunol. 3, (2003) 721–732.

[100] M. Xia, R. Huang, V. Guo, N. Southall, M.H. Cho, J. Inglese, C.P. Austin, M. Nirenberg Identification of compounds that potentiate CREB signaling as possible enhancers of long-term memory. Proc. Natl. Acad. Sci. U.S.A. 106(7) (2009) 2412-2417.

[101] X. Pan, E. Arauz, J.J. Krzanowski, D.F. Fitzpatrick, J.B. Polson, Synergistic interactions between selective pharmacological inhibitors of phosphodiesterase isozyme families PDE III and PDE IV to attenuate

proliferation of rat vascular smooth muscle cells. Biochem. Pharmacol. 48(4) (1994) 827-835.

[102] H. Matsuda, N. Watanabe, G.P. Geba, J. Sperl, M. Tsudzuki, J. Hiroi, M. Matsumoto, H. Ushio, S. Saito, P.W. Askenase, C. Ra. Development of atopic dermatitis-like skin lesion with IgE hyperproduction in NC/Nga mice. Int. Immunol. 9(3) (1997) 461-466.

Acknowledgements

First of all, I would like to express my sincere gratitude to my supervisor Professor. Joon Myong Song, who patiently set up a line of interesting questions, provided me with reasonable and testable hypothesis and effectively steered me toward the path of success. I could not have imagined having a better advisor and mentor for my Ph.D study. I would like to thank my thesis committee members, Prof. Jeong Hill Park, Prof. Sang Kook Lee, Prof. Jeeyeon Lee, Prof. Sungsu Park, and including my advisor, Prof. Joon Myong Song. The advice provided by them from different angles greatly broadened my view and shaped the progression and direction of the thesis book. My sincere thanks also goes to Dr. Parthasarathy Arumugam, who conducted all the in vitro and in vivo biology experiments, and also Dr. Goutam Kulsi who provided the molecular docking study results. Without they precious support it would not be possible to conduct this research. I am indebted to all my lab members for their dedicated collaborations.

I am also grateful to the college of pharmacy at Seoul National University, and National Research Foundation of Korea (NRF) for funding the research. Finally, I would like to thank my family. My lovely wife, Prabhavathy, has been a comforting presence, a steady companion and a source of joy throughout my PhD studies at SNU. Her support and spirit in life has been a

steady anchor during the highs and lows in the pursuit of my dream. Also, I am deeply indebted to my parents, my mother-in-law and my grandmother, who believed in me, encouraged me and were always there for me.